ISSN 2071-3592

童舟共濟五十載
再創百年新未來

since 1971

50

The 50th Anniversary of TTMHH

童綜合醫學雜誌

Tungs' Medical Journal
Special Issue September 2021

童綜合醫療社團法人 童綜合醫院
Tungs' Taichung MetroHarbor Hospital

榮獲JCI 國際醫療評鑑認證
JOINT COMMISSION INTERNATIONAL

TUNGS' MEDICAL JOURNAL

Editorial Office:

The Tungs' Medical Journal, Tungs' Taichung MetroHarbor Hospital.

No. 699, Sec. 8, Taiwan Blvd., Wuqi Dist., Taichung City 43503, Taiwan (R.O.C.)

E-Mail: Tungs_Journal@ms.sltung.com.tw

Tel.: 886-4-26581919 ext. 59045 Fax: 886-4-26582193

Printing Company:

Great C Printing Co.

Tel: 886-2-2302-3939 Fax: 886-2-2302-2036

Tungs' Medical Journal

CONTENTS IN BRIEF

EDITORIAL

REVIEW ARTICLE

ORIGINAL ARTICLE

CASE REPORT

Editorial

Incorporating Integrated Table Motion with Robotic Surgical Xi System: A Single Institutional Experience and Review of Literature

Min-Che Tung[1], Yen-Chuan Ou[1,*], Che-Hsueh Yang[1], Yi-Sheng Lin[1], Wei-Chuan Weng[1,2], Li-Hua Huang[1,3], Chin-Heng Lu[1], Chao-Yu Hsu[1,3]

[1]*Division of urology, Department of Surgery, Tungs' Taichung MetroHarbor Hospital, Taichung 435, Taiwan*
[2]*Department of Nursing, Jen-Teh Junior College of Medicine. Nursing and Management, Miaoli 356, Taiwan*
[3]*Rong Hsing Research Center for Translational Medicine, National Chung Hsing University, Taichung 402, Taiwan*

Received: Jun. 04, 2021; Accepted: Jun. 04, 2021

Abstract

This article presents a review of contemporary literature and describes our experiences in incorporating integrated table motion (ITM) into the da Vinci Xi system when performing robotic-assisted surgery. In our experience thus far, ITM has been a safe application that makes robotic-assisted surgeries more convenient, especially in deep pelvic manipulation or multi-target surgeries.

Key words: Urological cancer, Urological surgery, Robotic surgery, Table motion, da Vinci Xi

Introduction

With the recent advances in technology, surgeries have evolved from the traditionally open methods to laparoscopic ones, marking the age of minimally invasive and contemporary robotic surgery. In the past, surgery had been frequently linked with a melancholy disposition in patients and troublesome perioperative morbidities that frustrated attending surgeons. The introduction of minimally invasive surgery combined with fast-track perioperative care has helped surgeons considerably lower the risk of morbidities. Evidence supporting the benefits could be seen in milder inflammatory reactions after minimally invasive surgery than after open surgery[1]. The advantages of minimally invasive surgery have helped shorten hospital stays and improve patients' quality of life[2], especially in patients after extirpative surgeries. Equipped with similar skills in accessing surgical targets, robotic surgery features more delicate surgical manipulations than laparoscopic surgery at any desired angle. In fact, robotic-assisted surgery can be more specifically called computer-assisted surgery. With the console as the brain of the facility, surgeons are thus allowed to freely magnify the fields in three-dimensional fashion and access any corner of the human body. Unlike the rigid equipment of laparoscopic surgery, the nimble hinge can simulate the joints of a human body, allowing sophisticated tractions, repairs, and incisions to nearly any target. Even in some surgeries such as trans-abdominal hernioplasty, surgeons can perform the operation without assistants after the ports are established.

The advantages of robotic-assisted system are especially appreciated when dealing with targets in deep narrow spaces such as pelvic organs. Given the inverted triangle shape of pelvis, access is limited to a narrow working space. The conditions are even worse when the targets are located at the deep distal end

*Correspondence to: Dr. Yen-Chuan Ou, Division of urology, Department of Surgery, Tungs' Taichung MetroHarbor Hospital, No. 699, Sec. 8, Taiwan Blvd., Wuqi Dist., Taichung City 43503, Taiwan, (R.O.C.)

of this inverted triangle, obscuring the surgical fields. To further visualize pelvic surgical fields, the surgical practice of the Trendelenburg position to separate the entrails from the deep pelvis would be adopted. However, this steep head-down position, ranging from 20 to 40 degrees, could significantly impact the cardiovascular condition of the patient and, even more, compromise the airway and lead to laryngeal edema. One of the major revisions of Intuitive Robotic Surgical Systems from Si to Xi is that it allows self-targeting to operator-assigned targets. In the Si system, any change of position requires undocking all settled arms and re-docking of desired ports. However, the self-targeting and wireless connection abilities of the Xi system can be optimized with the adjunct of integrated table motion (ITM; TruSystem™ 7000dV OR Table by Trumpf Medical, Saalfeld, Germany). Using Bluetooth connection, ITM enables surgeons to run their operations without undocking settled arms and change positions without interrupting ongoing procedures. This can also benefit patients, since surgical positions can be more freely adjusted according to patients' conditions. Thus, vulnerable groups such as older populations and compromised cardiovascular patients can be more securely monitored.

Materials and Methods

Studies were retrieved using the search terms "(Integrated Table Motion[MeSH Terms]) AND ((remote operations robotics) OR (remote operation robotics[MeSH Terms]))" on PubMed, Medline, Scopus, Web of Science, The Cochrane Library, and Embase, and only literature above case series would be considered in this review. Robotic-assisted operative data from October 17, 2020, to April 17, 2021, were abstracted from our records in the anesthesia department and wards. A descriptive review was utilized to summarize the contemporary literature and descriptive statistical methods were used to conclude our experiences. This is a brief editorial perspective and PRISMA guidelines would not be required. Data analyses were performed using SPSS software version 26.0 (IBM Corp., Armonk, NY, USA).

Results

Seven articles initially met our criteria for analysis. After excluding duplicates, four articles[3-6] were included in the final analysis and are listed in Table 1. One[3] of the four studies was retrieved from the supplementary page in a journal with only the abstract available.

A total of 61 male patients who underwent either radical or simple prostatectomy and 6 patients who underwent nephroureterectomy were the subjects included in the analysis. The patients' data are listed in Table 1. As obtained from medical records, the median blood pressure was 133/71 (range: 109–156/61–89) mmHg and 129/69 (range: 104–147/65–77) mmHg before and after ITM, respectively. The median heart rates were 71 (range: 65–88) bpm and 69 (rang: 56–77) bpm before and after ITM, respectively. Blood pressure and heart rate did not vary significantly during the operation. Endotracheal tubes were all removed successfully in the postoperative room by anesthesiologists. No complications above Clavien–Dindo grade 2 were noted.

Discussion

The ITM has been used since 2015, and in official recommendations, the ideal characteristics of patients indicated for ITM includes a body mass index below 45 kg/m^2, age over 18 years old, and health conditions suitable for minimally invasive surgeries. Patients allergic to materials of the table, unable to fit in the table, or unable to get low enough to facilitate docking cannot undergo surgery with the ITM. All contemporary studies of ITM analyzed in this study involved colorectal, gynecological, and urological surgeries[3-6], indicating that the most beneficial effect of ITM lies in operations requiring deep-organ dissections or involving extreme positions. In our urological surgeries, we found that the ITM helped maintain a steady blood pressure and heart rate in steep head-down patient positions, such as during radical prostatectomy and cystectomy, and ease the process of ports alterations during multi-target surgeries such as nephroureterectomy.

Radical prostatectomy and pelvic surgeries

Just like colorectal and gynecological surgeries, urological organs such as the prostate and bladder are located in deep pelvis as well. In the distal narrow end of pelvis, a total of three major organs including prostate, bladder and rectum, are seated here. Asides

Table 1. Review of literature ad our data.

	Specialties	Age	[1]BMI; [2]ASA grade	Mean console time	Blood loss	Mean [3]ITM moves	Intra-operative conversion	post-operative stay	complications / management
Lamb et al.	Genitourinary- 1. 12 male: radical prostatectomy	Average: 66.0 years old	Not mentioned	135 minutes	400 ml	Not mentioned	No	1 day	1. Hematuria/catheter washout 2. [4]NSTEMI/medical control
Morelli et al.	Colorectum- 1. Seven patients: anterior resection of the rectum with total mesothelial excision 2. Two patients: right colectomy 3. One patient: sigmoidectomy	Not mentioned	Not mentioned	237 minutes (median: 227 minutes; range: 128-450 minutes)	82 ml (median: 25 ml; range: 10-500 ml)	1. 3.3 (median: 3; range: 2-6); right colectomy: 3; anterior resection of the rectum and sigmoidectomy: 3.37 2. Mean duration in each ITM move: 99 seconds (median: 77 seconds; range: 12-380 seconds); right colectomy: 59 seconds; anterior resection of the rectum and sigmoidectomy: 108 seconds	No	12.4 days (median: 6 days; range: 5-60 days)	No
Panteleimonitis et al.	Colorectum- 1. 29 paients: anterior resection of the rectum 2. Four patients: abdominoperineal excision	Median: 59 years old ([5]IQR: 59.5-75.5 years old)	[1]BMI: 29 (range:25.6-31) k/m^2 [2]ASA: I: one patients II:27 patients III: four patients	331 minutes ([5]IQR: 249-372 minutes)	20 ml ([5]IQR: 20-45 ml)	Not mentioned	No	6.5 days ([5]IQR: 4-8 days)	1. Small bowel obstruction/ conservative supports 2. Chyle leak/diagnostic laparoscopy
Giannini et al.	Gynecology: 1. 10 patients: Total hysterectomy	Average: 58.6 years old (41-77 years old)	[1]BMI:26.3 (range:18-37) kg/m^2 [2]ASA: II: nine patients III: one patient	152 minutes (range: 120-240 minutes)	Average: 52 ml (media: 210 ml)	3.3 (range:1-6)	No	3.6 days (median: 3 days; range: 2-5 days)	No
Min Che Tung et al.	Genitourinary- 1. 61 patients; radical prostatectomy	Average: 65.90 years old (median: 64.5 years old; range: 55-74 years old)	[1]BMI: 27.12 (range:20.11- 30.23) kg/m^2 [2]ASA: II: 52 patients III: nine patients	Median: 110 minutes (range: 80-240 minutes)	Average: 129.19 ml (median: 120ml; range: 10-400 ml)	Median: 1 (range: 0-1)	No	Median: 7 days (range: 3-14 days)	1. Two patients: Ileus/ conservative support
Min Che Tung et al.	Genitourinary- 1. Six patients: Nephroureterectomy	Average: 61 years old (median: 62 years old; range: 59-72 years old)	[1]BMI:26.56 kg/m^2 [2]ASA: II:4 patients III:2 patients	Median: 280 minutes (range: 20-350 minutes)	Median: 50 ml (range: 30-100 ml)	Median: 1 (range:0-1) Undocking and re-docking: 1. Median: 1 (range:0-1)	No	Median: 15 days (range: 10-61 days)	No

[1] Body Mass index; [2]American Society of Anesthesiologists; [3]Integrated Table Motion; [4]Non-ST elevation myocardial infarction; [5]Interquartile range

from these, uterus and its adnexa will join this space if patients are the female. After incising the endopelvic fascia and exploring deep into the pelvis, the steep head-down position would be required to optimize the surgical fields. In radical prostatectomy, this position is especially important for the manipulation of membranous urethra and bladder–urethra anastomosis. Furthermore, the intrinsic sphincter is seated inside membranous urethra, which should be kept as intact as possible to prevent incontinence in men and significantly improve quality life after radical prostatectomy. At the same time, quality, watertight suturing of the bladder neck to the urethra stump is essential to shorten the urinary tract recovery.

To achieve this purpose, ITM could fully exert its pros in operations. To clearly identify the prostate–bladder neck margin and the incised prostate–urethra margin, the steep head-down position is often adopted during the surgery. However, this position will induce several physiological changes. In the cardiovascular aspect, the position will increase venous return and elevate mean arterial pressure. In the pulmonary aspect, functional residual volume will be reduced, and temporary atelectasis will be induced by cephalic compression due to elevated abdominal pressure. If physiological changes are combined with excessive intraoperative fluid, the removal of the endotracheal tube will possibly be hampered by laryngeal edema. In the neurological aspect, intra-cranial and ocular pressure will be raised. Thus, intraoperative monitoring for patients with this position will always be attended by anesthesiologists. The application of ITM in surgery helps anesthesiologists with the timely adjustments of overt physiological changes without interrupting ongoing procedures. In our medical records, blood pressure was steadily maintained during radical prostatectomy with the use of ITM, and no airway complications were observed. In our experience, ITM adjunctive to robotic-assisted radical prostatectomy is a safe and feasible method.

Radical nephroureterectomy

Unlike radical prostatectomy or cystectomy, nephroureterectomy requires patients in the right or left decubitus position. Although these are not extreme positions, this operation needs surgical fields from the abdomen to the distal end of the ureter, which is also located deep in the pelvis. At the end of this surgery, a watertight seal to the bladder cuff will need to be performed. In the da Vinci Si system, the settled ports would need to be undocked and re-docked after switching the fields. This will take a while to change the original settings and re-settle the robotic cart. With this consideration, a lot of urologists will prefer laparoscopic surgery over robotic systems. However, with the new Xi system, urologists only need to undock the two working ports, and employ the self-target function via the camera port, enabling them to switch among multiple targets without needing to move robotic carts. Meanwhile, the nephroureterectomy requires a surgical field in the abdomen packed with organs. Changing positions will sometimes allow the separation of these organs from the surgical field. In fact, in our experience, a median of one ITM use will be adopted per operation.

Future perspectives

Ever since the first large comparative study[7] conducted in the United States, better oncological outcomes and continence recovery has been demonstrated in robotic-assisted radical prostatectomy. The use of robotic systems in minimally invasive surgeries has dramatically risen worldwide. The da Vinci Xi system brings together guidance, self-diagnosis, education, and integration functions to usher in the computerized era in surgery. Among these functions, the ability to integrate with other facilities is especially exciting and extends the possibilities of future applications. To create a more optimized environment, a lot of adjuncts have been developed. ITM is one of them. Its use in robotic-assisted surgery is safe without any minor or major complications. With the dawn of 5G, vastly enhanced connectivity will soon be integrated to deliver high-volume of data speeds with ultra-low latency, which would upgrade the ability of the robotic system to the next level. Aside from ITM, we anticipate upcoming new adjuncts that will help advance the computerized age of surgery. In April 2021, we were among the few hospitals equipped with two robotic Xi systems in Taiwan, and our robotic surgery-performing cases had reached the second place nationwide in the last one year. We wholeheartedly believe that we would be able to provide optimized benefits for patients under our endeavors.

Acknowledgements

We thank for the efforts making Taichung MetroHarbor Hospital greater from all the administrative and medical staffs in the past fifty years. May our friends be blessed with the good health and wealth in this pandemic period.

Disclosure statement

This review did not receive any specific grant from funding agencies in the public,commercial, or not-for-profit sectors.

Disclosure of interest

The corresponding author, Yen Chuan Ou, is listed as one of customers promoting TruSystem™ 7000dV OR Table at website https://www.trumpfmedical.com/en/solutions/robotic-or/trusystem-7000dv/.

Data availability statement

The authors confirm that the data supporting the findings of this study is available within the article or its supplementary materials

Reference

1. Kehlet H, Holte K. Review of postoperative ileus. Am J Surg. 2001 Nov; 182(5A Suppl): 3S-10S. doi: 10.1016/s0002-9610(01)00781-4.
2. Kehlet H, Wilmore DW. Multimodal strategies to improve surgical outcome. Am J Surg. 2002 Jun; 183(6): 630-41. doi: 10.1016/s0002-9610(02)00866-8.
3. Lamb, B. W., Alghazo, O., Goad, J., Upton, E., Hiller, J., Lawrentschuk, N., & Murphy, D. The da Vinci© Xi surgical system with integrated Table Motion can reduce the need for Trendelenburg position without compromising surgical parameters. BJU International 2018 121 Supplement 1 (46)
4. Morelli L, Palmeri M, Guadagni S, Di Franco G, Moglia A, Ferrari V, Cariello C, Buccianti P, Simoncini T, Zirafa C, Melfi F, Di Candio G, Mosca F. Use of a new integrated table motion for the da Vinci Xi in colorectal surgery. Int J Colorectal Dis. 2016 Sep; 31(9): 1671-3. doi: 10.1007/s00384-016-2609-3.
5. Panteleimonitis S, Harper M, Hall S, Figueiredo N, Qureshi T, Parvaiz A. Precision in robotic rectal surgery using the da Vinci Xi system and integrated table motion, a technical note. J Robot Surg. 2018 Sep; 12(3): 433-436. doi: 10.1007/s11701-017-0752-7.
6. Giannini A, Russo E, Mannella P, Palla G, Pisaneschi S, Cecchi E, Maremmani M, Morelli L, Perutelli A, Cela V, Melfi F, Simoncini T. First series of total robotic hysterectomy (TRH) using new integrated table motion for the da Vinci Xi: feasibility, safety and efficacy. SurgEndosc. 2017 Aug; 31(8): 3405-3410. doi: 10.1007/s00464-016-5331-x.
7. Finkelstein J, Eckersberger E, Sadri H, Taneja SS, Lepor H, Djavan B. Open Versus Laparoscopic Versus Robot-Assisted Laparoscopic Prostatectomy: The European and US Experience. Rev Urol. 2010 Winter; 12(1):35-43.

達文西 Xi 系統與連動床之應用：單一中心經驗與文獻回顧

童敏哲[1] 歐宴泉[1,*] 楊哲學[1] 林益聖[1] 翁瑋駿[1,2]
黃立華[1,3] 呂謹亨[1] 許兆畬[1,3]

[1]童綜合醫療社團法人童綜合醫院 外科部泌尿科
[2]仁德醫護管理專科學校護理科
[3]中興大學生命科學院轉譯醫學所

受文日期：民國 110 年 06 月 04 日；接受刊載：民國 110 年 06 月 04 日

摘要

本篇文章的目的是回顧有關於達文西手術連動床的文獻，並同時表述此連動床與達文西 Xi 手術系統於童綜合醫院的使用經驗。在我們過去的經驗裡，此連動床在提升達文西機械手臂手術方便性方面是安全可行的，其效益在深部骨盆腔手術尤為顯益。

關鍵詞：泌尿腫瘤、泌尿手術、機械手臂手術、連動床、達文西 Xi 系統

* 通訊作者：歐宴泉醫師 童綜合醫療社團法人童綜合醫院 外科部泌尿科
43503 臺中市梧棲區臺灣大道八段 699 號

Review Article

Mini-review: Immunotherapy in Bladder Urothelial Cancer in Taiwan: Present and Future Perspective

Yen-Chuan Ou[1,2], Kuang-Hsi Chang[1,3,#], Hung-Lin Chen[1,4,*]

[1]Department of Medical Research, [2]Department of Urology, Tungs' Taichung MetroHarbor Hospital, Taichung, Taiwan
[3]General Education Center, [4]Department of Nursing, Jen-Teh Junior College of Midicine, Nursing and Management

Received: Nov. 16, 2020; Accepted: Feb. 17, 2021

Abstract

Bladder cancer is the most common malignancy in the urinary system. The major type of bladder cancer is urothelial cancer, which accounts for 90% of all bladder cancers in the United States and Europe. Recently approved immunotherapy drugs offer a promising alternative to treating locally advanced urothelial cancer. The new immunotherapy is delivered by immune checkpoint inhibitors. The molecular mechanism of this immunotherapy involves blocking the activation of the PD-1/PD-L1 signaling pathway. Programmed death-1 ligand (PD-L1) is a protein receptor expressed on the surface membrane of cancer cells. Its function is to bind with PD-1 on the surface of immune cells to activate the cell death program in immune cells. From 2016 to 2017, the U.S. Food and Drug Administration approved the applications for five immune checkpoint inhibitor drugs for second-line urothelial cancer treatment, namely, pembrolizumab, atezolizumab, nivolumab, durvalumab, and avelumab. All five drugs are also currently available in Taiwan. Many patients are interested to know the efficacy of immune checkpoint drugs in urothelial cancer. Here, we discuss results of the first- and second-line clinical trials for these checkpoint inhibitors to provide patients and clinicians the information to select the most suitable immunotherapy drug.

Key words: Immunotherapy, PD-1/ PD-L1, immune checkpoint inhibitors, bladder urothelial cancer

Introduction

Bladder cancer is the most common malignancy in the urinary system. The major type of bladder cancer is urothelial cancer, which accounts for 90% of all bladder cancers in the United States and Europe. Nonurothelial bladder cancers are more commonly found in other places of the world. Sometimes, urothelial cancer also affects the renal pelvis, ureter, and urethra. In the clinical setting, 25% of bladder cancer patients were diagnosed with muscle infiltration, cancer cell metastasis, or progressing cancer cell metastasis[1]. Systemic chemotherapy is the standard treatment for locally advanced urothelial cancer patients who cannot undergo surgery or have metastatic malignancies. Although the chemotherapy response rate is high at the beginning, the survival period is only around 15 months, and the 5-year survival rate is about 15%[2]. When systemic chemotherapy does not prevent cancer progression, second-line chemotherapy drugs will be administered, even though the effect is limited. Recently approved immunotherapy drugs offer a promising alternative to treating locally advanced urothelial cancer.

The new immunotherapy is delivered using immune checkpoint inhibitors. The molecular mechanism of this immunotherapy is based on blocking the activation of the PD-1/PD-L1 signaling pathway. Programmed death-1 ligand (PD-L1) is a protein expressed on the surface membrane of

#co-first author
*Correspondence to: Hung-Lin Chen, Department of Medical Research, Tungs' Taichung MetroHarbor Hospital, No. 699, Sec. 8, Taiwan Blvd., Wuqi Dist., Taichung City 43503, Taiwan, (R.O.C.)

cancer cells. Its function is to bind with PD-1 on the surface of immune cells to activate the cell death program in immune cells. This in turn enables cancer cells to avoid death by inducing cell death in immune cells instead[3,4]. In other words, cancer cells possess a special molecular adaption that induces apoptosis in natural killer cells. As a result, the immune system loses the ability to identify and attack cancer cells. The novel immune checkpoint inhibitors are antibody drugs which can bind to PD-1 or PD-L1. This binding interrupts PD-1 and PD-L1 interaction, inhibiting the ability of cancer cells to suppress the activation of the immune system. Consequently, it helps recover the number of immune cells that can identify and shrink tumors. Currently, checkpoint inhibitors have been shown to improve the survival rate in non-small cell lung cancer, malignant melanoma, and advanced renal cell carcinoma[5]. Because of their encouraging findings in cancer therapy, Dr. James P. Allison and Dr. Tasuku Honjo received the Nobel Prize in Medicine for their discovery of the biological mechanism of the PD-1/PD-L1 checkpoint pathway[6,7,8].

From 2016 to 2017, the U.S. Food and Drug Administration (FDA) approved the applications for five immune checkpoint inhibitor drugs for second-line urothelial cancer treatment, which are pembrolizumab, atezolizumab, nivolumab, durvalumab, and avelumab. These drugs are also currently available in Taiwan. Patients desire to know the efficacy of immune checkpoint drugs in urothelial cancer[9]. We discuss the results of the first- and second-line clinical trials for these checkpoint inhibitors here and provide information to enable physicians and patients make an informed decision with regards the use of immunotherapy.

Immunotherapy as first-line treatment

Due to age or complications such as impaired renal function, neuropathy, or heart failure, up to 50% of patients with advanced urothelial cancer are not suitable for cisplatin chemotherapy. Immunotherapy thus provides a feasible second option for treatment. Although immunotherapy as first-line treatment is currently under evaluation, the initial results of clinical trials on immunotherapy drugs support the viewpoint that immunotherapy can be used as first-line drug treatment in urothelial cancer.[10,11] However, more clinical trials and longer follow-up periods are required to establish this. Pembrolizumab (PD-1 antibody) and atezolizumab (PD-L1 antibody) are currently being evaluated in clinical trials as first-line treatment.

A phase II study of pembrolizumab recruited 370 patients with advanced urothelial cancer who were not suitable for cisplatin therapy. Half of these patients had renal impairment, and the average age was 74 years old. The treatment duration was up to two years. Around the 9.5-month of follow-up, the objective response rate was reported at about 24%, including 5% with complete response and 19% with partial response (Table 1)[10]. Among those patients with positive treatment response, those with a high PD-L1 expression showed higher responses. However, patients with low PD-L1 expression still exhibited some response to the treatment. Therefore, PD-L1 expression could be considered a sufficient index instead of a necessary index when patients select immunotherapeutic treatment.

In a phase II multicenter single-arm clinical trial, atezolizumab was administered to 119 patients with urothelial cancer who suffered from advanced or metastatic bladder cancer and were not suitable for cisplatin chemotherapy. During approximately 17 months of follow-up, 27 patients (23%) showed objective response rates, including 11 patients with complete responses (Table 1). The median overall survival duration for the entire research was 16 months[11]. In April 2017, atezolizumab received conditional approval from the U.S. FDA as the initial treatment for patients who are not suitable for platinum-based chemotherapy.

Table 1. Immunotherapy as the first-line treatment of bladder urothelial cancer

	Antibody	n	objective response rate (n)		
			overall	complete response	partial response
Pembrolizumab[10]	PD-1	370	24% (89)	5% (17)	19% (72)
Atezolizumab[11]	PD-L1	119	23% (27)	9% (11)	14% (16)

Immunotherapy as second-line treatment

The five immune checkpoint inhibitors were approved by the U.S. FDA for the second-line treatment of urothelial cancer patients who had received platinum-based treatment.

Clinical trial results showed that pembrolizumab prolonged the overall survival rate of patients with metastatic urothelial cancer, which worsened after first-line platinum-based chemotherapy. In a phase III clinical trial, 542 patients who relapsed or worsened after platinum-based therapy were randomly classified into a pembrolizumab group (n = 270) or a chemotherapy group (n = 272) (Table 2). Compared with the chemotherapy group, the overall survival in the pembrolizumab group significantly increased about 3 months. In addition, the objective response rate and adverse reactions in the pembrolizumab group were significantly better than those in the chemotherapy group[12].

Atezolizumab is a PD-L1 inhibitor. Although the initial approval of atezolizumab was based on the results of phase I and phase II studies in which patients had been treated with platinum-based drugs, the most extensive data for atezolizumab were obtained from a phase III clinical trial. The study enrolled 931 metastatic urothelial cancer patients who had received platinum-based chemotherapy (Table 2). All subjects were randomly assigned to the atezolizumab group (n = 467) or chemotherapy group (n = 464)[13]. Compared with the chemotherapy group, the atezolizumab group had a higher objective response rate and a lower incidence of toxicity. The role of PD-L1 expression in this atezolizumab study was also evaluated. Patients with a higher PD-L1 expression also achieved a better response to atezolizumab (overall response rate: 23% atezolizumab vs 13.4% chemotherapy)[13].

Nivolumab is a PD-1 inhibitor and was approved by the FDA in February 2017. In the phase I and phase II studies, nivolumab achieved a significant response rate in patients with metastatic urothelial cancer that progressed despite receiving first-line treatment. In a larger group of two published phase II studies, 270 patients received nivolumab treatment. The overall objective response rate obtained was 19.6% (Table 2). The PD-L1 expression level did not affect the response rate, but it affected the overall survival duration. The median overall survival duration in patients with PD-L1 expression < 1 and ³ 1% were 6.0 and 11.3 months, respectively. Nivolumab prolonged survival to around 5 months[14].

Avelumab is a PD-L1 inhibitor that was approved for the treatment of advanced urothelial cancer with response failure to platinum-based chemotherapy. A study evaluated 161 patients who received avelumab treatment after platinum-based therapy. According to a comprehensive analysis, the objective response rate in the entire study was 17% (Table 2). Six percent of responsive patients showed a complete response, whereas 11% had a partial response. In addition, the study also showed that patients with PD-L1 expression had a higher response rate (overall response rate: 24% vs 14%)[15].

Durvalumab is a PD-L1 inhibitor. In a phase I/II research, 191 patients received durvalumab treatment. Except for 1 patient, all patients received first-line chemotherapy, 95% of whom received platinum-based chemotherapy. Thirty-four patients (17.8%) showed objective responses, including 7 cases who achieved a complete response and 27 cases who achieved a partial response (Table 2). Cases with high PD-L1 expression showed a higher response rate to durvalumab. The 1-year overall survival rate in the study was 55%[16].

Table 2. Immunotherapy as the second-line treatment of bladder urothelial cancer

	Antibody	n	objective response rate (n)		
			overall	complete response	partial response
Pembrolizumab[12]	PD-1	270	21.1 % (57)	-	-
Atezolizumab[13]	PD-L1	467	13.4% (62)	3% (16)	10% (46)
Nivolumab[14]	PD-1	265	19.6% (52)	2% (6)	17% (46)
Avelumab[15]	PD-L1	161	17% (27)	6% (9)	11% (18)
Durvalumab[16]	PD-L1	191	17.8% (34)	3.7% (7)	14.1% (27)

Perspectives

Although PD-1/PD-L1 immune checkpoint inhibitors are better than traditional chemotherapy in terms of survival duration and adverse reactions, the response rates of immune checkpoint inhibitor drugs are only around 20%-30%. Increasing the response rate will be crucial in order for immunotherapy to be effective in bladder urothelial cancer. The abovementioned trials indicate that PD-L1 expression is a potential index factor for immune checkpoint inhibitor therapy. A higher response rate was observed in patients with high PD-L1 expression in urothelial cancer cells. Therefore, PD-L1 expression can be used as an indicator of the efficacy of immune checkpoint inhibitor drugs and to select for candidate patients for immunotherapy.

Furthermore, when immunotherapy drugs inhibit PD-1–induced immune cell death, quickly amplifying the immune cells to target cancer cells is the next critical step. Thus, patients need to have a strong immune system ready for activation. In this scenario, the immune status of patients could be used as an index for evaluating the efficacy of immune checkpoint inhibitors. Moreover, simultaneously enhancing the immune system during immunotherapy should be implemented to increase the response rate. One study showed that the combination of IL-2 and PD-L1 blockade had a synergic effect on human chronic infections and cancer[17].

In addition to monotherapy, PD-1/PD-L1 inhibitors can be used in combination treatments to improve the outcomes of other cancer medications. In a phase III trial, overall survival was significantly prolonged with the addition of maintenance avelumab to best supportive care. Overall survival at 1 year was 71.3% in the avelumab group and 58.4% in the control group, which received supported care alone[18].

Immunotherapy also includes immune cell therapy. Immune cell therapy enhances the immune system to kill cancer by injecting *in vitro* expended, genetically engineered T cells or patient's NK cells and dendritic cells[19]. However, the treatment is expensive, and the treatment efficacy varies because immune cell therapy is highly customized. Since cell immunotherapy cases are currently limited in Taiwan, we did not explore them in this article.

Since immunotherapy is not fully supported by the national health insurance, the cost of immunotherapy prevents its more widespread use. For patients who are highly suitable for immunotherapy, the National Health Insurance Bureau has specifically allocated NTD 800 million for 800 eligible patients (cancer patients with eight types of cancer, including bladder cancer) since 2018 to alleviate the financial burden of the treatment[20].

Conclusions

Immune checkpoint inhibitor drugs have demonstrated considerable effects with regards improving treatment response and survival rates compared with systemic chemotherapy. As this review reveals, patients with high PD-L1 expression may benefit the most from these recently approved treatments. Although the response rate of immunotherapy is only 20%-30% in bladder urothelial cancer, some potential factors and applications can be implemented to potentially improve the response rate.

Reference

1. Kamat, Ashish M et al. "Bladder cancer." Lancet (London, England) vol. 388,10061 (2016): 2796-2810. doi:10.1016/S0140-6736(16)30512-8
2. von der Maase, H et al. "Gemcitabine and cisplatin versus methotrexate, vinblastine, doxorubicin, and cisplatin in advanced or metastatic bladder cancer: results of a large, randomized, multinational, multicenter, phase III study." Journal of clinical oncology : official journal of the American Society of Clinical Oncology vol. 18,17 (2000): 3068-77. doi:10.1200/JCO.2000.18.17.3068
3. Hodi, F Stephen et al. "Biologic activity of cytotoxic T lymphocyte-associated antigen 4 antibody blockade in previously vaccinated metastatic melanoma and ovarian carcinoma patients." Proceedings of the National Academy of Sciences of the United States of America vol. 100,8 (2003): 4712-7. doi:10.1073/pnas.0830997100
4. Iwai, Yoshiko et al. "PD-1 blockade inhibits hematogenous spread of poorly immunogenic tumor cells by enhanced recruitment of effector T cells." International immunology vol. 17,2 (2005): 133-44. doi:10.1093/intimm/dxh194
5. Hargadon, Kristian M et al. "Immune checkpoint blockade therapy for cancer: An overview of FDA-approved immune checkpoint inhibitors." International immunopharmacology vol. 62 (2018): 29-39. doi:10.1016/j.intimp.2018.06.001
6. Ishida, Y et al. "Induced expression of PD-1, a novel member of the immunoglobulin gene superfamily, upon programmed cell death." The EMBO journal vol. 11,11 (1992): 3887-95.
7. Leach, D R et al. "Enhancement of antitumor immunity by CTLA-4 blockade." Science (New York, N.Y.) vol. 271,5256 (1996): 1734-6. doi:10.1126/science.271.5256.1734

8. Press release: The Nobel Prize in Physiology or Medicine 2018. NobelPrize.org. Nobel Media AB 2020. Thu. 12 Nov 2020. https://www.nobelprize.org/prizes/medicine/ 2018/press-release/
9. Vasekar, Monali et al. "Immunotherapy in Bladder Cancer." Current molecular pharmacology vol. 9,3 (2016): 242-251. doi:10.2174/1874467208666150716120945
10. Balar, Arjun V et al. "First-line pembrolizumab in cisplatin-ineligible patients with locally advanced and unresectable or metastatic urothelial cancer (KEYNOTE-052): a multicentre, single-arm, phase 2 study." The Lancet. Oncology vol. 18,11 (2017): 1483-1492. doi:10.1016/S1470-2045(17)30616-2
11. Balar, Arjun V et al. "Atezolizumab as first-line treatment in cisplatin-ineligible patients with locally advanced and metastatic urothelial carcinoma: a single-arm, multicentre, phase 2 trial." Lancet (London, England) vol. 389,10064 (2017): 67-76. doi:10.1016/S0140-6736(16)32455-2
12. Bellmunt, Joaquim et al. "Pembrolizumab as Second-Line Therapy for Advanced Urothelial Carcinoma." The New England journal of medicine vol. 376,11 (2017): 1015-1026. doi:10.1056/NEJMoa1613683
13. Powles, Thomas et al. "Atezolizumab versus chemotherapy in patients with platinum-treated locally advanced or metastatic urothelial carcinoma (IMvigor211): a multicentre, open-label, phase 3 randomised controlled trial." Lancet (London, England) vol. 391,10122 (2018): 748-757. doi:10.1016/S0140-6736(17)33297-X
14. Sharma, Padmanee et al. "Nivolumab in metastatic urothelial carcinoma after platinum therapy (CheckMate 275): a multicentre, single-arm, phase 2 trial." The Lancet. Oncology vol. 18,3 (2017): 312-322. doi:10.1016/S1470-2045(17)30065-7
15. Patel, Manish R et al. "Avelumab in metastatic urothelial carcinoma after platinum failure (JAVELIN Solid Tumor): pooled results from two expansion cohorts of an open-label, phase 1 trial." The Lancet. Oncology vol. 19,1 (2018): 51-64. doi:10.1016/S1470-2045(17)30900-2
16. Powles, Thomas et al. "Efficacy and Safety of Durvalumab in Locally Advanced or Metastatic Urothelial Carcinoma: Updated Results From a Phase 1/2 Open-label Study." JAMA oncology vol. 3,9 (2017): e172411. doi:10.1001/jamaoncol.2017.2411
17. West, Erin E et al. "PD-L1 blockade synergizes with IL-2 therapy in reinvigorating exhausted T cells." The Journal of clinical investigation vol. 123,6 (2013): 2604-15. doi:10.1172/JCI67008
18. Powles, Thomas et al. "Avelumab Maintenance Therapy for Advanced or Metastatic Urothelial Carcinoma." N Engl J Med. Vol. 383,13 (2020):1218-1230. doi:10.1056/NEJMoa2002788
19. Mohanty, Rimjhim et al. "CAR T cell therapy: A new era for cancer treatment (Review)." Oncology reports vol. 42,6 (2019): 2183-2195. doi:10.3892/or.2019.7335
20. 癌症免疫檢查點抑制劑藥品給付規定,國健署 https://www.nhi.gov.tw/Content_List.aspx?n=7157A9A3E2A3B110&topn=3FC7D09599D25979

免疫治療在台灣泌尿上皮癌的現況與願景

歐宴泉[1,2] 張光喜[1,3,#] 陳鴻霖[1,4,*]

童綜合醫療社團法人童綜合醫院 [1]醫學研究部 [2]泌尿科
仁德醫護管理專科學校 [3]通識中心 [4]護理科

受文日期：民國 109 年 11 月 16 日；接受刊載：民國 110 年 02 月 17 日

摘要

膀胱癌是泌尿系統最常見的惡性腫瘤。根據美國及歐洲統計報告，有九成的膀胱癌屬於泌尿上皮細胞癌。近年來，免疫檢查點抑制劑成為局部晚期泌尿上皮癌病人熱門討論的新穎療法。免疫檢查點抑制劑的生物機制在於阻絕 PD-1/PD-L1 的訊息傳遞。PD-L1 是表現在癌細胞表面的一種蛋白，它的功能是與免疫細胞表面上的 PD-1 受體結合，啟動該免疫細胞的自我死亡程序，最終癌細胞便可遠離免疫系統的攻擊而存活在體內。藉由免疫檢查點抑制劑阻斷 PD-1/PD-L1 的訊息傳遞，自體免疫系統便可辨認及殺死癌細胞。在 2016 至 2017 年，美國食品藥物管理局核准 5 種免疫檢查點抑制劑作為泌尿上皮癌的二線治療，台灣食品藥物管理局近期也給予核可（Pembrolizumab, Atezolizumab, Nivolumab, Durvalumab, and Avelumab）。此篇文章在於討論這些新穎免疫檢查點抑制劑在泌尿上皮癌作為一線與二線的臨床試驗結果，提供醫師與病患在進行治療計畫時可以做為參考的資料。

關鍵詞：免疫治療、免疫檢查點抑制劑、膀胱泌尿上皮癌

共同第一作者
* 通訊作者：陳鴻霖博士 童綜合醫療社團法人童綜合醫院 醫學研究部
43503 臺中市梧棲區臺灣大道八段 699 號

Review Article

Bioimpedance Spectroscopy and Fluid Management in Dialysis Patients: From Laboratory to Clinic

Tsai-Kun Wu, Hong-Bin Chen, Chang-Hsu Chen, Tien-Yu Tseng, Paik-Seong Lim*

Renal Division, Internal Medicine, Tungs' Metroharbor Hospital, Taichung, Taiwan

Received: Dec. 30, 2020; Accepted: Mar. 08, 2021

Abstract

Many patients on dialysis are older adults with numerous comorbid conditions and poor nutritional health. Improving fluid and nutritional status are major treatment goals for patients on dialysis, who should regularly receive both fluid as well as nutritional assessment by dialysis staff. Anthropometric and body composition assessments provide important nutritional status information. However, most assessment methods have a limited application in patients on dialysis because dialysis alters their hydration status. On the other hand, body composition estimates from single- and multifrequency bioelectrical impedance in healthy individuals are well established. However, most bioelectrical impedance methods employ some form of predictive modeling to obtain estimated outcomes have some inherent problems in patients on dialysis.

A body composition monitor based on bioimpedance spectroscopy (BIS) with modified fluid and physiological models has been developed in recent years to detect excessive fluid in patients on dialysis. Due to its non-invasive and easy-to-perform characteristics, it has been increasingly applied as a bedside tool to evaluate patients' fluid status in many dialysis facilities worldwide. Furthermore, BIS is also useful in assessing nutritional status and adequacy of patients on dialysis in the clinical setting. We present a rigorous review of the recent publications that address these issues.

Key words: body bioimpedance, nutrition, fluid management, dialysis

Introduction

Fluid overload (FO) and malnutrition are challenging problems in patients with advanced chronic kidney disease (CKD) or end-stage renal disease. FO is associated with morbid conditions such as lower-extremity edema, anasarca, ascites, pulmonary vascular congestion or edema, hypertension, left ventricular hypertrophy, and worsening heart failure[1]. FO is an independent predictor of all-cause or cardiovascular mortality in patients on dialysis[2]. Strict volume control strategies might reduce blood pressure and left ventricular hypertrophy progression[3] and improve the outcomes of patients on dialysis[4]. Some recent studies demonstrated that FO is an independent risk factor of the combined outcome of all-cause or cardiovascular morbidity in non-dialysis patients with advanced CKD[3,4]. On the other hand, fluid depletion may result in intradialytic hypotension, myocardial ischemia leading to potentially significant loss of white matter in the brain and of residual renal function[5]. Older patients are now the rule rather than the exception in hemodialysis (HD). In most registries, they are the fastest-growing group of incident patients on dialysis[6]. Much grimmer predicted life expectancies for older patients could be due to higher comorbidity rates for cardiovascular diseases, FO, malnutrition, inflammation, depression, and cognitive disturbances[7]. Since fluid status is a key factor influencing the quality of life and life

*Correspondence to: Paik-Seong Lim MD, PhD., Renal Division, internal medicine, Tungs' Metroharbor Hospital, Taichung, Taiwan, No. 699, Sec. 8, Taiwan Blvd., Wuqi Dist., Taichung City 43503, Taiwan, (R.O.C.)

expectancy in the dialysis population, optimal fluid volume management is both a major treatment goal and a challenging clinical condition for dialysis staff. Clinical assessment of hydration status is not only time consuming but also requires specific clinical skills and may be relatively imprecise. Various strategies have been proposed to attain optimal fluid status in patients on dialysis, but each has its own limitation[8]. Bioimpedance spectroscopy (BIS) may serve as an easily applicable clinical tool in the assessment of dry weight in patients on dialysis. Over the past decade, a number of observational and intervention trials have significantly elucidated on its promising clinical utility.

Assessment of body composition in patients on dialysis

Protein-energy wasting syndrome is quite common in patients on dialysis and severely affects their short-term survival. Along this line, the assessment of body composition in patients on dialysis is clinically important. Current techniques used to assess body composition in patients on dialysis include subjective global assessment, anthropometric measurements, dual energy X-ray absorptiometry (DEXA), single-frequency bioimpedance analysis (BIA), and multifrequency BIS. Anthropometric assessments provide important nutritional status information about patients on dialysis. However, most anthropometric and body composition methods have a limited application in patients on dialysis because dialysis itself alters the hydration status of patients and also carries the assumptions used by these methods. DEXA is the most widely used and most thoroughly studied measurement technology for patients on dialysis[9]. Despite its detailed and accurate assessment, this method is expensive, requires technical expertise, and cannot be repeated frequently due to some X-ray exposure during the examination. Additionally, few dialysis clinics have direct access to DEXA systems. On the other hand, body composition estimates from single- and multifrequency bioelectrical impedance in healthy individuals are well established. However, most bioelectrical impedance methods employing some form of predictive modeling to obtain estimated outcomes have some inherent problems in patients on dialysis. The measurement of body compartments with different BIS devices do have a high inter-method variability that is probably due to the equations used. Rigorous validation is crucial for the useful application of BIS.

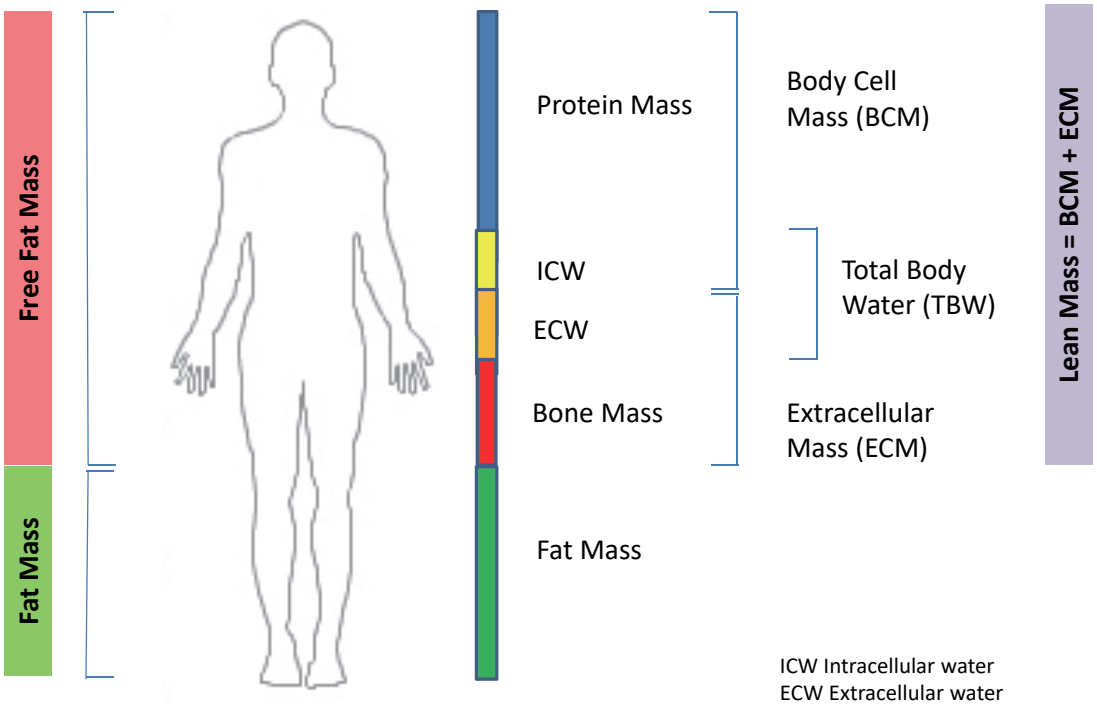

Fig. 1 Nutrient composition of the human body.

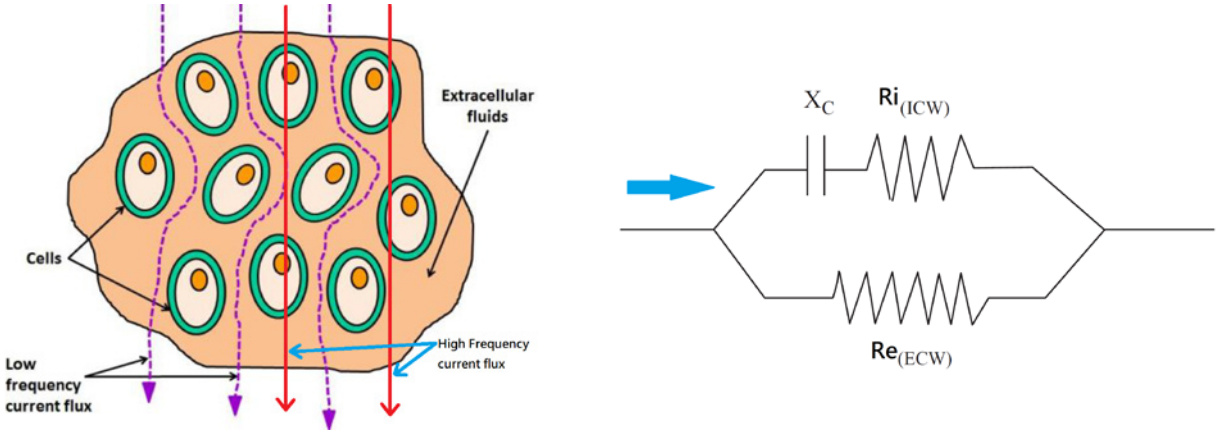

Fig. 2 Principles of bioimpedance spectroscopy. (a) Flow of electrical current through biological tissue: Low-frequency currents (f→0) flow around the cells through the extracellular fluid, whereas high-frequency currents (f→∞) penetrate the cell membranes and flow through the intracellular and extracellular fluids. (b) Diagram of an electrical circuit used to interpret measured data in BIS. Two parallel electrical conductors; Re (ECW); Ri (ICW); isolated by a cell membrane; tissue may act as a conductor or isolator. The electrical current goes through the line with the lowest resistance (Re).

Mechanism of BIS

BIS is a noninvasive, low-cost technology that can accurately measure fluid status and tissue composition in the clinical setting. The basic mechanism underlying bioimpedance may be rather complex for a practicing physician and will be briefly discussed here. The body is commonly modeled as a series of tissue and fluid compartments as shown in Figure 1. Body composition analysis is basically the clinical assessment of tissue and fluid distribution. Bioimpedance administers a weak alternating electrical current at one or more radiofrequencies through leads attached to surface electrodes to characterize the conductive and nonconductive tissues and fluid components of the body. When excited by this current, biologic tissues show a complex electrical bioimpedance that varies with tissue composition. The applied alternating current is easily conducted by water- and electrolyte-rich tissues such as blood and muscle and is poorly conducted by fat, bone, and air-filled spaces (Figure 2). The frequency-dependent opposition produced by the conducting tissue components to the flow of electric current is called impedance (Z). Geometrically, impedance can be expressed as the vector comprising two frequency-dependent parameters—resistance (R) and reactance (Xc). Resistance is the opposition to the flow of an alternating current through intracellular and extracellular ionic solutions. Reactance represents the delay in the conduction or passage of the administered current through

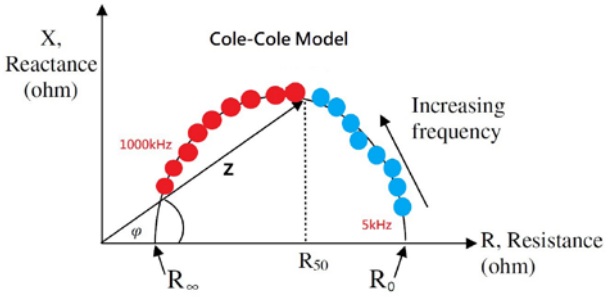

Fig. 3 Variations in impedance with frequency on bioimpedance spectroscopy. Resistances extrapolated at zero (R_0) and infinite (R_∞) frequencies. Semicircular distribution of the resulting reactance and resistance data using a non-linear, least-squares fitting curve according to the Cole–Cole model. φ, phase angle; Z, impedance; R_{50},.

cell membranes, tissue interfaces, and nonionic substances. Capacitance or capacitive reactance is a function of reactance that arises when cell membranes that store energy discharge as the current passes through them. Hence, the magnitude of reactance depends on the number of capacitors through which the current must pass. These two components are expressed in ohms (Ω) and may be graphically represented by vectors (Figure 3).

Body Composition Monitor, a novel BIS

The Body Composition Monitor (BCM; Fresenius Medical Care, Bad Homburg, Germany) is a novel BIS device that has been designed and used to assess fluid status in CKD patients[10-15]. BCM measures

resistance and reactance at 50 frequencies from 5 kHz and 1 MHz. The impedance obtained then undergoes complex modeling based on the classic Cole model[16] and Hanai mixture theory[16-18] to estimate fluid volumes and, in turn, lean tissue, adipose tissue, normohydration weight, and overhydration. The accuracy of body composition measurements has been validated against available gold standard reference methods[18,19]. However, the underlying assumptions introduced into equations may be appropriate only across a certain range of body compositions. These constants may introduce error to the volume estimates when applied in individuals with excessive adiposity and those with fluid retention. To account for this error, Moissl et al.[18] developed a model adjusted for body mass index that independently predicted extracellular and intracellular water and substantially improved BIS estimates, particularly for intracellular water. In the Moissl equations, intracellular water resistivity is not assumed to be static, as in the previous Hanai-based mixture equations, but rather changes with increasing fat. This approach greatly improved volume estimates in subjects at both extremes of the body mass index range, but substantial variability was still observed at the individual level[19]. Chamney et al.[20] further developed the method by creating a so-called three-compartment (3C) body model based on data from healthy adults. This model differentiates between normohydrated lean tissue mass, adipose tissue mass, and a virtual "overhydration" compartment. Differences between the 3C model and the two-compartment (2C) one expressed by single-frequency BIA can be explained by different arrangements of body composition compartments, which are based on differences in the hydration status of the compartments (Figure 4). The 2C model cannot distinguish excess volume due to fluid retention, hence, predictions for fat-free mass are influenced by the presence of fluid status[21]. The BCM, based on the 3C model, distinguishes body fat and lean mass from pathologic fluid retention (overhydration)[20]. The measurement of BCM is simple, fast, and highly reproducible. In addition, the noninvasive nature of bioimpedance makes it particularly well suited for measuring longitudinal changes in hydration and nutrition statuses. These important issues in long-term patients on dialysis are related to clinical outcomes and can be assessed objectively by BCM. Recently, several studies sought to identify the direct effects of BCM on important clinical outcomes[2,13,22-33]. In this review, we aimed to update the clinician on the current status of the application and outcomes of BCM-BIS in dialysis units.

FO and hemodynamic status

Achieving optimal fluid balance is a major challenge in routine dialysis practice, given the difficulties in obtaining so-called dry weight or normal hydrated weight estimates. Clinically, dry weight is defined as the lowest weight a patient can tolerate without developing intra- or inter-dialytic symptoms. The dry weight method is limited by the fact that some liters of fluid may accumulate in the body before edema

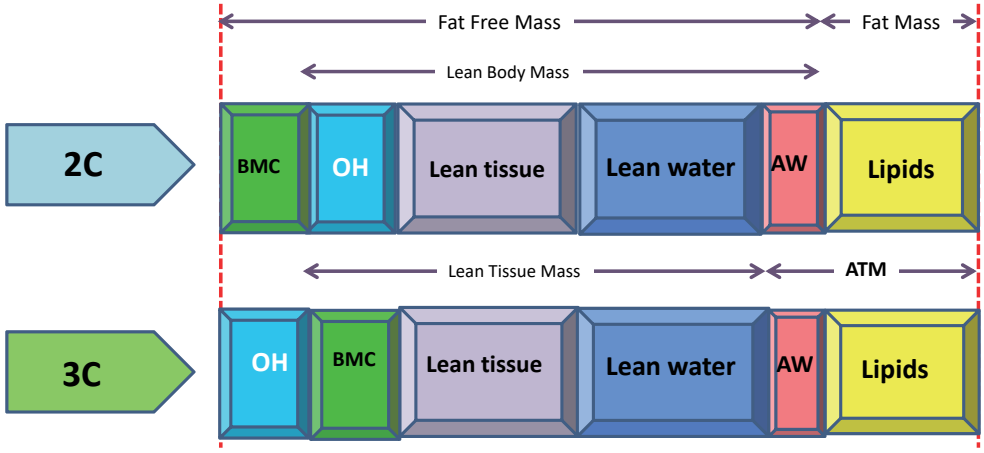

Fig. 4 Schematic diagram of human body compartments: 2C vs 3C models.
2C, two-compartment model; 3C, three- compartment model; OH, overhydration; BMC, bone mineral content; AW, adipose water; ATM, adipose tissue mass.

becomes clinically evident. It also does not account for changes in lean body mass, fat mass, or nutritional status over time. Using an overestimated dry weight may lead to hypertension, left ventricular hypertrophy, and congestive heart failure. On the other hand, an underestimated dry weight may lead to intradialytic hypotension, fatigue, impaired quality of life, and occlusion of arteriovenous shunts.

In recent years, several studies have found that FO assessed by BIS appears to be high in patients on dialysis, ranging around 27.4%–46.4% using different criteria. Accumulating evidence has highlighted blood pressure and volume status as key predictors of outcomes among patients receiving maintenance dialysis[26,34,35]. Efforts to develop standard best practices in managing blood pressure and volume in dialysis have been hampered by an absence of widely available, accurate, and objective measures of extracellular volume status. To this date, managing blood pressure and volume in dialysis involves weighing multiple clinical factors and risk considerations, as well as considering patient lifestyle and preferences, all within a narrow therapeutic window for avoiding acute or chronic volume-related complications, which are tedious and challenging. Hence, controlling the notorious impact of FO in this population is considered an unmet clinical need, and effective clinical strategies specifically aimed at optimizing the control of FO have been sought to improve the outcomes in these patients. Advances in bioimpedance technology have enabled a more accurate scientific exploration of dry weight to achieve optimal volume status in patients on HD[36].

Complications of FO

Establishing the relationship between FO and hypertension by BCM has provided a better strategy for hypertension control in some centers[37]. An early observational study by Wizemann et al.[2] showed that patients with hyperhydration had a significantly higher mortality rate than patients with normohydration. The cutoff threshold for overhydration was set to 15% relative to the extracellular water. The hydration state indicated by fluid parameters in BCM is an important independent predictor of mortality in patients on chronic HD. These findings were confirmed in larger groups of patients, as well as in meta-analyses[23,25,26,31]. In a report from the MONDO consortium including 8,883 patients, the authors found a significant correlation between mortality and incremental FO levels[31], whereas Zoccali et al.[26] found that this relationship was also stronger with prolonged periods of FO. Notably, they found that even mild levels of pre-dialytic FO (1.1–2.5 L) were associated with increased mortality. Two studies found that pre-dialytic fluid depletion was associated with increased mortality. Moreover, these studies[26,31] reported that pre-dialytic systolic blood pressure below 110 mm Hg was associated with increased mortality when combined with either pre-dialytic FO or fluid depletion. Surprisingly, post-dialytic fluid depletion appeared to be protective[31,38] in these patients. The relation between FO and mortality is also consistently found in in peritoneal dialysis and stage 4–5 CKD patients[15,28,39]. More recently, in patients with stage 5 CKD not undergoing dialysis, Han et al.[40] found that relative overhydration/extracellular water, systolic blood pressure, and serum phosphorus levels were independently associated with left ventricular mass index and that overhydration/extracellular water was independently associated with left ventricular hypertrophy. More recently, some studies demonstrated that the relationship between FO and mortality was independent from traditional cardiovascular risk factors. Hung et al.[11] noted an inverse relationship between FO and serum albumin and a positive relationship between FO and IL-6 levels. In addition, Decker et al.[41] observed the interrelation between clusters with FO (overhydration > +1.1 L pre-dialysis), inflammation (CRP levels > 6 mg/L), and malnutrition (lean tissue index below the 10th percentile of a control population). In the majority of their study subjects, FO was observed in combination with malnutrition and/or inflammation, and not as a single risk factor[41]. All three risk factors were found in 17.6% of patients, which is also the group with the highest risk of death. (hazard ratio [HR], 5.89; 95% confidence interval [CI]: 4.28–8.10). The concurrent presence of FO and inflammation (15%) was associated with a higher risk of death, which was not significantly increased in those patients who were only malnourished (6.5%). In another similar study, patients with the highest FO level and the lowest interdialytic weight gain level had the highest mortality risk[35]. The spontaneous decline in interdialytic weight gain may possibly reflect malnutrition[42]. In patients on peritoneal

dialysis, those who had FO on BCM had higher cardiac troponin-T levels and had a higher tendency to expire from cardiac-related deaths. A reduction in overhydration was correlated with reduced cardiac troponin-T levels[43].

Considering the complex interaction of risk factors in patients on dialysis, outcomes are best interpreted as a combination of the said factors. Moreover, CKD and heart disease frequently coexist, and the relationship between these two diseases is rather complex and difficult to define. Nevertheless, FO remained predictive of mortality even after adjustment for multiple risk factors[25,31].

BIS-guided treatment and outcomes

BCM can also provide objective normohydration targets, as demonstrated in some recent interventional studies[3,44-46]. Petr et al.[44] demonstrated that guiding patients toward normohydration targets by BCM led to better hypertension management in overhydrated patients, less intradialytic adverse events, and improved cardiac function. The potential benefit of BIS-guided treatment was subsequently assessed in several randomized controlled trials[3,45-53] (Table 1). The assessment of FO with BCM during a 1-year period showed better management of fluid status, resulting in regression of left ventricular mass index,

Table 1. Summary of Bioimpedance Guided Fluid Management Trials

Authors	Trial Design	N, HD/PD	Age (mean, SD)	Technology Use	Outcomes	Main Findings
Luo et al 2011[52]	RCT, open label; 3 months; 1 center	160, PD	60 ± 15	BCM	Fluid status	Less overhydration; BP reduction in BCM group
Onofriescu et al 2014[46]	RCT, open label;12 months; 1 center	131,HD	52 ± 13	BCM	Mortality	Lower all-cause mortality in BCM group
Hur et al 2013[3]	RCT, open label;12 months; 2 centers	156, HD	52 ± 12	BCM	LVM index	LVM reduced in BCM group; no significant change in BP
Ponce et al 2014[53]	RCT, cluster randomized; 12 monthsn open-access and a blinded group; 23 centers	189, HD	Openlabel: 65.8 ± 14.6 years; blind: 66.7 ± 15.1 years	BCM	Fluid status	Reduction of OH in both group(BCM less over hydrated);Hospitalization and survival rate was not significantly different
Tian 2015[55]	RCT, open label; 12 months; 1 center	240,PD	50 ± 15	MF-BIA; InBody 720	All-cause mortality	No significant effect on patient and technique survival
ABISAD-III Huan-Sheng 2016[45]	RCT, open albel; 12 months; 6 centers	298, HD	621 ± 2	BCM	All-cause hopsitalizations	All-cause hospitalization rate was not different. Incidence of acute fluid overload or CV-related events was lower
UK-Shanghai Bioimpedance Study Tan et al 2016[47]	Prospective open label randomized blinded to endpoint (PROBE);12 months; 4 centers	308, PD	56 ± 14	Longitudinal vector plot; BI 101 ASE (Akern, Italy)	Fluid status	Nonanuric subjects demonstrated stable fluid volumes irrespective of randomization; Hydration worsened in control anuric patients in Shanghai
COMPASS Trial Oh et al 2018[48]	RCT open; 12 months; 5 centers	PD, 137	52 ± 13	BCM	RRF; echocardiographic parameters or arterial stiffness	No additional benefit in volume control, RRF preservation, or CV parameters.
Yoon et al 2019[54]	RCT, open; label, 12 months; 8 centers	Non-anuric PD, 201	Control 53.9 ± 11.2 Study 55.3 ± 12.3	BCM	RRF, volume status, echocardiographic variables, CV events	Did not show an additional benefit to achieve euvolemia, and did not affect the decline in RRF No difference in echocardiographic variables or in CV event rates

BCM, body composition monitor; BP, blood pressure; CV, cardiovascular; HD, hemodialysis, LVM, left ventricular mass OH, overhydration; PD, peritoneal dialysis; RCT, randomized control trial; RRF residual renal function

decreased blood pressure, and improvement in arterial stiffness[47]. Onofriescu et al.[46] conducted a 2.5-year randomized controlled study comparing bioimpedance and clinical judgment alone to guide dry weight adjustment in patients on HD and reported improvements in both all-cause mortality and surrogate endpoints after strict volume control using bioimpedance. We had recently shown the frequent adjustment of post-dialysis target weight by BCM using an explicit algorithm for dry weight adjustment in patients with post-dialytic overhydration levels less than –2.0 or > 1.0 L[45]. During a 1-year period, we observed decreased acute FO or cardiovascular-related events, hypertension, and intra-dialysis hypotension with this strategy in non-diabetic patients (Figures 5a and 5b). However, in this randomized controlled trial, the primary outcome, hospitalization, was not met[45]. Similarly, Hur et al.[3] found that hospitalization rates did no differ significantly in a subgroup of BIA-guided treatment in HD patients.

Studies published so far on peritoneal dialysis using BIS-guided techniques did not result in an overall improvement of fluid state. Four recent randomized controlled trials did not support its routine use[47,48,54,55]. The COMPASS trial [48], which was a randomized controlled trial performed in non-anuric patients on peritoneal dialysis with residual renal function as the outcome parameter, found only minor changes in overhydration but did not reach the primary endpoint. Changes in the glomerular filtration rate over a 1-year period between the BIS-guided fluid management group and the control group did not differ (−1.5 ± 2.4 vs −1.3 ± 2.6 mL/min/1.73 m^2, p = 0.593). Overall, the degree of FO in the included patients was mild (mean overhydration around +1.5). Moreover, no differences were found in echocardiographic parameters or arterial stiffness at the end of follow-up between the two groups. Although longitudinal vector plot-based bioimpedance targets were provided to guide management in 308 patients on peritoneal dialysis in a UK–Shanghai peritoneal study[47], body composition remained relatively

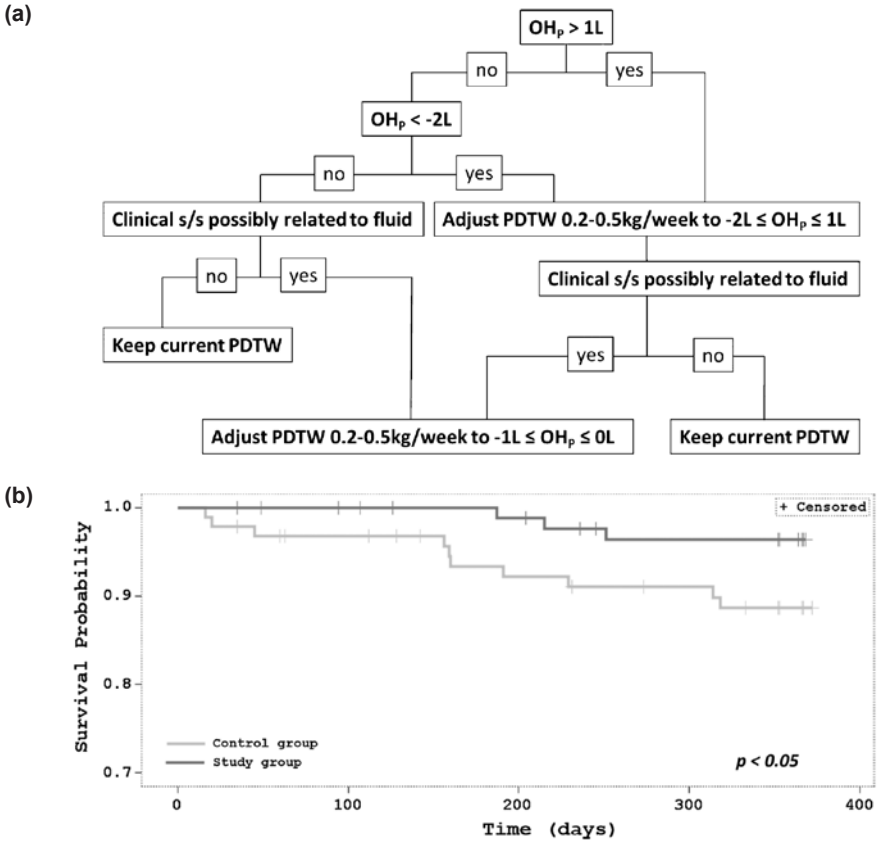

Fig. 5 (a) Algorithm for post-dialysis target weight adjustment using Body Condition Monitor bioimpedance spectroscopy (adapted from Ref. 49). (b) Kaplan–Meier analysis for acute fluid overload or cardiovascular event-free survival in non-diabetic patients in both groups.

stable in both BIA-guided intervention and control groups (routine clinical care) after 12-month follow-up, especially in the non-anuric subgroup (daily urine output > 200 mL). However, in control anuric Chinese patients, hydration worsened with increased extracellular/total body water ratio (+0.04; 95% CI: 0.01, 0.06). The authors concluded that the routine use of longitudinal bioimpedance to inform fluid management had minimal impact on patients on peritoneal dialysis.

Yoon et al.[54] also found that BIS-guided fluid management did not show an additional benefit toward achieving euvolemia and did not affect the decline in residual kidney function in patients on non-anuric peritoneal dialysis. In one recent randomized controlled study in 240 patients, Tian et al.[55] found that although BIA-guided fluid management resulted in a better FO status than the traditional clinical method, no significant effect was found on 1-year patient survival and technique survival in patients on peritoneal dialysis. The reasons behind the lower success rate in peritoneal dialysis trials compared with their HD counterparts remain unclear. Some of the reasons may be a less frequent adjustment of dry weight, which reduces the likelihood of attaining dry weight in patients on peritoneal dialysis. Until larger trials addressing the possible causes of such discrepancy are conducted, the evidence to support the routine use of BIS remains insufficient.

To date, most of these studies have been summarized in four meta-analyses[56-59]. Based on all these analyses, BIA-guided interventions for the correction of overhydration currently have little to no effect on all-cause or cardiovascular mortality. Nevertheless, BIA can result in significant fluid status changes and systolic blood pressure reduction in this vulnerable patient population. All meta-analyses on patients on HD found a relatively consistent improvement in hypertension control, which was related to the magnitude of the FO correction[22,56-59]. Tabinor et al.[25] found that overhydration > 15% (HR, 2.28; 95% CI: 1.56–3.34; P < 0.001) predicted mortality. Overhydration on BIA predicts mortality in patients on dialysis independent of the influence of comorbidity. On the other hand, the important question remains on whether reaching the target weight would carry a risk of compromising residual renal function and increase intradialytic instability. Pre-dialytic fluid depletion is also associated with increased mortality[22,38] and should be avoided. The optimal limit for dry weight assessed by BIS is obviously rather narrow. However, BIS can provide valuable and precise information that may assist in difficult decision making with regards fluid management instead of providing a simple target applied to all patients on dialysis.

Currently, the adjustment of dry weight emerges as the primary approach to fluid management in interventional trials. However, in real-world applications, such an approach has some drawbacks. Some of the main limiting factors that may hamper appropriate fluid removal will be encountered in daily practice, including poor compliance with fluid and water restriction, compromised cardiovascular status, patients with megafistula flow, malnutrition with hypoalbuminemia, and redistribution of body water in severely reduced lean body mass conditions. Some authors have recently suggested caution when using BIS devices interchangeably[60]. Currently, several commercially available devices employing bioimpedance technology are used in routine clinical practice. However, cross-validation studies between these BIS devices are scarce, and further assessments are needed. In addition, BIS should not be used as the sole determinant in guiding dry weight adjustment. The complete normalization of FO may not be possible without inducing severe intradialytic symptomatology. Undeniably, BIS-guided treatment can add valuable information to help solve the already complex decision-making around fluid management. Furthermore, at least for now, it is more useful in detecting longitudinal changes in body fluid composition and in adjusting for fluid removal rather than as a tool for guiding patients to achieve a specific target hydration status.

Conclusion

BCM provides an objective and clinically applicable assessment of hydration status and can thus mitigate the significant associations between FO and high mortality rate and cardiovascular events. BCM-guided dry weight adjustment improves blood pressure control and decreases intradialytic morbidities and possibly even mortality rate. Our results indicate that BIS contributes new information and is thus a promising tool for risk stratification of patients on dialysis. Larger-scale studies, particularly in patients

on peritoneal dialysis, are needed to establish the potential role and benefits of BIS-guided fluid management.

References

1. Kraemer M, Rode C, Wizemann V. Detection limit of methods to assess fluid status changes in dialysis patients. Kidney Int 2006;69:1609-20.
2. Wizemann V, Wabel P, Chamney P, Zaluska W, Moissl U, Rode C, et al. The mortality risk of overhydration in haemodialysis patients. Nephrol Dial Transplant 2009;24:1574-9.
3. Hur E, Usta M, Toz H, Asci G, Wabel P, Kahvecioglu S, et al. Effect of fluid management guided by bioimpedance spectroscopy on cardiovascular parameters in hemodialysis patients: a randomized controlled trial. Am J Kidney Dis 2013;61:957-65.
4. Onofriescu M, Siriopol D, Voroneanu L, Hogas S, Nistor I, Apetrii M, et al. Overhydration, Cardiac Function and Survival in Hemodialysis Patients. PLoS One 2015;10: e0135691.
5. Hassan K, Hassan D, Shturman A, Rubinchik I, Fadi H, Shadi H, et al. The impact of sub-clinical over-hydration on left ventricular mass in peritoneal dialysis patients. Int J Clin Exp Med 2015; 8:5890-6.
6. McDonald SP. Australia and New Zealand Dialysis and Transplant Registry. Kidney Int Suppl (2011) 2015;5:39-44.
7. Santoro A, Mancini E. Hemodialysis and the elderly patient: complications and concerns. J Nephrol 2010; 23 Suppl 15: S80-9.
8. Jaeger JQ, Mehta RL. Assessment of dry weight in hemodialysis: an overview. J Am Soc Nephrol 1999;10:392-403.
9. Kopple JD. National kidney foundation K/DOQI clinical practice guidelines for nutrition in chronic renal failure. Am J Kidney Dis 2001;37:S66-70.
10. Chen HS, Lee KC, Cheng CT, Hou CC, Liou HH, Lin CJ, et al. Application of Bioimpedance Spectroscopy in Asian Dialysis Patients (ABISAD): serial follow-up and dry weight evaluation. Clin Kidney J 2013;6:29-34.
11. Hung SC, Kuo KL, Peng CH, Wu CH, Lien YC, Wang YC, et al. Volume overload correlates with cardiovascular risk factors in patients with chronic kidney disease. Kidney Int 2014;85:703-9.
12. Mathew S, Abraham G, Vijayan M, Thandavan T, Mathew M, Veerappan I, et al. Body composition monitoring and nutrition in maintenance hemodialysis and CAPD patients--a multicenter longitudinal study. Ren Fail 2015;37:66-72.
13. Tsai YC, Tsai JC, Chen SC, Chiu YW, Hwang SJ, Hung CC, et al. Association of fluid overload with kidney disease progression in advanced CKD: a prospective cohort study. Am J Kidney Dis 2014;63:68-75.
14. van der Sande FM, van de Wal-Visscher ER, Stuard S, Moissl U, Kooman JP. Using Bioimpedance Spectroscopy to Assess Volume Status in Dialysis Patients. Blood Purif 2020;49:178-184.
15. Hung SC, Kuo KL, Peng CH, Wu CH, Wang YC, Tarng DC. Association of fluid retention with anemia and clinical outcomes among patients with chronic kidney disease. J Am Heart Assoc 2015;4:e001480.
16. Matthie JR. Bioimpedance measurements of human body composition: critical analysis and outlook. Expert Rev Med Devices 2008;5:239-61.
17. Khalil SF, Mohktar MS, Ibrahim F. The theory and fundamentals of bioimpedance analysis in clinical status monitoring and diagnosis of diseases. Sensors (Basel) 2014;14: 10895-928.
18. Moissl UM, Wabel P, Chamney PW, Bosaeus I, Levin NW, Bosy-Westphal A, et al. Body fluid volume determination via body composition spectroscopy in health and disease. Physiol Meas 2006;27:921-33.
19. Lim PS, Chen CH, Zhu F, Kotanko P, Jeng Y, Hu CY, et al. Validating Body Fat Assessment by Bioelectric Impedance Spectroscopy in Taiwanese Hemodialysis Patients. J Ren Nutr 2017;27:37-44.
20. Chamney PW, Wabel P, Moissl UM, Muller MJ, Bosy-Westphal A, Korth O, et al. A whole-body model to distinguish excess fluid from the hydration of major body tissues. Am J Clin Nutr 2007;85:80-9.
21. Broers NJ, Martens RJ, Cornelis T, Diederen NM, Wabel P, van der Sande FM, et al. Body composition in dialysis patients: a functional assessment of bioimpedance using different prediction models. J Ren Nutr 2015;25:121-8.
22. Dekker M, Konings C, Canaud B, Carioni P, Guinsburg A, Madero M, et al. Pre-dialysis fluid status, pre-dialysis systolic blood pressure and outcome in prevalent haemodialysis patients: results of an international cohort study on behalf of the MONDO initiative. Nephrol Dial Transplant 2018;33:2027-2034.
23. Dekker MJ, Marcelli D, Canaud BJ, Carioni P, Wang Y, Grassmann A, et al. Impact of fluid status and inflammation and their interaction on survival: a study in an international hemodialysis patient cohort. Kidney Int 2017;91:1214-1223.
24. Dekker MJE, Kooman JP. Fluid status assessment in hemodialysis patients and the association with outcome: review of recent literature. Curr Opin Nephrol Hypertens 2018; 27:188-193.
25. Tabinor M, Elphick E, Dudson M, Kwok CS, Lambie M, Davies SJ. Bioimpedance-defined overhydration predicts survival in end stage kidney failure (ESKF): systematic review and subgroup meta-analysis. Sci Rep 2018;8:4441.
26. Zoccali C, Moissl U, Chazot C, Mallamaci F, Tripepi G, Arkossy O, et al. Chronic Fluid Overload and Mortality in ESRD. J Am Soc Nephrol 2017;28:2491-2497.
27. Hwang SD, Lee JH, Lee SW, Kim JK, Kim MJ, Song JH. Risk of overhydration and low lean tissue index as measured using a body composition monitor in patients on hemodialysis: a systemic review and meta-analysis. Ren Fail 2018; 40:51-59.
28. Ng JK, Kwan BC, Chow KM, Pang WF, Cheng PM, Leung CB, et al. Asymptomatic fluid overload predicts survival and cardiovascular event in incident Chinese peritoneal dialysis patients. PLoS One 2018;13:e0202203.
29. Parthasarathy R, Oei E, Fan SL. Clinical value of body composition monitor to evaluate lean and fat tissue mass in peritoneal dialysis. Eur J Clin Nutr 2019;73:1520-1528.
30. Rymarz A, Gibińska J, Zajbt M, Piechota W, Niemczyk S. Low lean tissue mass can be a predictor of one-year survival in hemodialysis patients. Ren Fail 2018;40:231-237.
31. Vega A, Abad S, Macías N, Aragoncillo I, Santos A, Galán I, et al. Low lean tissue mass is an independent risk factor for mortality in patients with stages 4 and 5 non-dialysis chronic kidney disease. Clin Kidney J 2017;10:170-175.
32. Kim C, Kim JK, Lee HS, Kim SG, Song YR. Longitudinal changes in body composition are associated with all-cause mortality in patients on peritoneal dialysis. Clin

Nutr 2020.
33. Lin TY, Peng CH, Hung SC, Tarng DC. Body composition is associated with clinical outcomes in patients with non-dialysis-dependent chronic kidney disease. Kidney Int 2018; 93:733-740.
34. Assimon MM, Wang L, Flythe JE. Failed Target Weight Achievement Associates with Short-Term Hospital Encounters among Individuals Receiving Maintenance Hemodialysis. J Am Soc Nephrol 2018;29:2178-2188.
35. Hecking M, Moissl U, Genser B, Rayner H, Dasgupta I, Stuard S, et al. Greater fluid overload and lower interdialytic weight gain are independently associated with mortality in a large international hemodialysis population. Nephrol Dial Transplant 2018;33:1832-1842.
36. Barbosa-Silva MC, Barros AJ, Wang J, Heymsfield SB, Pierson RN, Jr. Bioelectrical impedance analysis: population reference values for phase angle by age and sex. Am J Clin Nutr 2005;82:49-52.
37. Vujicic B, Mikolasevic I, Racki S, Orlic L, Ljutic D, Bubic I. BCM--body composition monitor: a new tool for the assessment of volume-dependent hypertension in patients on maintenance haemodialysis. Coll Antropol 2013;37: 815-9.
38. Siriopol D, Siriopol M, Stuard S, Voroneanu L, Wabel P, Moissl U, et al. An analysis of the impact of fluid overload and fluid depletion for all-cause and cardiovascular mortality. Nephrol Dial Transplant 2019;34:1385-1393.
39. O'Lone EL, Visser A, Finney H, Fan SL. Clinical significance of multi-frequency bioimpedance spectroscopy in peritoneal dialysis patients: independent predictor of patient survival. Nephrol Dial Transplant 2014;29:1430-7.
40. Han BG, Lee JY, Choi SO, Yang JW, Kim JS. Relative overhydration is independently associated with left ventricular hypertrophy in dialysis naïve patients with stage 5 chronic kidney disease. Sci Rep 2020;10:15924.
41. Dekker MJE, Konings C, Canaud B, van der Sande FM, Stuard S, Raimann JG, et al. Interactions Between Malnutrition, Inflammation, and Fluid Overload and Their Associations With Survival in Prevalent Hemodialysis Patients. J Ren Nutr 2018;28:435-444.
42. Ye X, Dekker MJE, Maddux FW, Kotanko P, Konings C, Raimann JG, et al. Dynamics of Nutritional Competence in the Last Year Before Death in a Large Cohort of US Hemodialysis Patients. J Ren Nutr 2017;27:412-420.
43. Oei E, Paudel K, Visser A, Finney H, Fan SL. Is overhydration in peritoneal dialysis patients associated with cardiac mortality that might be reversible? World J Nephrol 2016; 5:448-54.
44. Machek P, Jirka T, Moissl U, Chamney P, Wabel P. Guided optimization of fluid status in haemodialysis patients. Nephrol Dial Transplant 2010;25:538-44.
45. Huan-Sheng C, Yeong-Chang C, Ming-Hsing H, Fan-Lieh T, Chu-Cheng L, Tsai-Kun W, et al. Application of bioimpedance spectroscopy in Asian dialysis patients (ABISAD-III): a randomized controlled trial for clinical outcomes. Int Urol Nephrol 2016;48:1897-1909.
46. Onofriescu M, Hogas S, Voroneanu L, Apetrii M, Nistor I, Kanbay M, et al. Bioimpedance-guided fluid management in maintenance hemodialysis: a pilot randomized controlled trial. Am J Kidney Dis 2014;64:111-8.
47. Tan BK, Yu Z, Fang W, Lin A, Ni Z, Qian J, et al. Longitudinal bioimpedance vector plots add little value to fluid management of peritoneal dialysis patients. Kidney Int 2016; 89:487-97.
48. Oh KH, Baek SH, Joo KW, Kim DK, Kim YS, Kim S, et al. Does Routine Bioimpedance-Guided Fluid Management Provide Additional Benefit to Non-Anuric Peritoneal Dialysis Patients? Results from COMPASS Clinical Trial. Perit Dial Int 2018;38:131-138.
49. Liu L, Sun Y, Chen Y, Xu J, Yuan P, Shen Y, et al. The effect of BCM guided dry weight assessment on short-term survival in Chinese hemodialysis patients : Primary results of a randomized trial - BOdy COmposition MOnitor (BOCOMO) study. BMC Nephrol 2020;21:135.
50. Patel HV, Annigeri RA, Kowdle PC, Rao BS, Seshadri R, Balasubramanian S, et al. Bioimpedance Spectroscopy-Guided Ultrafiltration Normalizes Hydration and Reduces Intradialytic Adverse Events in Hemodialysis Patients. Indian J Nephrol 2019;29:1-7.
51. Paunic Z, Dimkovic N, Dekleva-Manojlovic M, Markovic Nikolic N. SP464BIOIMPEDANCE SPECTROSCOPY VOLUME STATUS MONITORING AND HYPERTENSION IN HEMODIALYSIS PATIENTS: A PROSPECTIVE RANDOMIZIED STUDY. Nephrology Dialysis Transplantation 2016;31:i247-i248.
52. Luo YJ, Lu XH, Woods F, Wang T. Volume control in peritoneal dialysis patients guided by bioimpedance spectroscopy assessment. Blood Purif 2011;31:296-302.
53. Ponce P, Pham J, Gligoric-Fuerer O, Kreuzberg U. Fluid management in haemodialysis: Conventional versus Body Composition Monitoring (BCM) supported management of overhydrated patients. Portuguese Journal of Nephrology & Hypertension 2014;28:239-248.
54. Yoon HE, Kwon YJ, Shin SJ, Lee SY, Lee S, Kim SH, et al. Bioimpedance spectroscopy-guided fluid management in peritoneal dialysis patients with residual kidney function: A randomized controlled trial. Nephrology (Carlton) 2019; 24:1279-1289.
55. Tian N, Yang X, Guo Q, Zhou Q, Yi C, Lin J, et al. Bioimpedance Guided Fluid Management in Peritoneal Dialysis: A Randomized Controlled Trial. Clin J Am Soc Nephrol 2020; 15:685-694.
56. Tabinor M, Davies SJ. The use of bioimpedance spectroscopy to guide fluid management in patients receiving dialysis. Curr Opin Nephrol Hypertens 2018;27:406-412.
57. Beaubien-Souligny W, Kontar L, Blum D, Bouchard J, Denault AY, Wald R. Meta-Analysis of Randomized Controlled Trials Using Tool-Assisted Target Weight Adjustments in Chronic Dialysis Patients. Kidney Int Rep 2019;4: 1426-1434.
58. Covic A, Ciumanghel AI, Siriopol D, Kanbay M, Dumea R, Gavrilovici C, et al. Value of bioimpedance analysis estimated "dry weight" in maintenance dialysis patients: a systematic review and meta-analysis. Int Urol Nephrol 2017;49:2231-2245.
59. Scotland G, Cruickshank M, Jacobsen E, Cooper D, Fraser C, Shimonovich M, et al. Multiple-frequency bioimpedance devices for fluid management in people with chronic kidney disease receiving dialysis: a systematic review and economic evaluation. Health Technol Assess 2018;22:1-138.
60. Dejongh S, Farré R, Bammens B, Claes K, Kuypers D, Evenepoel P, et al. Discrepancies between bioimpedance spectroscopy devices in haemodialysis patients. Clin Kidney J 2020;13:906-908.

生物阻抗頻譜分析與透析病人的水分控制：由實驗室走入臨床

吳再坤　陳宏賓　陳昶旭　曾天佑　林柏松*

童綜合醫療社團法人童綜合醫院　腎臟內科

受文日期：民國 109 年 12 月 30 日；接受刊載：民國 110 年 03 月 08 日

摘要

許多透析病人為年長、罹患多重共病且營養狀況不良。透析醫護人員經由水分及營養規則性評估是改善病人水分及營養狀態的重要方法。經由人體及身體組成的量測方式，可以提供透析病人的重要營養訊息。然而，由於此些檢驗方式的預先假設，以及透析改變了體內水分的狀態，限制了此些測量於透析病人的應用性。另一方面，身體組成測量方式，是經由單一或多個電生物阻抗在健康民眾推估實驗而設立。此外，大多數電生物阻抗法推估出的預後模組，於透析病人存在其根本問題。

近幾年，根據生物阻抗頻譜分析水分及生理改變的型態，設計出監測透析病人體內是否水分過多組成的儀器。由於具有非侵襲性、使用方便等特性，全世界越來越多的透析機構及醫療人員運用此儀器於床邊評估透析病人水分。此外，生物阻抗頻譜分析儀對於評估營養狀況及透析病人的透析是否充足也有臨床重要性。我們回顧及整理近幾年此議題的文獻並提供重要相關性。

關鍵詞：生物阻抗、營養、水分、透析

* 通訊作者：林柏松醫師　童綜合醫療社團法人童綜合醫院　腎臟內科
43503 臺中市梧棲區臺灣大道八段 699 號

Tungs' Medical Journal 15 (2021)
The 50th Anniversary of TTMHH 24-30 DOI: 10.3966/207135922021091505004

Original Article

The Immediate Effect of Transcranial Direct Current Stimulation (tDCS) Combined with TENS for Chronic Cervical Myofascial Pain – a Randomized, Sham-Controlled Study

Yi-Chia Yeh[1,*], Min-Fang Kuo[2], Yen-Chun Wu[3]

[1]*Department of Physical Medicine & Rehabilitation , Tungs' Taichung MetroHarbor Hospital*
[2]*Department of Psychology and Neurosciences, Leibniz Research Centre for Working Environment and Human Factors, Dortmund, Germany*
[3]*Department of Physical Medicine & Rehabilitation, St. Joseph Hospital, Yunlin*

Received: Jan. 20, 2021; Accepted: Apr. 22, 2021

Abstract

Objective: We sought to clarify whether a combination treatment of transcranial direct current stimulation (tDCS) and transcutaneous electrical nerve stimulation (TENS) could result in greater pain relief for patients with chronic cervical myofascial pain syndrome.
Methods: This study was a randomized, sham-controlled, crossover clinical trial. Ten patients with chronic cervical myofascial pain randomly received each of active tDCS/active TENS, active tDCS/sham TENS, and sham tDCS/active TENS stimulation. Visual analog scale and pressure pain threshold scores were recorded immediately before and after each treatment by a blinded evaluator.
Results: The three treatment approaches all showed significant pain reduction effects (p = 0.00) compared with the baseline scores. The pain reduction percentage in tDCS/TENS, tDCS/sham TENS, sham tDCS/TENS were 35.41%, 30.27%, and 26.64%, respectively. However, none of the groups reached statistical significance, although a greater pain reduction was observed in the tDCS/TENS group (p = 0.543). No significant differences in trigger point sensitivity were noted in all treatment groups (p = 0.934). The results suggest that both tDCS and TENS increased the pain threshold without changing the trigger point activity directly, thus limiting the therapeutic effect of the combined treatment.
Conclusions: The results of this study suggest that tDCS combined with TENS or tDCS alone demonstrated the same therapeutic effect as TENS, but neither demonstrated superior effects.

Key words: transcranial direct current stimulation, transcutaneous electrical nerve stimulation, chronic myofascial pain

Introduction

Chronic cervical myofascial pain syndrome (MPS) is a common type of musculoskeletal pain. The most common clinical manifestations include muscle tightness, a limited range of motion, referred pain, taut bands, and trigger points[1]. Therapeutic approaches involving physical therapy, stretching, or trigger point injections have been used to manage MPS. However, frequent recurrences of the syndrome have been noted due to poor posture or stress.

Transcutaneous electrical stimulation (TENS) is often applied to trigger points to treat myofascial pain. The therapeutic effect results from peripheral nerve stimulation to the spinal cord to change the pain reception threshold, a process known as "gate control theory[2]." A previous study has shown that movements or passive stretching exercises leading to increased nociceptive input or motor cortex activity can enhance the pain-reducing effect of TENS[3].

*Correspondence to: Yi-Chia Yeh, Department of Physical Medicine & Rehabilitation, Tungs' Taichung MetroHarbor Hospital, No. 8, Chenggong W. St., Shalu Dist., Taichung City 433, Taiwan (R.O.C.)

Transcranial direct current stimulation (tDCS) is a newly developed non-invasive brain stimulation technique delivered over motor cortex via a weak, continuous direct current[4-6]. When the electrode is placed over the area of interest, anodal tDCS enhances cortical excitability, whereas cathodal stimulation causes inhibition[7-9]. Recent studies suggest that tDCS is effective at reducing pain for fibromyalgia, central pain from spinal cord injury, and chronic neuropathic pain, as well as in healthy volunteers[10-13]. A previous study revealed that patients with fibromyalgia experienced superior pain relief in anodal primary motor/cathodal supraorbital compared with anodal prefrontal/cathodal supraorbital[11]. The possible mechanism underlying the efficacy of pain relief resulting from the stimulation of the primary motor cortex is attributed to spinothalamic projection to the motor cortex[14].

A recent study suggests that TENS used for peripheral stimulation can augment the pain-reducing effect of tDCS on chronic neuropathic pain[10]. The possible mechanism of greater pain alleviation could be a higher level of pain threshold induced by tDCS as afferent stimulation to the motor cortex (increased excitability of motor cortex) when combined with TENS[10].

Our study aimed to evaluate the pain-reducing effect of the combined treatment of tDCS and TENS in patients with chronic cervical MPS. An additional group treated with TENS alone that was not previously compared with the tDCS treatment in a previous experiment was included for comparison in our study. We wanted to determine whether tDCS could reduce chronic nociceptive pain, as well as neuropathic pain, or change the trigger point sensitivity. We measured the visual analog scale (VAS) and pressure pain threshold scores immediately before and after three treatment types (tDCS/TENS, tDCS/sham TENS, or sham tDCS/ TENS) to evaluate the therapeutic effects of each group.

Materials and Methods

Study Design

This was a randomized, double-blind, sham-controlled study initiated after obtaining informed consent from the patients. The study was conducted according to the ethical standards of the Helsinki Declaration and was approved by the institutional ethics committee (IRB 9902-1, St. Joseph's Hospital).

Patients

Patients were selected by the medical doctors of the Department of Rehabilitation in a regional teaching hospital. The eligibility criteria were as follows: (1) diagnosis of cervical myofascial pain, (2) stable chronic pain lasting for 6 months, (3) VAS score larger or equal to 4, (4) aged between 18 and 65 years old, and (5) no other neurologic and/or psychiatric disease. Those who presented one of the following criteria were excluded: (1) intracranial metal implant or pacemaker, (2) pregnancy, and (3) undergoing any medication for central neurologic disorder. Since we only compared the VAS and pressure pain threshold scores before and immediately after the treatment, other therapies such as regular medication for pain relief, hot packs, or massages were not prohibited during our study. The treatment was not applied to the participants taking non-regular analgesics medication for pain relief.

Experimental Design

All the patients received the three treatments of active tDCS + active TENS, active tDCS + sham TENS, and sham tDCS + TENS in a randomized order. The wash-out interval was one week between each of treatment period.

tDCS

We applied saline-soaked sponge electrodes with the anodal electrode sized 5×5 cm^2 and cathodal electrode 7×7 cm^2. Direct current stimulation was delivered through a constant direct current stimulator (Chattanooga Intelect Mobile Combination, Chattanooga Group, USA). The participants received anodal stimulation of the primary motor cortex (M1) contralateral to the lesion side with the anode placed over C3 or C4 according to the international 10/20 EEG system and the cathode over the contralateral supraorbital area. Both electrodes were stabilized with elastic bandage. The current intensity of tDCS was 2 mA for 30 minutes in the treatment group. Ramping time was included in the 30 minutes. For the participants receiving sham tDCS, they would experience an initial itching sensation, same as the treatment group, when the stimulator was ramping up. Ramping down to zero would then be performed within 30 seconds.

TENS

The same stimulator in dual-channel mode was

applied, with one set of channels for TENS and the other for tDCS. TENS was applied on the participant's most painful trigger point of the trapezius with two 5 × 5 cm electrodes using a square pulse of 4–5Hz for 30 minutes. The active electrode was placed on the most painful trigger point, as evaluated using the pain threshold pressure meter before each treatment. In the group of patients treated with TENS, the intensity of the stimulator was gradually increased until the participants reported feeling a weak electrical stimulation. The intensity was then adjusted to just slightly below the threshold sensation (as a subthreshold stimulation) for 30 minutes. In the sham TENS treatment, the stimulator was gradually "turned off" after the initial weak electrical stimulation sensation. In the group receiving subthreshold stimulation, the participants were not able to distinguish whether they received true or sham treatment. All of the participants would only feel the TENS stimulation at the beginning of the stimulation.

Evaluation

Pain was assessed subjectively using the VAS. A 100-mm horizontal line was marked "no pain" from the left side and "most intense pain imaginable" on the right[18]. Pressure pain threshold was measured using a pressure algometer to assess objective trigger point sensitivity and quantify trigger points[15-17]. This instrument is a force gauge calibrated in kg/cm^2 attached to a plunger with a 1-cm round rubber tip on its end. The pain threshold (kg/cm^2) was measured by an experienced rehabilitation doctor. The trigger point of the upper trapezius was first identified, and then the tenderest point of one side was marked. The pressure pain threshold meter was placed on the marked point and a constantly increasing pressure (rate: 1 kg/cm^2/sec) was applied over the trigger point until the subject first felt a sensation of pain, then the pressure application was stopped, and the pain threshold was recorded. The same procedure was repeated three times, and the average pre- and post- treatment pressure pain thresholds were recorded. After the treatment, a trained evaluator who was blinded to the treatment group recorded the initial VAS scores and the pressure pain thresholds immediately after treatment. Monitoring for adverse responses was performed during and after the experiment sessions.

Statistical Analysis

Mixed analysis of variance (ANOVA) was performed for the statistical analysis. The condition and time of treatment were considered as fixed effects. The responses of the patients were recognized as random effects. The variables of the fixed-effects models in this study model included (1) pre-stimulation and post-stimulation times; (2) the combination of stimulation conditions of tDCS, TENS, and sham; and (3) the relationship between time and stimulation condition. Post-hoc comparison with multiple comparison adjustment was performed using the Bonferroni method. The percentage of pain reduction (pre-post VAS/preVAS) was used to evaluate the therapeutic effects. The baseline characteristics were also compared to assess the adequacy of our crossover design. All results are presented as mean, standard deviation, and standard error of the mean. Statistical significance was defined as a 2-tailed p value < 0.05.

Results

Ten patients (8 females) with a mean age of 38.1 ± 9.97 years were included in this study. The demographic and baseline clinical characteristics are described in Table 1.

All subjects tolerated the treatment well, and no adverse effects were reported. Only one subject (in the active tDSC/active TENS group) felt very sore over the trapezius immediately after treatment (VAS 3.5–4) due to the 30-minute immobilization during the treatment. This patient felt better after some range-of-motion exercise, but dropped out of the third session (TENS) because of early improvement (VAS < 3).

Mixed ANOVA was performed for each covariate, including time, stimulation condition, and the interaction between condition and time. A reduction in pain compared with baseline was found statistically significant by post-hoc analysis ($F[5,48] = 19.94$; $p = 0.00$) for the treatment approaches using tDCS/TENS (35.14% ± 4.73%; $p = 0.00$), tDCS/sham TENS (30.27% ± 5.47%; $p = 0.00$), and sham tDCS/TENS (26.64% ± 5.89%; $p = 0.00$). The analysis revealed no significant differences in VAS reduction percentage between the three treatment groups ($F[2,24] = 0.627$; $p = 0.543$) (Table 2). Furthermore, no significant difference was observed in pressure

Table 1. Demographics and Baseline Clinical Characteristics

	Age	Gender	Pain duration	Daily activity affected by pain	Had ever received other treatments
Patient 1	39	F	>3year	Yes	Yes
Patient 2	39	F	>3year	Yes	Yes
Patient 3	21	F	1-3 year	Yes	Yes
Patient 4	58	F	>3year	No	Yes
Patient 5	37	F	>3year	Yes	Yes
Patient 6	38	F	>3year	Yes	Yes
Patient 7*	31	M	1-3year	No	Yes
Patient 8	41	M	>3year	Yes	Yes
Patient 9	30	F	6months-1year	Yes	Yes
Patient 10	47	F	>3year	No	Yes
Mean(SD)	38.1(9.97)				

* Patient 7 dropout the TENS treatment due to early improvement with a VAS less than 3 after the 2nd interval.

Table 2. Pain reduction percentage - Difference between 3 treatment groups

Treatment	pre-post VAS/preVAS			Compared with baseline
	Mean	SD	SEM	*P*
TDCS/TENS	35.14	14.21	4.73	<0.00
tDCS/sham TENS	30.27	16.42	5.47	<0.00
Sham tDCS/ TENS	26.64	17.68	5.89	<0.00

Pain reduction percentage compared with baseline(%)
SD: standard deviation, SEM: standard error of mean

Table 3 Pressure pain threshold - Difference between 3 treatment groups

Treatment	Pre		Post		Difference(post-pre)	
	Mean	SD	Mean	SD	Mean	SE
tDCS/TENS	2.28	0.74	2.40	0.87	0.126	0.389
tDCS/sham TENS	2.30	0.66	2.09	0.68	-0.203	0.389
Sham tDCS/TENS	2.40	0.95	2.50	0.98	0.10	0.389

Algometer scores(kg/cm^2), SD: standard deviation, SE: standard error

pain threshold between the three treatment groups ($F[5,48] = 0.257$; $p = 0.934$) (Table 3). An analysis of the baseline information for the three groups was performed to determine whether a carryover effect occurred; showed no significant difference was observed ($p = 0.63$).

Discussion

This is the first study investigating the effects of tDCS on chronic MPS. The results revealed all of the three treatment approaches decreased the perception of pain immediately and significantly. However, no significant difference or change in trigger point sensitivity was found among the patients in all the treatment groups.

A previous study evaluating the effects of tDCS for fibromyalgia revealed significant pain reduction in M1 stimulation when compared with DLPFC or sham stimulation[11]. Furthermore, a previous study on the combined treatment with tDCS and TENS for chronic neuropathic pain showed greater pain reduction in tDCS/TENS compared with tDCS/sham TENS or sham stimulation[10]. Our study used the same duration and amplitude of tDCS stimulation (30 minutes, 2 mA) as the said study[10] for chronic neuropathic pain but varied the stimulation interval (1 week vs. 48 hours). To compare the difference in efficacy between tDCS

and TENS, we included an additional active TENS/sham tDCS group that was not analyzed in the previous study. Since many previous studies investigating tDCS for pain reduction had shown a significant difference between tDCS treatment and sham stimulation[10-13], the sham TENS/sham tDCS group was not included in this study.

An analysis of the therapeutic effects of TENS on trigger point sensitivity and VAS pain reduction found that TENS was effective in reducing myofascial pain without significantly changing the trigger point sensitivity[19]. We hypothesized that a combined application of TENS and tDCS might increase the pain threshold through peripheral and central mechanisms without directly changing the trigger point activity. Although the treatment used a combination of TENS and tDCS did not exhibit a superior effect over TENS treatment alone (p = 0.827), we still observed a tendency toward a higher pain reduction in the patients receiving tDCS/TENS treatment compared with those receiving tDCS alone or TENS alone, as presented in Table 2. One possible reason for our findings could be our small sample size. A larger enough sample size should be able to demonstrate more conclusively the significance and difference between the tDCS/TENS and TENS treatment approaches. Another possibility could be that neither tDCS nor TENS can change the trigger point activity. In that case, the therapeutic effect for myofascial pain would be limited since the treatment of myofascial pain is usually aimed to directly alter trigger point sensitivity[1]. Our study demonstrated that tDCS or TENS treatment can be effective for short-term pain relief but insufficient for long-term treatment of myofascial pain. Combining tDCS or TENS with stretching exercises may lead to superior pain reduction and also reduce trigger point sensitivity[16].

We did not observe similar findings as those in a previous study reporting a significantly greater pain reduction for chronic neuropathic pain in the group receiving tDCS/TENS treatment. One possible reason may be due to differences in the characteristics between chronic neuropathic pain and nociceptive pain.

This study has some limitations. First, this study analyzed a small sample size. However, the use of a crossover design could generate data equivalent to 30 subjects in a parallel study (30 subjects with 1 drop-out) and smaller within-subjects variability than between-subjects variability. Therefore, this study can be considered more powerful compared with that enrolling 29 patients in a parallel design.

Second, since a control group was not included in this study, the possibility of a placebo effect could not be ruled out. However, tDCS treatment has shown superior effects on pain reduction for chronic pain, fibromyalgia, and neuropathic pain compared with the control group in previous studies[10-13]. Therefore, sham tDCS/sham TENS was not included.

In this study, we found compatible therapeutic effects of tDCS and TENS in pain reduction for chronic cervical myofascial pain but not in trigger point sensitivity. Although no significant differences were found among the three treatment approaches, our results suggest that tDCS combined with TENS can induce better pain control. Further research with a larger sample size and the inclusion of stretching exercises is required to determine the effects on pain control and trigger point sensitivity reduction.

References

1. Travell JG, Simons DG. Myofascial Pain and Dysfunction: The Trigger Point Manual, Williams and Wilkins 1983.
2. Melzack R, Wall PD. Pain mechanism: a new theory. Science. 1965;150: 971-979.
3. Rakel B, Frantz R. Effectiveness of transcutaneous electrical nerve stimulation on postoperative pain with movement. J Pain. 2003;4:455-464.
4. Nitsche MA, Paulus W. Excitability changes induced in the human motor cortex by weak transcranial direct current stimulation. J Physiol. 2000;527: 633-639.
5. Nitsche, MA, Paulus W. Sustained excitability elevations induced by transcranial DC motor cortex stimulation in human. Neurology. 2001;57:1899-1901.
6. Poreisz C, Boros K, Antal A, et al. Safety aspects of transcranial direct current stimulation concerning healthy subjects and patients. Brain Research Bulletin. 2007;72:208-214.
7. Nitsche MA, Nitsche MS, Klein CC, et al. Level of action of cathodal DC polarization R inhibition of the human motor cortex. Clin Neurophysiol. 2003;114:600-604.
8. Nitsche, M.A., et al., Transcranial direct current stimulation: State of the art 2008, in Brain Stimul. 2008:p.206-223.
9. Gandiga PC, Hummel FC, L.G. Cohen LG. Transcranial DC stimulation (tDCS):a tool for double-blind sham-controlled clinical studies in brain stimulation. Clin Neurophysiol. 2006;117:845-850.
10. Boggio PS, Zaghi S, Villani AB, et al. Transcranial DC stimulation coupled with TENS for the treatment of chronic pain: a preliminary study. Clin J Pain. 2009;25:691-695.
11. Fregni F, Gimenes R, Valle AC, et al. A randomized, sham-controlled proof of principle study of transcranial direct current stimulation for the treatment of pain in fibromyalgia. Arthritis Rheum. 2006;54:3988-3998.
12. Fregni F, Boggio PS, Lima MC, et al. A sham-controlled, phase II trial of transcranial direct current stimulation

for the treatment of central pain in traumatic spinal cord injury. Pain. 2006;122:197-209.
13. Boggio PS, Zaghi S, Lopes M, et al. Modulatory effects of anodal transcranial direct current stimulation on perception and pain threshold in healthy volunteers. Eur J Neurol. 2008;15:1124-1130.
14. Padel Y, Relova JL. Somatosensory responses in the cat motor cortex. I. Identification and course of an afferent pathway. J Neurophysiol. 1991;66:2041-2058.
15. Fischer AA. Pressure threshold meter: Its use for quantification of tender spots. Arch Phys Med Rehabil. 1986;67: 836-838.
16. Jaeger B, Reeves JL. Quantification of changes in myofascial trigger point sensitivity with the pressure algometer fallowing passive stretch. Pain. 1986;27:203-210.
17. Reeves JL, Jaeger B, Graff-Radford SB. Reliability of the pressure algometer as a measure of myofascial trigger point sensitivity. Pain. 1986;24:313-321.
18. Seymour RA, Simpson JM, Charlton JE, et al. An evaluation of length and end phrase of visual analogue scales in dental pain. Pain. 1979;21:177-185.
19. Graff-Radford SB, Reeves JL, Baker RL, et al. Effects of transcutaneous electrical nerve stimulation on myofascial pain and trigger point sensitivity. Pain. 1989;37:1-5.

經顱直流電刺激術結合經皮神經電刺激對慢性頸部肌筋膜疼痛之立即效果

葉怡嘉[1] 郭旻芳[2] 吳炎村[3]

[1]童綜合醫療社團法人童綜合醫院 復健科
[2]德國萊布尼茲研究中心 神經心理科學部
[3]財團法人天主教若瑟醫院 復健科

受文日期：民國 110 年 01 月 20 日；接受刊載：民國 110 年 04 月 22 日

摘要

在近年來的研究中，發現經顱直流電刺激術合併經皮電刺激對於慢性頑固性神經疼痛患者有減輕疼痛的效果，並且比單獨使用經顱直流電刺激術或是對照組有更佳的止痛效果。 我們在本研究中，假設此種治療方式對慢性頸部肌筋膜疼痛症，相較於單獨使用經顱直流電刺激術或是經皮電刺激治療，會有更佳的治療效果。

本研究採用隨機控制及交叉設計方法。收案十名慢性斜方肌肌筋膜疼痛患者 , 每個人都接受三種不同的治療方式，經顱直流電刺激術（tDCS）結合經皮神經電刺激（TENS）(tDCS/TENS, tDCS/sham TENS, sham tDCS/TENS），在治療前後記錄視覺類比分數（visual analogue scale）及壓痛閾值 pressure pain threshold）。研究結果顯示本研究發現三種治療方式的疼痛減輕百分比都有達到顯著的意義，分別為 tDCS/ TENS 組（35.41%），tDCS/sham TENS 組（30.27%），sham tDCS/TENS 組（26.64%）。但三組之間比較並沒有統計上的差異（p= 0.543）。在肌筋膜疼痛點敏感度（trigger point sensitivity）上，三組間沒有統計上的差異（p=0.934）。此結果可能代表這三種治療都提高了疼痛閾值，但因沒有直接改變肌筋膜疼痛點的活性，造成合併兩種療法並未呈現更佳的的療效。

關鍵詞：經顱直流電刺激、經皮電刺激、慢性肌筋膜疼痛

* 通訊作者：葉怡嘉醫師 童綜合醫療社團法人童綜合醫院 復健科 43503 臺中市梧棲區臺灣大道八段 699 號

Original Article

Effect of Aromatherapy on Neuropathic Pain: A Meta-analysis of Randomized Controlled Trials

Chen-Pi Li[1,2], Chung-Hsin Yeh[3], Jui-Ting Yu[4], Wen-Chieh Liao[5,7], Ru-Yin Tsai[5,6,7,*]

[1]*Nurse Practitioner,* [4]*Division of Hematology/Medical Oncology, Department of Medicine, Tungs' Taichung MetroHarbor Hospital, Taiwan*
[2]*Department of Public Healthy,* [5]*Department of Anatomy, Faculty of Medicine, Chung Shan Medical University, Taichung, Taiwan*
[3]*Department of Neurology, Yuan Rung Hospital, Changhua*
[6]*College of Nursing and Health Sciences, Da-Yeh University, Changhua, Taiwan*
[7]*Department of Medical Education, Chung Shan Medical University Hospital, Taichung, Taiwan*

Received: Dec. 31, 2020; Accepted: Mar. 31, 2021

Abstract

Purpose: This study aimed to determine the effectiveness of aromatherapy on neuropathic pain severity in people suffering from neuropathy.
Design: A systematic literature review and meta-analysis was conducted.
Methods: Six databases (PubMed, Scopus, Science Direct, CINAHL, OVID, and The Cochrane Library) were searched for studies published between January 2010 and October 2020. Only randomized controlled trials (RCTs) aromatherapy intervention for people with neuropathic pain were included.
Results: This meta-analysis included four RCTs, comprising 246 participants in total. Neuropathic pain was significantly suppressed by aromatherapy intervention in both the massage and non-massage groups.
Conclusions: The meta-analysis findings suggest aromatherapy as an effective intervention for people with neuropathic pain. Aromatherapy could be considered an adjuvant in clinical neuropathic pain management for patients needing long-term anti-analgesic drug treatment or patients with neuropathic pain.

Key words: aromatherapy, essential oil, neuropathic pain, neuropathy, allodynia, hyperalgesia

Introduction

Neuropathic pain is the result of a primary lesion or dysfunction of the nervous system. Hyperalgesia and allodynia are well-documented symptoms of neuropathic pain in the clinical setting[1]. Although neuropathic pain responds to opioids, the results are unsatisfactory, and adjuvant drugs are frequently needed.

Recent systemic reviews[2,3] revealed that non-pharmacologic therapies utilized in neuropathic pain management include acupuncture[4,5], massage[6], reflexology[7], and aromatherapy[6,8-10]. Among these, aromatherapy was frequently used.

Aromatherapy is a modus of complementary medicine that can be applied through inhalation and massage. The possible mechanism may involve signals from the olfactory system stimulating the central nervous system to release neurotransmitters like dopamine and serotonin[11]. These neurotransmitters further alleviate neuropathic pain[12]. More than 40 plant extraction oils have been reported for therapeutic use[13]. Even though aromatherapy is commonly used, few empirical reviews have examined its effectiveness in reducing neuropathic pain. To date, no meta-analysis has extensively examined the effects of aromatherapy focus on neuropathic pain and management. The aim of this meta-analysis was to quantify

*Correspondence to: Dr. Ru-Yin Tsai, Department of Anatomy, Faculty of Medicine, Chung Shan Medical University, No. 110, Sec. 1, Jianguo N. Rd, Taichung, Taiwan (R.O.C.)

the effectiveness of aromatherapy on neuropathic pain management.

Materials and methods

Data Sources

To determine the effects of aromatherapy on neuropathic pain, randomized controlled trials published between January 2010 and October 2020 were retrieved from PubMed, Scopus, Science Direct, CINAHL, OVID, and The Cochrane Library. The keywords used consisted of "aromatherapy," "essential oil," "neuropathic pain," "neuropathy," "allodynia," "hyperalgesia," "neuralgias," "neuralgia," and "neurodynia." The database search was limited to clinical trials with human subjects. The Preferred Reporting Items for Systematic Reviews and Meta-Analysis (PRISMA) guidance was used. Articles identified in this manner were retrieved and their reference lists searched for additional relevant articles.

Eligibility Criteria

Studies were included if: (a) participants were diagnosed with neuropathic pain; (b) intervention included aromatherapy with/without massage; (c) different kinds of essential oils could be used in aromatherapy; (d) outcomes measured at least one on the visual analog scale (VAS); and (e) studies were described as randomized controlled trials (RCTs) in English. Studies were excluded if they pertained to: (a) participants were mixed patients with other kinds of chronic pain but not specifically categorized as neuropathic pain; and (b) conference proceedings, abstracts only, review articles, letters, discussions, and editorials.

Selection of Studies

The data screening and selection were performed independently by two authors (JTY and CPL) and were verified by a third author (RYT). One hard copy of all the articles was obtained and read in full. Details of the selection process are shown in the PRISMA flow diagram (Figure 1).

Data Extraction

Two authors (RYT and CPL) independently extracted data using a standardized data extraction form as described in the Cochrane Handbook[14]. The following data were extracted from the studies: author names, year of publication, study design, sample size, participants' demographics, duration of the intervention, pattern of pain, element of essential oil, descriptions of the intervention and control groups, and outcomes and their measurements.

Quality Assessment

The Cochrane Risk of Bias (Rob 2.0) tool was used to perform quality assessment of the included

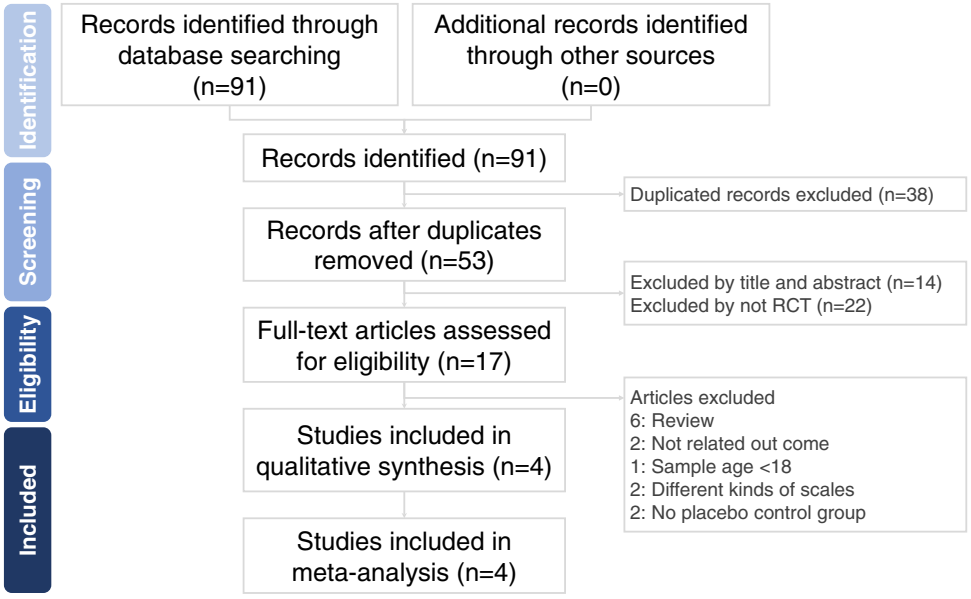

Fig. 1 PRISMA flow chart.

studies[15]. The following domains were assessed: bias arising from the randomization process, bias due to deviations from intended interventions, bias due to missing outcome data, bias in measurement of the outcomes, and bias in selection of the reported results. A study was judged to be at high risk of bias in at least one domain based on the results of this assessment.

Data Analysis

The primary end point for this study was the use of aromatherapy for neuropathic pain management. For each study, the standardized mean difference (SMD) of the VAS pain scores between the intervention and control groups was calculated. A random-effects model was employed to pool individual SMDs; all analyses were performed using Comprehensive Meta-Analysis software, version 3 (Biostat, Englewood, NJ, USA). Between-trial heterogeneity was determined using the I^2 test; value > 50% was regarded as considerable heterogeneity. Funnel plots and Egger's test were used to examine potential publication bias. Statistical significance was defined as p-value < 0.05, except for the determination of publication bias, which employed $p < 0.10$.

Results

Database Search and Characteristics of Included Patients

We retrieved 91 non-duplicate RCT citations and reviewed their titles and abstracts. Seventeen articles were included for detailed evaluation after eliminating references violating the inclusion criteria (Figure 1). With further careful reading, 13 records were eliminated due to being review articles[16-21], unrelated outcomes[22,23], patients were kids[24], different kinds of scales for measuring pain[10,25], and no placebo control group[9,26]. A final tally of four articles were included in this meta-analysis[6,8,27,28], three of which were double blind[8,27,28] and the fourth was single blind[6]. The final quantitative analysis included two hundred forty-six participants. The participant characteristics and study methodology are shown in Table 1.

Quality Assessment

The risk of bias was moderate across five domains in the included RCTs, and all RCTs were

Table 1. Summary of randomized placebo-controlled trials of aromatherapy for neuropathic pain.

Author, year	Patients' diagnosis	Enrolled sample number (Male/Female)	Average age, years	Enrolled criteria	Intervention oil	Frequency	Double-blind	Follow-up time	Outcome measurement	combine other therapy
Massage										
Gok Metin et al, 2017	Diabetic neuropathy	Intervention: 21 Placebo: 25	Intervention: 54.3±8.8 Placebo: 57.2±9.7	DN4 ≧ 4	rosemary, geranium, lavender, and eucalyptus	three times per week for a period of 4 weeks.	No	Before intervention and 2 and 4 weeks after intervention	DN4, Visual analog scale (VAS), and Neuropathic Pain Impact of Quality of Life (NePIQoL)	not mentioned
Non-Massage										
Eftekharsadat et al, 2018	Carpal tunnel syndrome (CTS)	Intervention: 24 (4/20) Placebo: 24 (3/21)	Intervention: 49.71±8.61 Placebo: 47.81±8.88	mild to moderate CTS	Lavender	one time per day	Yes	Before intervention and 40 days after intervention	Boston CTS questionnaire, VAS, pinch grip strength, and grip power	night wrist orthotic
Petramfar et al, 2016	neuropathic pain, diabetic neuropathy, and postsurgical neuropathic pain	Intervention: 46 Placebo: 46	Average age: 57.4	Detailed examination confirmed neuropathic pain	Ajwain	two times per day	Yes	Before intervention and 4 weeks after intervention	VAS, McGill pain questionnaire	not mentioned
Li L 2010	neuropathic pain	Intervention: 60 Placebo: 60	69±10	VAS 3~8	Neuragen PN®	approximately 0.75 ml per foot	Yes	9 hours after intervention	VAS	oral analgesics

Table 2 Assessment of methodological quality of included trials

RCT evaluated by RoB 2.0						
Author	Selecyion bias	Performance bias	Detection bias	Attrition bias	Reporting bias	Other
Eftekharsadat B et al, 2018	Some concerns	Low	Low	Low	Low	None
Gok Metin Z et al, 2017	Some concerns	Hihr	Low	High	High	None
Li L 2010	Low	Low	Low	Low	Low	None
Petramfar P et al, 2016	Low	Low	Low	Low	Some concerns	None

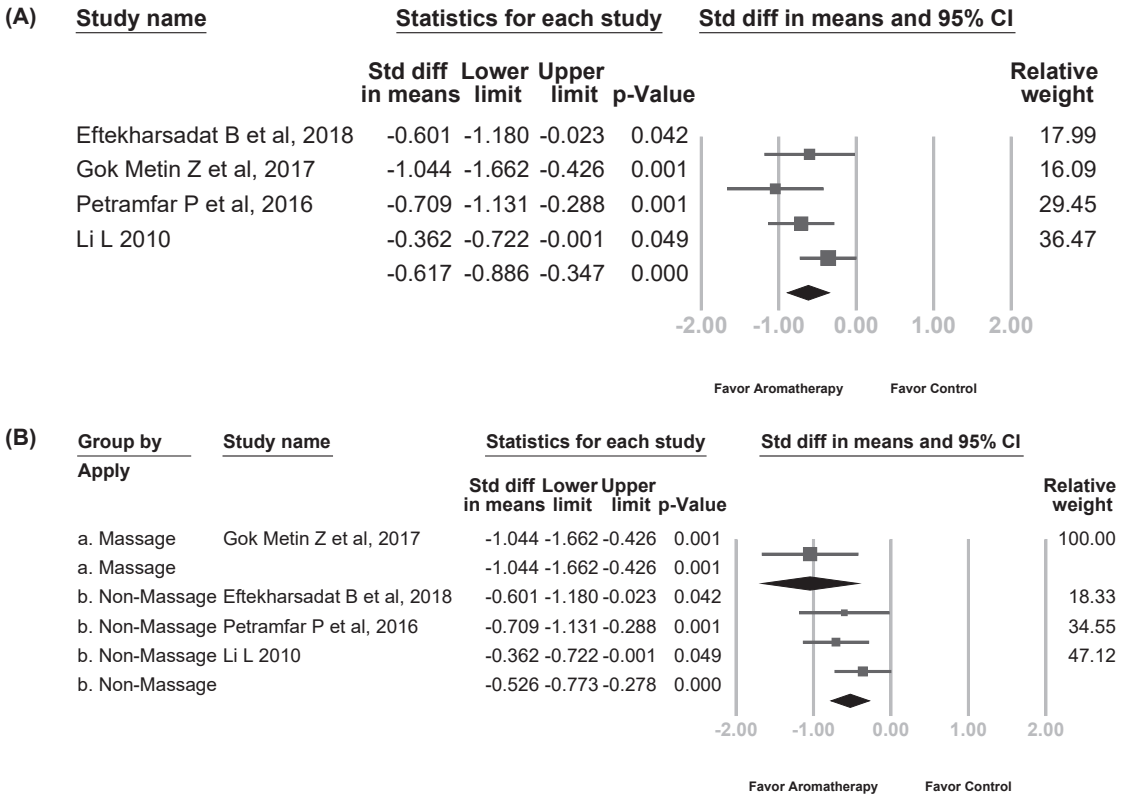

Fig. 2 The effect of aromatherapy on neuropathic pain measured using the visual analog scale, as compared with (a) placebo, overall effects, and (b) subgroup analysis.

limited in quality (Table 2). Two studies had some concerns of bias due to the small sample size[27] and selective reporting of results[8]. One study had a high risk of bias as the assessors were not blinded, deviations from intended interventions were noted, and bias in the outcome measurement was observed[6].

Effect of Aromatherapy on Neuropathic Pain

The overall SMD of aromatherapy versus control regarding neuropathic pain was −0.617 (95% confidence interval: −0.886 to −0.347). The subgroup analysis showed a significantly lower neuropathic pain level for aromatherapy versus control, both in the massage group (SMD: −1.044; 95% confidence interval: −1.662 to −0.426) and the non-massage group (SMD: −0.526; 95% confidence interval: −0.773 to −0.278) (Figures 2a and 2b). Regarding SMD heterogeneity, the I^2 was less than 0.001% in the non-massage group and <0.001% in the massage group.

Publishing Bias

The Egg's test indicated no significant publication bias regarding the overall SMD (p = 0.22203). The funnel plots for SMD of neuropathic pain are shown in Figure 3.

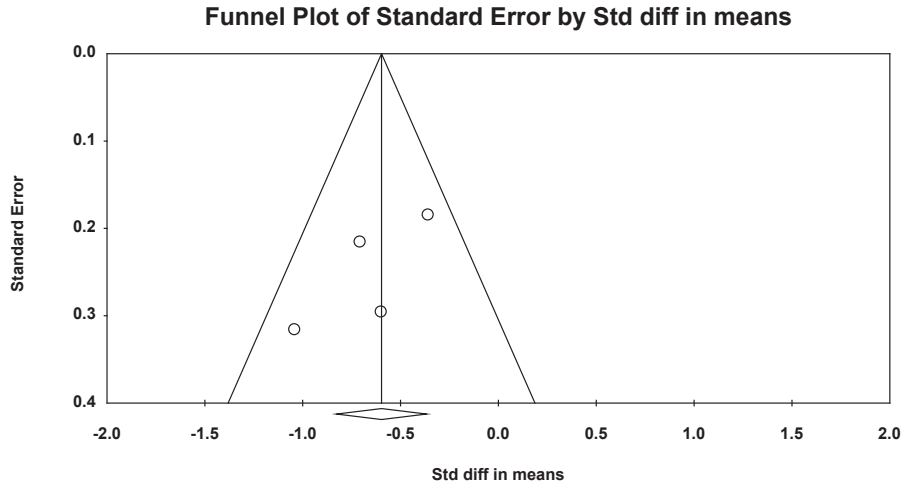

Fig. 3 Funnel plot for aromatherapy for neuropathic pain management compared with placebo.

Discussion

Aromatherapy has been widely studied in pain management[25,27]. This meta-analysis demonstrated that two types of aromatherapy used in managing neuropathic pain, massage and topical application, are superior to the control. The results suggest essential oils can be used in clinical practice for managing neuropathic pain.

Two studies reported that using different essential oils both significantly reduced pain scores, with no significant differences between the two intervention groups[9,26]. If an inert placebo control was tested in those two trials, more information could have been obtained on the relationship between aromatherapy and massage. Our statistical analysis showed that aromatherapy is significantly effective in relieving neuropathic pain, even without massage. Aromatherapy with massage was reported to confer more favorable and longer sustained effects than a massage alone in older people with knee osteoarthritis[29]. Seyyed-Rasooli et al.[30] found that, although both inhalation aromatherapy and aromatherapy massage significantly reduced pain scores in burn patients, inhalation aromatherapy was preferred to aromatherapy massage. In sum, we suggest inhalation aromatherapy as a low-cost, convenient, and more independent method than aromatherapy massage.

Aromatherapy is widely used in clinical conditions and is defined as the use of essential oils to promote therapeutic effects. Chemical molecules of essential oils pass through the olfactory system and relieve pain and promote physical, emotional, and mental health[31]. As we know, the olfactory system is the simplest path of perception[32]. Analgesic-like molecules in essential oils, especially monoterpenes and sesquiterpenes, have low molecular weight and high lipid solubility, so they can pass through the olfactory nerve, infiltrate the blood–brain barrier, and act on the central nervous system[33]. Moreover, compared with pharmacological drugs, essential oils have fewer side effects and more diverse applications, including inhalation[3,33]. Similarly, the essential oils used in the four studies evaluated in this meta-analysis mostly contained monoterpenes[8,26] or sesquiterpenes[6], which have significant anti-analgesic effects. Our findings indicate that inhalation might be the best application method for aromatherapy.

This meta-analysis has some limitations. The overall quality of the included studies was not optimal, and some of them had risks of performance and ascertainment biases. No uniform measure of neuropathic pain exists. The four studies included in the final pooled analysis examined treatments for nine different pain situations using different aromatherapy methods in the intervention, varying essential oils, and inconsistent control therapies. Eligible studies examining the efficacy of aromatherapy for managing neuropathic pain are currently lacking in the literature. While the size of the study allowed us to analyze the effectiveness of aromatherapy, a much larger-scale study is needed to evaluate adverse events.

Conclusion

Our data indicate that aromatherapy with or without massage significantly reduced neuropathic pain. Thus, the aroma of essential oils should be considered a safe, convenient, and independent addition to current neuropathic pain management. Although the present meta-analysis indicates positive effects in the use of aromatherapy for neuropathic pain management, the sample size is very small. Given the prevalence of aromatherapy, more RCT-type research is necessary to fully understand the clinical applications for its use. This meta-analysis suggests that aromatherapy can be used as an effective complementary treatment alternative for patients with neuropathic pain. However, only one study reported quality of life outcomes. Although long-term studies on the effectiveness of aromatherapy on neuropathic pain are also available, the number of studies included in the analysis was small. Well-designed studies with larger sample sizes and longer follow-up periods are needed to be able to draw firm conclusions on the effectiveness of aromatherapy in neuropathic pain relief.

Acknowledgements

The present study was supported by grants provided by the Tungs' Taichung MetroHarbor Hospital (TTMHH-108R0024) and Yuan Rung Hospital Da Yeh University Collaboration Project (DON0916).

References

1. Baron R, Maier C, Attal N, Binder A, Bouhassira D, Cruccu G, et al. Peripheral neuropathic pain: a mechanism-related organizing principle based on sensory profiles. Pain 2017;158:261-272.
2. Macone A, Otis JAD. Neuropathic Pain. Semin Neurol 2018;38:644-653.
3. Boyd A, Bleakley C, Hurley DA, Gill C, Hannon-Fletcher M, Bell P, et al. Herbal medicinal products or preparations for neuropathic pain. Cochrane Database Syst Rev 2019;4: CD010528.
4. Chen W, Yang GY, Liu B, Manheimer E, Liu JP. Manual acupuncture for treatment of diabetic peripheral neuropathy: a systematic review of randomized controlled trials. PLoS One 2013;8:e73764.
5. Dimitrova A, Murchison C, Oken B. Acupuncture for the Treatment of Peripheral Neuropathy: A Systematic Review and Meta-Analysis. J Altern Complement Med 2017;23: 164-179.
6. Gok Metin Z, Arikan Donmez A, Izgu N, Ozdemir L, Arslan IE. Aromatherapy Massage for Neuropathic Pain and Quality of Life in Diabetic Patients. J Nurs Scholarsh 2017; 49:379-388.
7. Dalal K, Maran VB, Pandey RM, Tripathi M. Determination of efficacy of reflexology in managing patients with diabetic neuropathy: a randomized controlled clinical trial. Evid Based Complement Alternat Med 2014;2014:843036.
8. Petramfar P, Moein M, Samani SM, Tabatabaei SH, Zarshenas MM. Trachyspermum ammi 10 % topical cream versus placebo on neuropathic pain, a randomized, double-blind, placebo-controlled trial. Neurol Sci 2016;37:1449-55.
9. Musharraf MU, Ahmad Z, Yaqub Z. Comparison of topical capsaicin and topical turpentine Oil for treatment of painful diabetic neuropathy. J Ayub Med Coll Abbottabad 2017;29:384-387.
10. Noh GO, Park KS. Effects of aroma self-foot reflexology on peripheral neuropathy, peripheral skin temperature, anxiety, and depression in gynaecologic cancer patients undergoing chemotherapy: A randomised controlled trial. Eur J Oncol Nurs 2019;42:82-89.
11. Lv XN, Liu ZJ, Zhang HJ, Tzeng CM. Aromatherapy and the central nerve system (CNS): therapeutic mechanism and its associated genes. Curr Drug Targets 2013;14:872-9.
12. Obata H. Analgesic Mechanisms of Antidepressants for Neuropathic Pain. Int J Mol Sci 2017;18.
13. Lakhan SE, Sheafer H, Tepper D. The Effectiveness of Aromatherapy in Reducing Pain: A Systematic Review and Meta-Analysis. Pain Res Treat 2016;2016:8158693.
14. Higgins JPT, Cochrane Collaboration. Cochrane handbook for systematic reviews of interventions. Hoboken, NJ: Wiley-Blackwell, 2020.
15. Sterne JAC, Savovic J, Page MJ, Elbers RG, Blencowe NS, Boutron I, et al. RoB 2: a revised tool for assessing risk of bias in randomised trials. BMJ 2019;366:l4898.
16. Zimpel SA, Torloni MR, Porfírio GJM, Flumignan RLG, da Silva EMK. Complementary and alternative therapies for post-caesarean pain. Cochrane Database of Systematic Reviews 2020.
17. Ball EL, Owen-Booth B, Gray A, Shenkin SD, Hewitt J, McCleery J. Aromatherapy for dementia. Cochrane Database of Systematic Reviews 2020.
18. Shin ES, Seo KH, Lee SH, Jang JE, Jung YM, Kim MJ, et al. Massage with or without aromatherapy for symptom relief in people with cancer. Cochrane Database of Systematic Reviews 2016.
19. Hu RF, Jiang XY, Chen J, Zeng Z, Chen XY, Li Y, et al. Non-pharmacological interventions for sleep promotion in the intensive care unit. Cochrane Database of Systematic Reviews 2015.
20. Cameron M, Chrubasik S. Oral herbal therapies for treating osteoarthritis. Cochrane Database of Systematic Reviews 2014.
21. Fellowes D, Barnes K, Wilkinson SSM. Aromatherapy and massage for symptom relief in patients with cancer. Cochrane Database of Systematic Reviews 2008.
22. Seol GH, Kang P, Lee HS, Seol GH. Antioxidant activity of linalool in patients with carpal tunnel syndrome. BMC Neurol 2016;16:17.
23. Bahr T, Allred K, Martinez D, Rodriguez D, Winterton P. Effects of a massage-like essential oil application procedure using Copaiba and Deep Blue oils in individuals with hand arthritis. Complementary Therapies in Clinical Practice 2018;33:170-176.

24. Malachowska B, Fendler W, Pomykala A, Suwala S, Mlynarski W. Essential oils reduce autonomous response to pain sensation during self-monitoring of blood glucose among children with diabetes. J Pediatr Endocrinol Metab 2016;29:47-53.
25. Izgu N, Ozdemir L, Bugdayci Basal F. Effect of Aromatherapy Massage on Chemotherapy-Induced Peripheral Neuropathic Pain and Fatigue in Patients Receiving Oxaliplatin: An Open Label Quasi-Randomized Controlled Pilot Study. Cancer Nurs 2019;42:139-147.
26. Motilal S, Maharaj RG. Nutmeg extracts for painful diabetic neuropathy: a randomized, double-blind, controlled study. J Altern Complement Med 2013;19:347-52.
27. Eftekharsadat B, Roomizadeh P, Torabi S, Heshmati-Afshar F, Jahanjoo F, Babaei-Ghazani A. Effectiveness of Lavendula stoechas essential oil in treatment of mild to moderate carpal tunnel syndrome: A randomized controlled trial. J Hand Ther 2018;31:437-442.
28. Li L. The effect of Neuragen PN on neuropathic pain: A randomized, double blind, placebo controlled clinical trial. BMC Complement Altern Med 2010;10:22.
29. Pehlivan S, Karadakovan A. Effects of aromatherapy massage on pain, functional state, and quality of life in an elderly individual with knee osteoarthritis. Jpn J Nurs Sci 2019;16:450-458.
30. Seyyed-Rasooli A, Salehi F, Mohammadpoorasl A, Goljaryan S, Seyyedi Z, Thomson B. Comparing the effects of aromatherapy massage and inhalation aromatherapy on anxiety and pain in burn patients: A single-blind randomized clinical trial. Burns 2016;42:1774-1780.
31. Tang SK, Tse MY. Aromatherapy: does it help to relieve pain, depression, anxiety, and stress in community-dwelling older persons? Biomed Res Int 2014;2014:430195.
32. Merrick C, Godwin CA, Geisler MW, Morsella E. The olfactory system as the gateway to the neural correlates of consciousness. Front Psychol 2014;4:1011.
33. de Sousa DP. Analgesic-like activity of essential oils constituents. Molecules 2011;16:2233-52.

芳香療法對神經病理性疼痛的影響：隨機對照試驗之薈萃分析

李偵碧[1,2] 葉宗勳[3] 俞瑞庭[4] 廖玟潔[5,7] 蔡如愔[5,6,7,*]

童綜合醫療社團法人童綜合醫院 專科護理師[1] 血液腫瘤科[4]
中山醫學大學 公共衛生研究所[2] 醫學系解剖學科[5]
[3]員榮醫療社團法人員榮醫院 神經內科
[6]大葉大學 護理健康學院
[7]中山醫學大學附設醫院 醫學教育部

受文日期：民國 109 年 12 月 31 日；接受刊載：民國 110 年 03 月 31 日

摘要

目的：本研究主要目的是確認芳香療法對緩解神經病理性疼痛的有效性。
設計：本研究利用系統性文獻回顧和薈萃分析。
方法：本研究檢索六個數據庫（PubMed，Scopus，Science Direct，CINAHL，OVID 和 Cochrane 圖書館），探討 2010 年 1 月至 2020 年 10 月之間發表的研究。僅收集對神經病理性疼痛患者進行芳香療法干預的隨機對照試驗（RCT）。
結果：這項薈萃分析包括四個 RCT 實驗，總共 246 名參與者。經過芳香療法干預，無論是按摩組或非按摩組均可顯著緩解神經病理性疼痛。
結論：從薈萃分析研究結果，我們認為芳香療法對於神經病理性疼痛患者是一種有效的干預措施。對於需要長期使用鎮痛藥物或患有神經病理性疼痛之患者，芳香療法可被視為臨床神經病理性疼痛管理的輔助藥物。

關鍵詞：芳香療法、精油、神經病理性疼痛、神經病變、痛覺敏感、痛覺過敏

* 通訊作者：蔡如愔副教授 中山醫學大學醫學系解剖學科 台中市建國北路一段 110 號

Original Article

Use Neural Networks to Detect Pneumothorax on X-ray Images

Jen-Ta Yu[1,+], Yan-Rui Lin[2,+], Chih-Chun Lai[2], Yu-Kang Chang[3], Tung-Kuo Huang[4], Cheng-Chun Lee[5], Neng-Chuan Tseng[6], Yao-Te Tsai[7,*], Shao-Jen Weng[8,*]

[1]Superintendent Room, [2]Department of Information Technology, [3]Department of Medical Research, [4]Premium Health Exam Center, [5]Department of Medical Imaging, [6]Division of Nuclear Medicine, Tungs' Taichung MetroHarbor Hospital, Taichung, Taiwan
[7]Department of International Business, Feng Chia University, Taichung, Taiwan
[8]Department of Industrial Engineering and Enterprise Information, Tunghai University, Taichung, Taiwan

Received: Dec. 08, 2020; Accepted: Feb. 19, 2021

Abstract

Background and Purpose: Chest X-Ray (CXR) imaging is an essential first-line diagnostic tool for pneumothorax, a virtually life-threatening condition. The insertion of a chest tube to drain air is the main therapeutic method for pneumothorax. This research aimed to develop an artificial intelligence (AI) model for identifying pneumothorax on CXR. Furthermore, we created an auxiliary AI model for recognizing an inserted chest tube. Although pneumothorax can be life-threatening, the presence of the chest tube means the pneumothorax is under treatment. In the clinical scenario, a fresh pneumothorax is emergent, but pneumothorax after chest tube treatment is not. Therefore, we proposed a combined AI model to distinguish the newly onset emergent condition from the condition after treatment.
Method: We trained a neural network based on MobileNet V2 to do the binary classification of whether a pneumothorax has occurred or not. The dataset was labeled by three radiologic technologists and reviewed by a radiologist. The same techniques were also applied to the AI model for the chest tubes.
Results: The accuracy for pneumothorax and chest tube identification on the test dataset was 92.19% and 98.22%, respectively. The areas under the receiver operating characteristic curve were 0.9638 (pneumothorax) and 0.9968 (chest tube). The inference time of each image ranged 0.21–0.6 second.
Discussions: The AI models achieved satisfactory results and can be further integrated into the Hospital Information System (HIS) in the future to assist in the early detection of emergent pneumothorax.

Key words: neural network, deep learning, chest, X-ray, pneumothorax, chest tube

Introduction

The term "pneumothorax" indicates an air leak within the pleural space, which leads to lung collapse. Early detection and early treatment would reduce the risk of progression to life-threatening tension pneumothorax. A chest tube is one of the most common and efficient treatments for re-expanding the lung[1]. Several examinations are used to detect pneumothorax (e.g., chest radiography, computed tomography, and ultrasonography). Chest radiography (CXR) is considered the most convenient and affordable first-line examination over computed tomography (CT) and ultrasonography (US). In addition, CXR could be the only imaging modality that is available in suburban hospitals. Although CT is the gold standard for pneumothorax detection, it is a time-consuming task, which results in delayed diagnosis[2]. Therefore, it is

[+]These authors contributed equally to this work
*Correspondence to: Dr. Yao-Te Tsai, Department of International Business, Feng Chia University, No. 100, Wenhwa Rd., Seatwen, Taichung, 40724, Taiwan (R.O.C.)
Dr. Shao-Jen Weng, Department of Industrial Engineering and Enterprise Information, Tunghai University, No. 1727, Sec.4, Taiwan Boulevard, Xitun District, Taichung, 407224, Taiwan (R.O.C.)

usually used when the physician could not identify pneumothorax on CXR images.

In Taiwan, hospitals generate a huge volume of CXR images. According to the Taiwan Ministry of Health and Welfare statistics[3], the number of licensed radiologists in 2019 was 1,213. This makes the interpretation of CXR images a very time-consuming task for radiologists. Decision support systems to help radiologists efficiently interpret CXR images and make an accurate diagnosis are thus urgently needed. Fortunately, innovations in information technology in recent years have brought tremendous benefits to medical imaging. One of the most successful applications thus far is artificial intelligence (AI). AI denotes a set of computer programs that allow computers to both understand and develop intelligent entities that simulate human decision making[4]. Medical imaging diagnostic systems using deep learning have become the most dominant area for medical AI applications[5].

Deep learning algorithms emerged from the traditional neural network algorithm. With more neurons and hidden layers, deep learning algorithms are able to create higher-level features from data inputs such as images[6]. Through the transformation, highly complicated functions can be learned iteratively. Previous studies have presented promising evidence of the applications of deep learning algorithms in medical images. Wang et al[7]. proposed a hybrid convolutional neural network (CNN) to detect and locate eight common thorax disease patterns by analyzing more than 100,000 X-ray images. Rajpurkar et al[8]. developed a CNN model for detecting pneumonia with 121 layers. Ayan and Ünver[9] applied deep learning algorithms in detecting pneumonia. Although various techniques were used, these studies all showed that the accuracy of detecting thoracic diseases using deep learning algorithms outperforms radiologist performance.

This research aimed to develop an AI model for identifying pneumothorax on CXR. In addition, we created an auxiliary AI model for recognizing the chest tube. Although a pneumothorax can be life-threatening, the coexistence of the chest tube means the pneumothorax is under treatment. In the clinical scenario, a fresh pneumothorax is emergent, but pneumothorax after chest tube treatment is not. Therefore, we aimed to determine whether these two AI models could correctly distinguish between a newly onset emergent pneumothorax from one arising after treatment.

Material and Methods

Data Collection

We developed the pneumothorax and chest tube AI models. A total of 292,201 de-identified and de-linked CXR images, along with the radiology reports, from 2017 to 2019 were collected from the hospital system. The de-identification process eliminates privacy issues by removing names, sex, age, date of birth, and other identification. This study was approved by the Institutional Review Board (IRB) of Tungs' Taichung MetroHarbor Hospital (TTMHH_IRB No: 107073 and No: 109024).

Data Processing

First, text mining was performed to search for reports using the keyword "pneumothorax" to get the presumed positive dataset. Another search was performed to do the reverse, that is, to search for reports without the keyword to get the presumed negative dataset.

Second, the presence of pneumothorax was clearly labeled on the CXR images in the datasets by three radiological technologists, with one radiologist who reviewed the labels. The same process was performed to produce the chest tube datasets. The purpose of this step was to assure the quality and consistency of labeling and to minimize error. A total of 1,912 images were labeled in the pneumothorax dataset. In the labeling results, 605 were positive (with pneumothorax), and 1,307 were negative (without pneumothorax). The positive/negative (P/N) ratio obtained was 1:2.16. In the chest tube dataset, 2,250 images were labeled, with 1,378 positive, and 872 negative. The P/N ratio was 1.58. The imaging data were subsequently segmented into the training set, validation set, and test set. The training set was used to train the deep learning model, the validation set to tune the hyperparameters and determine the best model, and the test set to examine the model accuracy and other metrics. The proportions of these three sets were about 80%, 10%, and 10%, respectively (Table 1).

Third, data augmentation was performed. Several image processing techniques applied in this phase included rescale, random perspective,

grayscale jitter, rotation, random horizontal flip, and random vertical flip. These image-processing techniques created more variations and representations of the images to train the model to generalize better.

Data analysis

Finally, we used MobileNetV2[10], a classical CNN architecture, as the training model. In this model, the image was the input, and the output was the probability (a number between 0 and 1) of pneumothorax. During the training, the probability threshold was arbitrarily assigned as 0.5 to classify positive and negative cases. We selected the checkpoint where the accuracy of the validation dataset was highest and generated the best AI model. The Youden index search was then applied to the validation dataset to seek a better threshold and optimize the accuracy. The F1-score, precision, sensitivity, specificity, and area under the receiver operating characteristic curve (AUROC) were used to measure the model performance. The F1-score, the harmonic mean of recall and precision, is a common metric for binary classification. Sensitivity and specificity measure the number of correctly identified positives and negatives. AUROC can be used to measure the correctness regardless of data unbalancing.

Table 1. Data statistics

		pneumothorax	Chest tube
Training	Positive	484	1,102
	Negative	1,046	698
Validate	Positive	60	138
	Negative	130	87
Test	Positive	61	138
	Negative	131	87
Total		1,912	2,250

Results

We selected the models with the best accuracy on the validation dataset and evaluated their performances with the test datasets. The results are shown in Table 2. For detecting pneumothorax in the validation set, 183 true positives (TPs) and true negatives (TNs) were found, whereas 7 images were not analyzed correctly. For detecting chest tubes in the validation set, 224 TPs and TNs were found, with 1 image identified as a false positive (FP). The number of FP and false negative (FN) slightly increased in both test sets, with 9 FPs and 6 FNs in the pneumothorax test dataset, and 1 FP and 3 FNs in the chest tube test dataset. Since a two-stage algorithm was implemented, the confusion matrix of the testing data of the pneumothorax on the chest cube model was also identified (Appendix A). We detected 1 out of 1 images with both pneumothorax and chest tube, and 5 out of 5 images with chest tube only.

The results showed that when the model was applied to out-of-sample images, the model still provided sufficient detecting power. Table 2 shows the performance data of the pneumothorax model on the test dataset (F1-score: 0.8800; precision: 0.8594; sensitivity: 0.9016; specificity: 0.9313; accuracy:

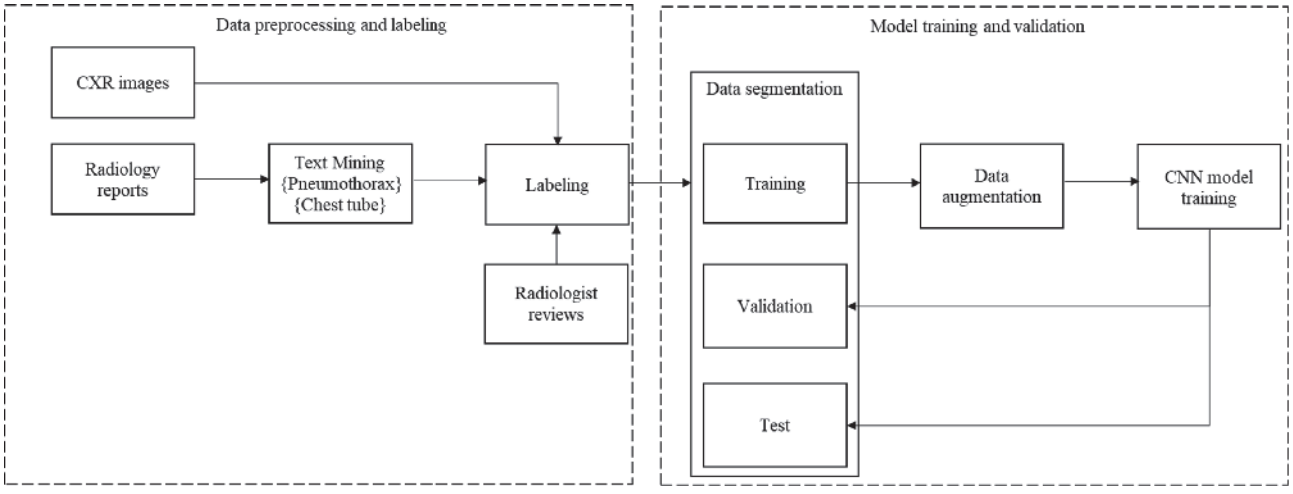

Fig. 1 CNN framework used to detect pneumothorax and chest tube.

Table 2. Results of image identification and model evaluation

Label	Dataset	Metrics					
		F1 score	Precision	Sensitivity	Specificity	Accuracy	AUROC
Pneumothorax	Validation	0.9402	0.9649	0.9167	0.9846	0.9632	0.9685
	Test	0.8800	0.8594	0.9016	0.9313	0.9219	0.9638
Chest tube	Validation	0.9964	0.9928	1.0000	0.9885	0.9956	0.9997
	Test	0.9854	0.9926	0.9783	0.9885	0.9822	0.9968

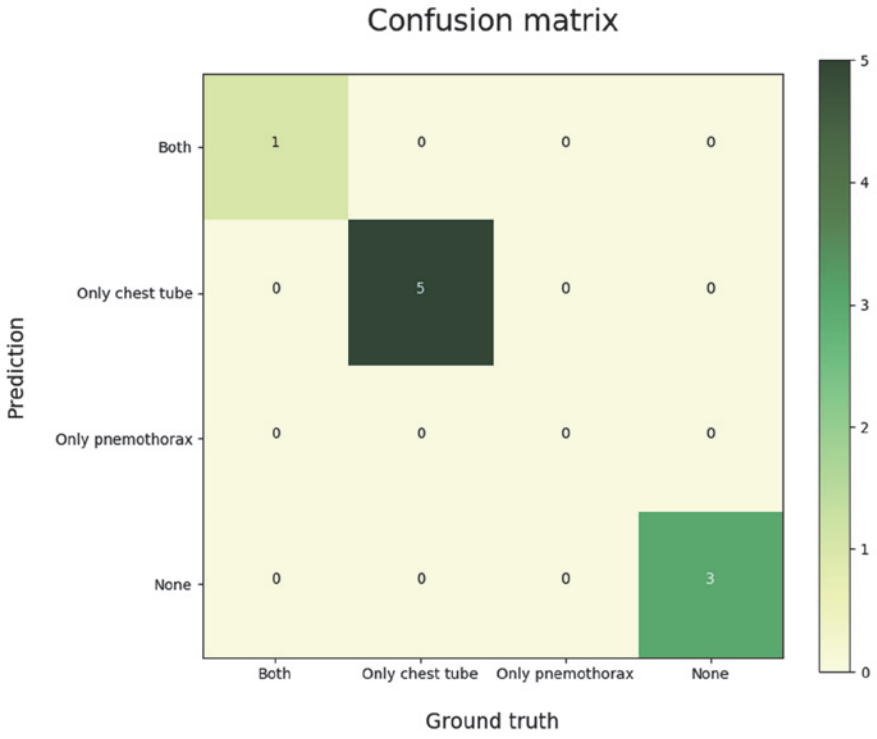

Appendix A Confusion matrix of the testing data of pneumothorax on the chest cube model.

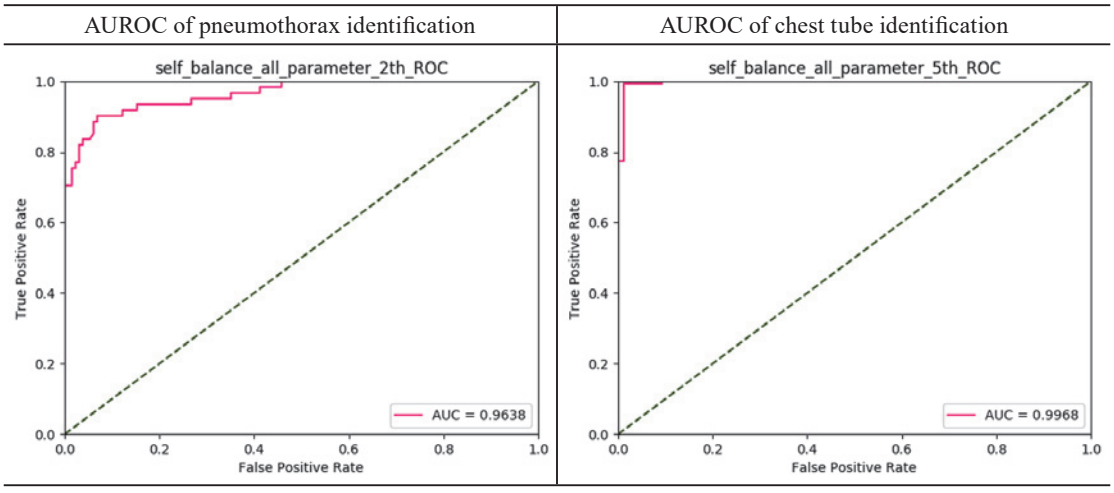

Appendix B AUROC of pneumothorax and chest tube model

0.9219, AUROC: 0.9638). The data indicate that this AI model remained robust even with the new dataset. Furthermore, the metrics for the chest tube AI model showed that the model performed even better than the pneumothorax one (F1-score: 0.9854; precision: 0.9926; sensitivity: 0.9783; specificity: 0.9885; accuracy: 0.9822; AUROC: 0.9968). The AUROC of the two models are shown in Appendix B. The Youden index optimization obtained the thresholds of 0.5054 for pneumothorax and 0.6656 for chest tubes on the validation datasets. However, this change did not improve the accuracy of our original setting (threshold = 0.5) on the test datasets. The inference time of the pneumothorax AI model's on a 768 × 768 pixel CXR image took only 0.6 second, whereas that of the chest tube AI model on a 512 × 512 pixel CXR image took 0.2 second.

We use the class activation mapping (CAM) technique to generate heat maps that highlighted the pneumothorax location (Figures 2B, 2D, and 2F). The

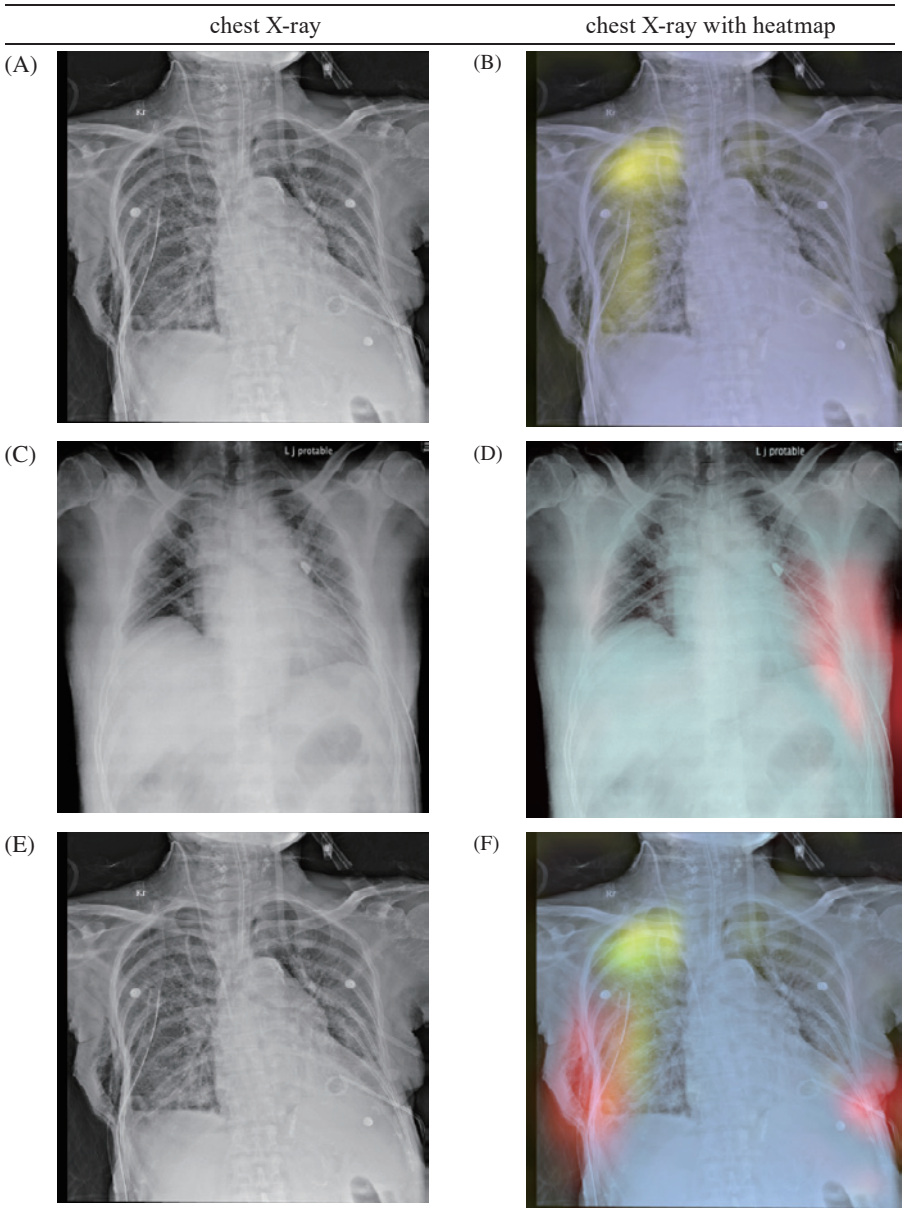

Fig. 2 Representative images of (A) pneumothorax, (C) chest tube, (E) coexisting pneumothorax and chest tube, and their (B, D, and F) corresponding heat map images, respectively. The (B) bright yellow area indicates the location of the pneumothorax. The (D) red area indicates the location of the left-side chest tube. The (F) bright yellow area highlights the pneumothorax in the right upper thorax, whereas the red areas depict the right-side chest tube and the pigtail drainage tube through the left chest wall.

heat map precisely indicates the extent of the pneumothorax extent both in the right thorax and the left costo-phrenic angle (Figure 2B).

Discussion

Deep learning techniques have been widely applied in medical imaging in recent years. Four types of applications are usually involved: image classification, image detection, image segmentation, and image registration. Image classification in deep learning generally involves categorizing into binary or multi-class disease parameters[11]. Liu et al[12]. reviewed studies on deep learning methods of classifying diseases using medical imaging and found that ophthalmic diseases, cancers, trauma and orthopedics, and respiratory diseases were the primary diseases in the imaging field. Image detection refers to localizing objects on the images, such as using bounding boxes on the target areas[13,14]. The applications of deep learning in image segmentation could help physicians identify precise outlines of objects. Image registration is the process of aligning multiple types of image contents. A comprehensive review of deep learning in image registration was conducted by Fu et al[15]. Regardless of the deep learning methods or medical imaging types, these studies aimed to provide a more accurate and faster disease recognition system for physicians. On top of that, the AI-based results showed promising evidence compared with the performance of healthcare professionals[12].

Our study applied the CNN model (MobileNetV2) in identifying pneumothorax and chest tubes on CXR images. These classification models demonstrated superior performance (AUC = 0.9638 and 0.9968 for pneumothorax and chest tube, respectively; accuracy = 0.9219 and 0.9822 for pneumothorax and chest tube, respectively). Previous studies have used deep learning algorithms in detecting and localizing pneumothorax and chest tubes on either CXR images or CT images. For example, Gooßen et al[16]. applied three deep learning algorithms in detecting and localizing pneumothorax and obtained AUCs of 0.96, 0.93, and 0.92. Wang et al[17]. proposed a CNN model to localize pneumothorax, and obtained an AUC of 0.80–0.86 from six settings. Park et al[18]. also applied deep learning techniques in detecting pneumothorax after biopsy on CXR images and compared results with those of previous studies. They obtained a sensitivity of 0.78–0.954 and a specificity of 0.78–0.964.

We identify three valuable contributions of our study. First, we highlighted the importance of quality control in labeling. With highly consistent, two-stage labeling (labeled by radiology technologists and then verified by one radiologist), the deep learning model could learn the precise image characteristics based on unambiguous ground truth. The high accuracy and AUC obtained support this argument. Second, an ensemble of pneumothorax and chest tube AI models in one prediction process can enhance the clinical usability of AI. The presence of both pneumothorax and chest tube on a CXR image implies that the patient with pneumothorax has been treated by chest tube drainage. In other words, this ensemble AI can accurately distinguish emergent, newly onset

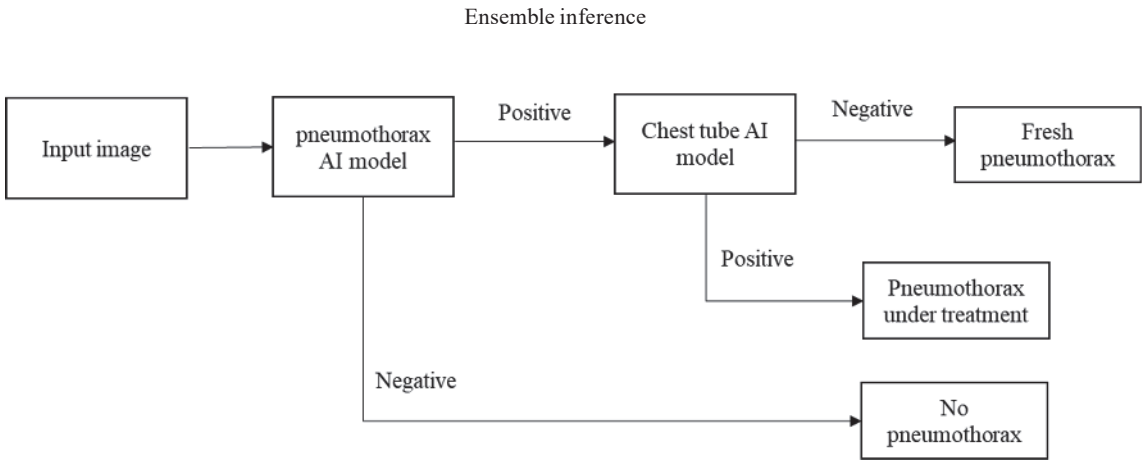

Fig. 3 Framework of pneumothorax diagnosis using the proposed AI model.

pneumothorax from non-emergent post-treatment pneumothorax (Figure 3). Lastly, the automatic localization by CAM technique provides a visualization of the spread of the pneumothorax and helps users identify the lesions quicker. Unlike object detection or segmentation techniques, it gets rid of the burden of manually drawing the disease area while labeling and thus spares a lot of labeling time.

This study has limitations. First, the sample size is limited because imaging staff usually do not have much time and extra physical energy for labeling. Second, the precision (0.8594) for the pneumothorax model is not satisfactory, which results in a high frequency of false readings based on the low prevalence of the disease. Thus, continuous improvement of the AI model and the quality of data labeling is imperative. The development of more sophisticated ensemble models that satisfy clinical requirements should be considered in future studies.

Conflicts of interest

All authors have no conflicts of interest to declare.

Acknowledgment

This study was funded by the project (TTMHH-R1100002, TTMHH-108R0038, and TTMHH-108R0039) of Tungs' Taichung MetroHarbor Hospital.

Reference

1. Thelle A, Gjerdevik M, SueChu M, Hagen OM, Bakke P. Randomised comparison of needle aspiration and chest tube drainage in spontaneous pneumothorax. Eur Respir J. 2017;49(4):1601296.
2. Zhang M, Liu Z-H, Yang J-X, et al. Rapid detection of pneumothorax by ultrasonography in patients with multiple trauma. Crit Care. 2006;10(4):R112.
3. Ministry of Health and Welfare. Statistics of Medical Care Institution's Status & Hospital Utilization 2019. Published 2020. Accessed November 25, 2020. https://www.mohw.gov.tw/cp-4932-54834-2.html
4. Russell S, Norvig P. Artificial intelligence: a modern approach. In: 4th ed. Pearson; 2020:1-2.
5. Yu K-H, Beam AL, Kohane IS. Artificial intelligence in healthcare. Nat Biomed Eng. 2018;2(10):719-731.
6. Ravì D, Wong C, Deligianni F, et al. Deep learning for health informatics. IEEE J Biomed Heal informatics. 2016;21(1):4-21.
7. Wang X, Peng Y, Lu L, Lu Z, Bagheri M, Summers RM. Chestx-ray8: Hospital-scale chest x-ray database and benchmarks on weakly-supervised classification and localization of common thorax diseases. In: Proceedings of the IEEE Conference on Computer Vision and Pattern Recognition.; 2017:2097-2106.
8. Rajpurkar P, Irvin J, Zhu K, et al. Chexnet: Radiologist-level pneumonia detection on chest x-rays with deep learning. arXiv Prepr arXiv171105225. Published online 2017.
9. Ayan E, Ünver HM. Diagnosis of Pneumonia from Chest X-Ray Images Using Deep Learning. In: 2019 Scientific Meeting on Electrical-Electronics & Biomedical Engineering and Computer Science (EBBT). IEEE; 2019:1-5.
10. Sandler M, Howard A, Zhu M, Zhmoginov A, Chen L-C. Mobilenetv2: Inverted residuals and linear bottlenecks. In: Proceedings of the IEEE Conference on Computer Vision and Pattern Recognition. IEEE; 2018:4510-4520.
11. Pandey SK, Janghel RR. Recent deep learning techniques, challenges and its applications for medical healthcare system: A review. Neural Process Lett. 2019;50(2):1907-1935.
12. Liu X, Faes L, Kale AU, et al. A comparison of deep learning performance against health-care professionals in detecting diseases from medical imaging: a systematic review and meta-analysis. lancet Digit Heal. 2019; 1(6):e271-e297.
13. Ghesu FC, Georgescu B, Mansi T, Neumann D, Hornegger J, Comaniciu D. An artificial agent for anatomical landmark detection in medical images. In: International Conference on Medical Image Computing and Computer-Assisted Intervention. Springer; 2016:229-237.
14. Zheng Y, Liu D, Georgescu B, Nguyen H, Comaniciu D. 3D deep learning for efficient and robust landmark detection in volumetric data. In: International Conference on Medical Image Computing and Computer-Assisted Intervention. Springer; 2015:565-572.
15. Fu Y, Lei Y, Wang T, Curran WJ, Liu T, Yang X. Deep learning in medical image registration: a review. Phys Med Biol. 2020;65(20):20TR01.
16. Gooßen A, Deshpande H, Harder T, et al. Deep Learning for Pneumothorax Detection and Localization in Chest Radiographs. arXiv Prepr arXiv190707324. Published online 2019.
17. Wang H, Gu H, Qin P, Wang J. CheXLocNet: Automatic localization of pneumothorax in chest radiographs using deep convolutional neural networks. PLoS One. 2020;15(11):e0242013.
18. Park S, Lee SM, Kim N, et al. Application of deep learning–based computer-aided detection system: detecting pneumothorax on chest radiograph after biopsy. Eur Radiol. 2019;29(10):5341-5348.

使用類神經網絡在 X 光影像上檢測氣胸

游人達[1,+] 林彥瑞[2,+] 賴治群[2] 張祐剛[3] 黃棟國[4]
李政君[5] 曾能泉[6] 蔡耀德[7,*] 翁紹仁[8,*]

童綜合醫療社團法人童綜合醫院
院長室[1] 資訊部[2] 醫學研究部[3] 高級健康檢查中心[4] 放射診療科[5] 核子醫學部[6]
[7]逢甲大學 國際經營與貿易學系
[8]東海大學 工業工程與經營資訊學系

受文日期：民國 109 年 12 月 08 日；接受刊載：民國 110 年 02 月 19 日

摘要

背景及目的：Chest X-Ray（CXR）影像為診斷氣胸最重要之第一線工具，氣胸會對生命造成威脅，而放置胸管來引流空氣為目前治療氣胸的主要方式。本研究之主要目的為建立 AI 模型來判讀 CXR 影像上有無氣胸，並且建立輔助的模型偵測胸管，雖氣胸會對生命造成威脅，但胸管的存在則表示已接受治療。在臨床上，影像判讀出有胸管則表示氣胸的症狀已非緊急，因此本研究提出一結合的 AI 模型來分辨新形成及接受治療過後的氣胸。本研究旨在使用 AI（Artificial Intelligence）作為胸部影像判讀的輔助工具，使準確率提昇及品質均一化，與提昇診斷的效率。

方法：本研究基於 MobileNet V2 的類神經網路方式將有無氣胸做二元分類，輸入資料庫是由放射師做標註並由放射科醫師審查，胸管亦是以同樣方法標註。

結果：對氣胸及胸管的辨識準確度可達 92.19% 及 98.22%，AUC 值分別為 0.9638 及 0.9968，每張影像的判讀時間更僅只有 0.21 至 0.6 秒。

討論：本 AI 模型達到令人滿意的結果並能在未來導入醫療資訊系統，以用於協助緊急氣胸之早期偵測。

關鍵詞：類神經網路、深度學習、胸部、X 光、氣胸、胸管

[+] 第一作者
* 通訊作者：蔡耀德助理教授 逢甲大學 國際經營與貿易學系 台中市 40724 西屯區文華路 100 號
翁紹仁教授 東海大學 工業工程與經營資訊學系 407224 台中市西屯區台灣大道四段 1727 號

Original Article

Clinical Characteristics of Spinal Muscular Atrophy

Hueng-Chuen Fan[1,2,5], Yu-Kang Chang[2,5], Bio-Chia Show[3], Yi-Yu Chen[2], Li-Ting Wang[4], Hui-Ching Yang[4], Ching-Shiang Chi[1,*]

[1]Department of Pediarics, [2]Department of Medical research, [3]Department of Clincal pathology, [4]Department of Nursing, Tungs' Taichung MetroHarbor Hospital, Taichung, Taiwan
[5]Jen-Teh Junior College of Medicine, Nursing and Management, Miaoli, Taiwan.

Received: Jul. 01, 2020; Accepted: Aug. 12, 2020

Abstract

Spinal muscular atrophy (SMA) is a genetic disorder. The mutated homozygous *SMN1* affects the survival of motor neurons in the spinal cord, ultimately leading to muscle atrophy and weakness, which often cause scoliosis, joint contractures, and restrictive lung function resulting in frequent pneumonia and death. The definite diagnosis of SMA relies on typical clinical characteristics, electromyogram changes, muscle biopsy, changes in serum creatine kinase levels, and gene analysis. Advancements in molecular and bio-technology have generated several promising therapeutic approaches aimed at treating SMA, which was once thought to be incurable. This study aimed to summarize the clinical characteristics of SMA and provide comprehensive information regarding the disease that would be valuable in improving current medical care and in clinical trials involving patients with SMA in a local teaching hospital.

Key words: Spinal muscular atrophy (SMA), survival motor neuron (SMN)

Introduction

Spinal muscular atrophy (SMA) is an inherited degenerative disease involving α motor neurons that cause hypotonia, reduced to absent deep tendon reflexes, symmetrical proximal weakness, muscle atrophy, paralysis, and even death in childhood[1, 2]. The International SMA Consortium classification system classifies SMA into three types based on the wide array of clinical manifestations, severity, age at onset, achievement of milestones, prognosis, and typical life span of patients[3,4]. Type I SMA (Werdnig–Hoffman disease; MIM# 253300) is the most severe form, with clinical onset generally occurring before the age of 6 months, wherein which the child never achieves the ability to sit. Type II SMA (MIM# 253550) is of intermediate severity, with onset between 7–18 months. Most patients with type II SMA are able to sit without support but can never stand and walk independently. They usually survive beyond 10 years. Type III SMA (Kugelberg–Welander disease; MIM# 253400) is a mild form of the disease with onset after the age of 18 months. Even with proactive respiratory and nutritional management, patients with type I typically die in the first 2 years of life. Both SMA type II and III may lose motor milestones over time[5].

SMA is autosomal recessive; however, autosomal dominant and X-linked inheritance has been documented[6]. The reported incidence is about 1 in 10,000 live births with a carrier frequency of 1 in 50[7]. Consanguineous marriage increases the risk of the disease in the family. Genetic studies have mapped the locus for the three clinical types of SMA to chromosome 5q13 and refined it to the location of the survival motor neuron (*SMN*) gene[8]. Two highly homologous copies of *SMN*, telomeric *SMN* (*SMN1*) and centromeric *SMN* (*SMN2*), have been identified[8]. Approximately 94% of patients with SMA were homozygous for the absence of *SMN1*, leaving the subject with a limited amount of SMN

*Correspondence to: Dr. Ching-Shiang Chi, Department of Pediarics, Tungs' Taichung MetroHarbor Hospital, No.699, Sec. 8, Taiwan Blvd., Taichung City 435, Taiwan (R.O.C.)

protein produced by the remaining copies of *SMN2*[9]. *SMN2* is a duplication of *SMN1* that differs by only 5 nucleotides. As the protein generated by the *SMN2* is rapidly degraded, motor neurons in the spinal and cranial regions will selectively and progressively degenerate, leading to weakness, debilitation, and death[10]. Therefore, the amount of SMN protein is inversely correlated with the severity of disease[8]. Moreover, several compound heterozygous subjects with various deletions and point mutations have been reported[11]. The complete absence of the SMN protein in cells has also been found lethal in mice embryo and other organisms[12], suggesting a likelihood of prenatal onset and death. The American College of Medical Genetics has recommended the routine carrier screening for SMA in the general population because of its high carrier frequency and disease severity[13].

The accurate assessment of SMA motor function in combination with *SMN* gene studies helps determine the functional prognosis. The expanded Hammersmith functional motor scale (HFMSE)[14] can accurately assess the functional ability of patients with SMA and has been correlated with the primary outcome in a randomized clinical trial. In this study, we aimed to describe the clinical characteristics of SMA, including sex, onset age, gene data, prenatal history, delivery modes, birth weight, and clinical manifestations. We used the HFMSE to measure the motor functions of subjects with SMA and to correlate the findings with their genetic data.

Patients and methods

Subjects and enrolled criteria

This was a retrospective chart review of patients with SMA hospitalized in a local teaching hospital from January 2015 to December 2019. The data evaluated in this study were as follows: (i) inpatient and outpatient records with a diagnosis of SMA, International Classification of Disease 2008 code (Code numbers 335.0, 335.10, 335.11, and 335.19); (ii) demographic features including prenatal history, birth weight, presenting complaints at admission or at healthcare seeking, consanguinity, developmental delay or early death/s within the family, onset age (defined as the age at which the first abnormalities became evident, based on the descriptions from parents about the first signs of weakness, delayed motor milestones, or loss of functions), sex, disease progression, involvement of respiratory or bulbar muscles, joint contracture, scoliosis, and pneumonia; (iii) symptoms including generalized hypotonia, muscle weakness in upper or all limbs, muscle atrophy, tongue fasciculation, and decreased or absent deep tendon reflexes[1]; (iv) motor function evaluation with the HFMSE (lower scores indicate poorer motor function)[15]; and (v) genetic analysis. All patients were diagnosed with SMA based on the criteria established by the International SMA Consortium[3]. This study was approved by the institutional ethical review committee (IRB No: 108035).

Genetic studies

Genomic DNA from peripheral whole blood was prepared by standard phenol/chloroform extraction procedures[16]. Quantitative real-time polymerase chain reaction was used to detect the numbers of SMN1 and *SMN2* copies to determine *SMN1* and *SMN2* expressions. The *SMN* copies were amplified using the forward primer 5¢ -AATGCTTTTTAACATCCATATAAAGCT-3¢ and the reverse primer 5¢ -CCTTAATTTAAGGAATGTGAGCACC -3¢ under the following amplification conditions: one cycle at 50°C for 2 min, one cycle at 95°C for 10 min, followed by 40 cycles of 95°C for 15 sec and 60°C for 1 min for a total volume of 25 mL containing 50 ng of genomic DNA, 0.3 mM of each primer, 13 mL Platinum qPCR Supermix-UDG (Invitrogen, Karlsruhe, Germany), 0.5 mM 6-carboxy-X-rhodamine (ROX) as a passive reference (Invitrogen), 2 mM $MgCl_2$, and 100 nmol of each probe. Quantification and analysis were performed using an ABI Prism 7000 sequence detection system. All procedures were modified from those described in a previous study[17]. All patients' genetic studies were performed by the Sofiava Genomics Co., Ltd., Taipei, Taiwan.

Statistical analysis

All values were expressed as mean ± standard deviation. The quantification data on the *SMN2* copy numbers and HFMSE scores were analyzed using Student's t-test. A p value < 0.05 was considered statistically significant.

Results

Functional assessment of SMA

The chart review retrieved seven eligible

cases involving three boys and four girls for further analysis. Five patients (71.4%) were SMA types II, and two patients (28.6%) were SMA type III (Table 1). No SMA type I were identified in this study considering this classification entails rapid disease progression, a short life span, and high mortality. The onset age varied considerably from 12 months to as late as 36 months. Motor functions were evaluated with HFMSE, which contains 33 items that are divided into sitting, rolling, transitions/crawling, standing/stepping, transitions/kneeling, squat/jumping, and climbing stairs. Each item is scored on a scale of 0–2. The total scores for SMA type II and SMA type III ranged from 16 to 21 and from 53 to 61, respectively.

Correlation between motor function and SMN2 copy number in SMA

In this study, all patients showed homozygous deletions of *SMN1* (100%). Molecular studies showed that the number of *SMN2* copies in SMA types II and III were 3 and 4, respectively (Table 1). The statistical analysis showed that *SMN* copy number was significantly correlated with the functional assessment results (Figure 1, $p < 0.005$).

Clinical features of SMA

No prenatal anomalies were noted in the chart records. The mean birth weights for SMA types II and III were 3389 ± 434.2 g and 3055 ± 572.8 g,

Table 1. Onset age, sex, classification, *SMN* copy number, and functional assessment with the Expanded Hammersmith Functional Motor Scale of patients with spinal muscular atrophy

Case	1	2	3	4	5	6	7
Onset age (Mo) /Gender	12/F	13/F	36/M	12/F	12/F	36/M	15/M
SMA type	II	II	II	II	II	III	III
SMN2 copy No	3	3	3	3	3	4	4
HFMSE							
Sitting	2	3	1	2	2	6	8
Rolling	2	1	1	1	1	5	9
Transitions/Crawling	8	5	5	6	6	14	16
Standing/stepping	2	2	2	2	2	5	5
Transitions/kneeling	3	3	3	3	3	12	12
Squat/jumping	1	1	1	1	1	3	3
Stairs	3	3	3	4	3	8	8
Total	21	18	16	19	18	53	61

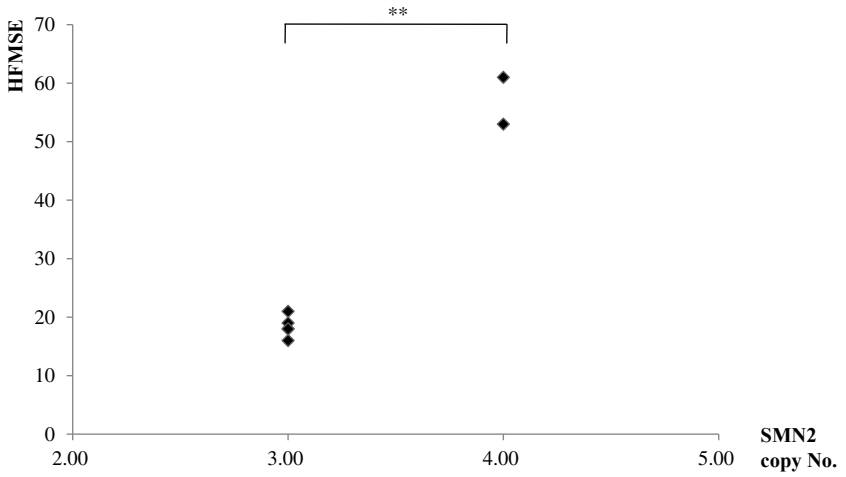

Fig. 1 Correlation between *SNM2* copy number and the Expanded Hammersmith Functional Motor Scale (HFMSE) score. Each black diamond represents a subject with SMA. ** $p < 0.005$.

Table 2. Clinical manifestations of patients with SMA

Type	SMA II	SMA III
Case no. n (%)	5 (71.4)	2 (28.6)
Prenatal anomalies	–	–
Birth weight (g)	3389±434.2	3055±572.8
Onset age (mo)	17±10.6	25.5±14.8
Floppy at birth	5 (100)	0 (0)
Delayed motor milestones	5 (100)	2 (100)
Weakness: only legs	3 (60)	2 (100)
arms and legs	2 (40)	0 (0)
Muscle atrophy	5 (100)	0 (0)
Tongue trembling	2 (40)	0 (0)
Bulbar paralysis	0 (0)	0 (0)
Paradoxical breath	0 (0)	0 (0)
Decreased or absent DTR	5 (100)	0 (0)
Pneumonia	5 (100)	2 (100)
Scoliosis	2 (40)	1 (50)
Joint contracture	5 (100)	1 (50)

respectively. The mean onset age for SMA types II and III was 17 ± 10.6 months and 25.5 ± 14.8 months, respectively (Table 2). Symptoms analysis showed that infantile hypotonia was only found in SMA type II (100%) and none in type III. All patients regardless of SMA type had a history of delayed achievement of motor milestones. Forty percent of patients with SMA type II and none with SMA type III showed weakness in both arms and legs. Furthermore, 60% of patients with SMA type II and 100% of patients with SMA type III showed weakness involving bilateral legs. These findings confirm the greater disease severity in SMA type II than in SMA type III. Muscle atrophy and decreasing or absent deep tendon reflex were only observed in all patients with SMA type II. Furthermore, 40% of patients with SMA type II presented with tongue fasciculations. No bulbar paralysis and paradoxical paralysis were found in any patient. The chart review further revealed that all patients had prior history of pneumonia. Orthopedic deformities such as scoliosis were found in two cases (40%) with SMA type II and one with type III (50%), whereas joint contracture was observed in all patients with type II (100%) and in one with type III (50%).

Discussion

Onset age and age at achievement of motor function milestones are important parameters in the disease course of SMA and in classification by clinical type[15]. In this study, the average ages of onset for SMA types II and III were 17 ± 10.6 and 25.5 ± 14.8 months, respectively. Zerres et al.[18] retrospectively analyzed the natural history of 445 patients with SMA and found that the age of onset for types II and III were 8.6 ± 4.4 months and 17.9 ± 7.2 months, respectively. Souchon et al.[19] retrospective investigated 63 patients with SMA types II and III in Canada and observed that onset age in types II and III were 0.8 ± 0.3 years and 1.8 ± 1.5 years, respectively. The discrepancy between our study and others may be due to the recall effect. Nevertheless, our results showed that the onset age for type II was earlier than that for type III. A slightly high prevalence of females was noted in the present study, which may be due to the small sample size. In previous reports, patients with SMA have been predominantly male[20,21].

Although the disease progresses later in the life span, patients with SMA exhibit a wide range of motor functions, from being very weak, unable to sit, and unable to play sports. Subjective and easy quantitative assessments are needed to evaluate these motor functions, and the scales should be specific and to the unique motor behaviors age-appropriate[22]. Several motor scales have been established to evaluate patients with SMA, such as the Children's Hospital of Philadelphia Infant Test of Neuromuscular Disorders designed for SMA type I[23], Bayley Scales of Infant Development for assessing motor function in normal children[24], Hammersmith Infant Neuromuscular Examination Section 2[25] for SMA infants[26], HFMS[27] for SMA type II with limited mobility[27], and HFMSE. The HFMSE was built upon the HFMS by incorporating 13 items from the Gross Motor Function Measure, an instrument designed for patients with cerebral palsy[28]. It consists of 33 activities with a maximum item scoring of 66. Each item is scored from 0 for unable to perform, 1 for performs with modification/adaptation, to 2 for performs without modification. The higher the total score, the greater the patient's motor function[15]. HFMSE can accurately represent the clinical picture and functional ability of patients with SMA and has been used as the primary outcome measure in a randomized clinical trial in SMA[14].

Homozygous deletion of *SMN1* is the gold standard for the diagnosis and absence of exon

7 and/or exon 8 in *SMN1*. This deletion has been observed in 95% of SMA cases[29,30]. Such mutations in the *SMN1* alter RNA processing to inhibit SMN protein production, leading to the pathophysiology of SMA. The *SMN2* is a near-identical copy but with a critical difference at the exon 7 or 8 splice site, which causes a reduced amount of full-length protein to be translated[31]. As several reports concluded that no difference in the frequencies of the *SMN1* exon 7 and/or 8 deletion among the three SMA phenotypes[32], the present study therefore did not further investigate the incidence rates of mutated *SMN* exons 7 and 8.

Furthermore, 95% of patients with SMA type I have only 1–2 copies of *SMN2*, whereas almost all patients belonging to type III had 3 or more copies[33], suggesting that patients with multiple copies may generate more full-length proteins that in turn lessen severity. In the present study, patients with SMA type II had 3 *SMN2* copies, whereas patients with SMA type III had 4 *SMN* copies. The data not only showed that the total HFMSE scores were positively correlated with *SMN2* copy number, thus affirming that clinical motor function is correlated with *SMN2* copy number[34], but also showed that the total HFMSE scores of female patients with SMA type II were higher than male patients with SMA type II, demonstrating that that clinical course of SMA is more severe in males than in females[20].

No consanguineous marriages and no family members with early deaths or with developmental delays prior to death were found in our cases, although a high prevalence of SMA has been reported in Middle East Asia because consanguineous marriages are very common in that region[35]. Different cultural backgrounds may affect the incidence rate of SMA. Many patients with SMA may have had prenatal onset, and most were SMA type I[7,36]. No patients had prenatal onset in the present study.

A paper reported that lower birth weight may be linked to poor prognosis of SMA type I[37]. The birth weight in our cases was within the normal range because most patients enrolled in the study were SMA type II or III, although a retrospective study showed 20% of SMA type II who died at 15 years and 4.9% of SMA type III who had retained ambulatory function in their teenage years were floppy infants at birth[38]. In our series, only cases with SMA type II showed floppiness at birth and were subsequently confined to a wheelchair. No cases with type III showed floppiness at birth. Our results suggest that patients with SMA type II tended to present floppiness at birth.

Studies showed that 75% of SMA type II maintained the ability to sit after the age of 7 years independent of onset age; in the type III group, 50% of patients with onset before 2 years lost the ability to walk[39]. In the present study, patients with both SMA types II and III all showed delayed motor milestones, and medical records showed that patients with SMA type II progressively became confined to a wheelchair after disease onset. However, patients with type III showing delayed motor milestones were still ambulatory. Therefore, delayed motor milestones do not necessarily correlate with motor function prognosis.

Bulbar paralysis and paradoxical breathing are common in SMA type I and very rarely in types II and III[40], which is compatible with our findings. Muscular weakness is the cardinal symptom of SMA. This study showed that weakness in the legs occurred in 60% of SMA type II and 100% of SMA type III. However, weakness in the arms and legs only presented in SMA type II but not in type III, suggesting that patients with SMA types II and III may present variable levels of weakness in different limbs. Muscle atrophy, tongue fasciculations, and areflexia were noted in SMA type II but not in SMA type III.

Bone- and joint-associated deformity is common in SMA[41]. In this study, 100% of SMA type II and 50% of type III developed joint contractures and foot deformities. Scoliosis is also more common in type II than in type III[18,42]. We noted that muscular weakness led to progressive scoliosis in some of our cases. The combination of respiratory muscle weakness and scoliosis may result in restrictive lung disease[41], leading to a high incidence of pneumonia (100% in types II and III). Convergently, these variable features and the spectrum of disease severity in SMA suggest that SMA is not solely a lower motor neuron disease but a multi-system disorder.

This study had several limitations. First, this study only enrolled 7 patients. Larger samples are needed to further explain the relationships between genetic data and clinical manifestations of SMA. Second, this study is retrospectively designed. A prospective study may have fewer potential sources of bias and confounding factors than a retrospective one. Third, this study is cross-sectional

in design. A longitudinal study will be able to describe developments and changes in the characteristics of the patients with SMA over a longer observation period and thus will be able to elucidate the impacts of *SMN* copy numbers and clinical presentations. These limitations may have led to some biases in the analysis of the clinical characteristics in the present study.

Patients with SMA demonstrate a wide array of characteristics and spectrum of severity. Making an accurate diagnosis and classification is currently challenging because of the variable features and onset age of SMA. Our findings confirm that SMA may be a multi-system disorder but is not solely a disease of lower motor neuron function. Increased understanding of the etiology and pathogenesis of SMA in recent years has led to the development of several potential therapeutic approaches such as nusinersen, a modified antisense oligonucleotide that modulates the splicing of the *SMN2* mRNA transcript. It is the first drug approved for all types of SMA. Gene therapy, such as Zolgensma, has been approved by the U.S. Food and Drug Administration. The approval was based on a clinical trial using adeno-associated virus vectors encoding *SMN*, which reported positive results in survival and motor milestones achievement[43]. In addition, progress has been made on other specific approaches, such as the modulation of *SMN2* transcripts[44-46], neuroprotection[47-49], and the use of stem cells[50]. Based on these developments, therapeutic approaches aimed at treating SMA will soon create meaningful changes in the treatment and clinical management of SMA.

Consent and ethical approval

The current study was approved by the institutional review board (IRB) of Tungs' taichung metroharbor hospital, Taichung, Taiwan (approval number 108035). IRB issued consent for waiver of informed consent for this retrospective chart review study.

Acknowledgments

This work was supported by grants from the Tungs' MetroHarbor Hospital (TTMHH-109C00002, TTMHHR0001, and TTMHH-109R0002). The funders had no role in the study design, data collection and analysis, decision to publish, or preparation of the manuscript.

Reference

1. Hausmanowa-Petrusewicz I, Vrbova G. Spinal muscular atrophy: a delayed development hypothesis. Neuroreport 2005;16:657-61.
2. Swoboda KJ, Prior TW, Scott CB, McNaught TP, Wride MC, Reyna SP, et al. Natural history of denervation in SMA: relation to age, SMN2 copy number, and function. Ann Neurol 2005;57:704-12.
3. Munsat TL, Davies KE. International SMA consortium meeting. (26-28 June 1992, Bonn, Germany). Neuromuscul Disord 1992;2:423-8.
4. Zerres K, Rudnik-Schoneborn S. 93rd ENMC international workshop: non-5q-spinal muscular atrophies (SMA) - clinical picture (6-8 April 2001, Naarden, The Netherlands). Neuromuscul Disord 2003;13:179-83.
5. Kaplan JC. Gene table of monogenic neuromuscular disorders (nuclear genome only) Vol 19. No 1 January 2009. Neuromuscul Disord 2009;19:77-98.
6. Salahshourifar I, Shafeghati Y, Golkar Z, Najmabadi H. Molecular analysis of the neuronal apoptosis inhibitory protein gene in families with spinal muscular atrophy. Arch Iran Med 2007;10:509-13.
7. Lunn MR, Wang CH. Spinal muscular atrophy. Lancet 2008;371:2120-33.
8. Lefebvre S, Burglen L, Reboullet S, Clermont O, Burlet P, Viollet L, et al. Identification and characterization of a spinal muscular atrophy-determining gene. Cell 1995;80: 155-65.
9. Wirth B, Herz M, Wetter A, Moskau S, Hahnen E, Rudnik-Schoneborn S, et al. Quantitative analysis of survival motor neuron copies: identification of subtle SMN1 mutations in patients with spinal muscular atrophy, genotype-phenotype correlation, and implications for genetic counseling. Am J Hum Genet 1999;64:1340-56.
10. Kolb SJ, Kissel JT. Spinal muscular atrophy: a timely review. Arch Neurol 2011;68:979-84.
11. Lorson CL, Hahnen E, Androphy EJ, Wirth B. A single nucleotide in the SMN gene regulates splicing and is responsible for spinal muscular atrophy. Proc Natl Acad Sci U S A 1999;96:6307-11.
12. Cheng D, Cote J, Shaaban S, Bedford MT. The arginine methyltransferase CARM1 regulates the coupling of transcription and mRNA processing. Mol Cell 2007;25:71-83.
13. Prior TW, Professional P, Guidelines C. Carrier screening for spinal muscular atrophy. Genet Med 2008;10:840-2.
14. Pera MC, Coratti G, Forcina N, Mazzone ES, Scoto M, Montes J, et al. Content validity and clinical meaningfulness of the HFMSE in spinal muscular atrophy. BMC Neurol 2017;17:39.
15. Glanzman AM, O'Hagen JM, McDermott MP, Martens WB, Flickinger J, Riley S, et al. Validation of the Expanded Hammersmith Functional Motor Scale in spinal muscular atrophy type II and III. J Child Neurol 2011;26:1499-507.
16. Lee MY, Cheng SN, Chen SJ, Huang HL, Wang CC, Fan HC. Polymorphisms of the beta2-adrenergic receptor correlated to nocturnal asthma and the response of terbutaline nebulizer. Pediatr Neonatol 2011;52:18-23.
17. Su YN, Hung CC, Li H, Lee CN, Cheng WF, Tsao PN, et al. Quantitative analysis of SMN1 and SMN2 genes based on DHPLC: a highly efficient and reliable carrier-screening test. Hum Mutat 2005;25:460-7.
18. Zerres K, Rudnik-Schoneborn S. Natural history in prox-

imal spinal muscular atrophy. Clinical analysis of 445 patients and suggestions for a modification of existing classifications. Arch Neurol 1995;52:518-23.
19. Souchon F, Simard LR, Lebrun S, Rochette C, Lambert J, Vanasse M. Clinical and genetic study of chronic (types II and III) childhood onset spinal muscular atrophy. Neuromuscul Disord 1996;6:419-24.
20. Ar Rochmah M, Shima A, Harahap NIF, Niba ETE, Morisada N, Yanagisawa S, et al. Gender Effects on the Clinical Phenotype in Japanese Patients with Spinal Muscular Atrophy. Kobe J Med Sci 2017;63:E41-E44.
21. Chung BH, Wong VC, Ip P. Spinal muscular atrophy: survival pattern and functional status. Pediatrics 2004;114:e548-53.
22. Finkel RS, Hynan LS, Glanzman AM, Owens H, Nelson L, Cone SR, et al. The test of infant motor performance: reliability in spinal muscular atrophy type I. Pediatr Phys Ther 2008;20:242-6.
23. Glanzman AM, Mazzone E, Main M, Pelliccioni M, Wood J, Swoboda KJ, et al. The Children's Hospital of Philadelphia Infant Test of Neuromuscular Disorders (CHOP INTEND): test development and reliability. Neuromuscul Disord 2010;20:155-61.
24. Bayley N. Bayley Scales of Infant and Toddler Development: Administration Manual. 3rd. San Antonio, TX: Harcourt Assessment, 2006.
25. Haataja L, Mercuri E, Regev R, Cowan F, Rutherford M, Dubowitz V, et al. Optimality score for the neurologic examination of the infant at 12 and 18 months of age. J Pediatr 1999;135:153-61.
26. Bishop KM, Montes J, Finkel RS. Motor milestone assessment of infants with spinal muscular atrophy using the hammersmith infant neurological Exam-Part 2: Experience from a nusinersen clinical study. Muscle Nerve 2018; 57:142-146.
27. Krosschell KJ, Maczulski JA, Crawford TO, Scott C, Swoboda KJ. A modified Hammersmith functional motor scale for use in multi-center research on spinal muscular atrophy. Neuromuscul Disord 2006;16:417-26.
28. O'Hagen JM, Glanzman AM, McDermott MP, Ryan PA, Flickinger J, Quigley J, et al. An expanded version of the Hammersmith Functional Motor Scale for SMA II and III patients. Neuromuscul Disord 2007;17:693-7.
29. Beattie CE, Carrel TL, McWhorter ML. Fishing for a mechanism: using zebrafish to understand spinal muscular atrophy. J Child Neurol 2007;22:995-1003.
30. Zhang Z, Lotti F, Dittmar K, Younis I, Wan L, Kasim M, et al. SMN deficiency causes tissue-specific perturbations in the repertoire of snRNAs and widespread defects in splicing. Cell 2008;133:585-600.
31. Monani UR, Lorson CL, Parsons DW, Prior TW, Androphy EJ, Burghes AH, et al. A single nucleotide difference that alters splicing patterns distinguishes the SMA gene SMN1 from the copy gene SMN2. Hum Mol Genet 1999;8:1177-83.
32. Vijzelaar R, Snetselaar R, Clausen M, Mason AG, Rinsma M, Zegers M, et al. The frequency of SMN gene variants lacking exon 7 and 8 is highly population dependent. PLoS One 2019;14:e0220211.
33. Mailman MD, Heinz JW, Papp AC, Snyder PJ, Sedra MS, Wirth B, et al. Molecular analysis of spinal muscular atrophy and modification of the phenotype by SMN2. Genet Med 2002;4:20-6.
34. Feldkotter M, Schwarzer V, Wirth R, Wienker TF, Wirth B. Quantitative analyses of SMN1 and SMN2 based on real-time lightCycler PCR: fast and highly reliable carrier testing and prediction of severity of spinal muscular atrophy. Am J Hum Genet 2002;70:358-68.
35. Ibrahim S, Moatter T, Saleem AF. Spinal muscular atrophy: clinical spectrum and genetic mutations in Pakistani children. Neurol India 2012;60:294-8.
36. Koul R, Al Futaisi A, Chacko A, Rao V, Simsek M, Muralitharan S, et al. Clinical and genetic study of spinal muscular atrophies in Oman. J Child Neurol 2007;22:1227-30.
37. Park HB, Lee SM, Lee JS, Park MS, Park KI, Namgung R, et al. Survival analysis of spinal muscular atrophy type I. Korean J Pediatr 2010;53:965-70.
38. Tonali P, Servidei S, Uncini A, Restuccia D, Galluzzi G. Clinical study of proximal spinal muscular atrophy. Report on 89 cases. Ital J Neurol Sci 1984;5:423-32.
39. Russman BS, Buncher CR, White M, Samaha FJ, Iannaccone ST. Function changes in spinal muscular atrophy II and III. The DCN/SMA Group. Neurology 1996;47:973-6.
40. Kolb SJ, Kissel JT. Spinal Muscular Atrophy. Neurol Clin 2015;33:831-46.
41. Wijngaarde CA, Stam M, Otto LAM, van Eijk RPA, Cuppen I, Veldhoen ES, et al. Population-based analysis of survival in spinal muscular atrophy. Neurology 2020;94:e1634-e1644.
42. Zerres K, Wirth B, Rudnik-Schoneborn S. Spinal muscular atrophy--clinical and genetic correlations. Neuromuscul Disord 1997;7:202-7.
43. Mendell JR, Al-Zaidy S, Shell R, Arnold WD, Rodino-Klapac LR, Prior TW, et al. Single-Dose Gene-Replacement Therapy for Spinal Muscular Atrophy. N Engl J Med 2017; 377:1713-1722.
44. Bertini E, Dessaud E, Mercuri E, Muntoni F, Kirschner J, Reid C, et al. Safety and efficacy of olesoxime in patients with type 2 or non-ambulatory type 3 spinal muscular atrophy: a randomised, double-blind, placebo-controlled phase 2 trial. Lancet Neurol 2017;16:513-522.
45. Finkel RS, Chiriboga CA, Vajsar J, Day JW, Montes J, De Vivo DC, et al. Treatment of infantile-onset spinal muscular atrophy with nusinersen: a phase 2, open-label, dose-escalation study. Lancet 2016;388:3017-3026.
46. Nizzardo M, Simone C, Salani S, Ruepp MD, Rizzo F, Ruggieri M, et al. Effect of combined systemic and local morpholino treatment on the spinal muscular atrophy Delta7 mouse model phenotype. Clin Ther 2014;36:340-56 e5.
47. Chali F, Desseille C, Houdebine L, Benoit E, Rouquet T, Bariohay B, et al. Long-term exercise-specific neuroprotection in spinal muscular atrophy-like mice. J Physiol 2016; 594:1931-52.
48. Lewelt A, Krosschell KJ, Stoddard GJ, Weng C, Xue M, Marcus RL, et al. Resistance strength training exercise in children with spinal muscular atrophy. Muscle Nerve 2015;52:559-67.
49. Madsen KL, Hansen RS, Preisler N, Thogersen F, Berthelsen MP, Vissing J. Training improves oxidative capacity, but not function, in spinal muscular atrophy type III. Muscle Nerve 2015;52:240-4.
50. Adami R, Bottai D. Spinal Muscular Atrophy Modeling and Treatment Advances by Induced Pluripotent Stem Cells Studies. Stem Cell Rev Rep 2019;15:795-813.

脊髓性肌肉萎縮症的臨床特徵

范洪春[1,2,5] 張祐剛[2,5] 邵寶釵[3] 陳怡妤[2] 王俐婷[4] 楊惠菁[4] 遲景上[1,*]

童綜合醫療社團法人童綜合醫院 兒童醫學部[1] 醫學研究部[2] 臨床病理科[3] 護理部[4]
[5]仁德醫護管理專科學校護理科

受文日期：民國 109 年 07 月 01 日；接受刊載：民國 110 年 08 月 12 日

摘要

脊髓肌肉萎縮症（SMA）是一種基因的疾病。由於突變的同型合子存活運動神經元（SMN）影響脊髓上的運動神經元，最終導致肌肉萎縮和無力，造成脊柱側彎，關節攣縮和侷限性肺功能，導致經常性肺炎以及死亡。SMA 的確認診斷主要依據臨床特徵、肌電圖的變化、肌肉切片、血清中肌酐酸激酶以及基因檢查。SMA 以往被認為是無法治療的疾病，先進的分子醫學技術以一直持續改進、改善、深具意義的方式，發展出具有潛力有前景的 SMA 治療方法。因此，本研究想以一個教學醫院近 5 年的病歷，來分析 SMA 病人的臨床特徵，包括性別、發病年齡、基因、產前病史、生產模式、出生體重以及臨床症狀，除了可以提供 SMA 的完整訊息，改善醫療照護，更有助執行患有 SMA 病人的臨床試驗。

關鍵詞：脊髓肌肉萎縮症、同型合子存活運動神經元

* 通訊作者：遲景上醫師 童綜合醫療社團法人童綜合醫院 兒童醫學部
43503 臺中市梧棲區臺灣大道八段 699 號

Original Article

Hysteroscopic Resection and Laparoscopy in Fertility-Sparing Surgery for Early Endometrial Cancer and Complex Atypical Hyperplasia: A Single Institutional Experience

Kim-Seng Law*

Department of Obstetrics and Gynecology, Tungs' Taichung Metroharbor Hospital, Taichung, Taiwan

Received: Jul. 24, 2020; Accepted: Oct. 21, 2020

Abstract

Background and purpose: To analyze the oncological and fertility outcomes in patients with early endometrial cancer (EC) or complex atypical hyperplasia (CAH) treated with hysteroscopic tumor resection with or without laparoscopic staging before progestin treatment.

Methods: This study evaluated women undergoing hysteroscopic resection of tumors diagnosed as early endometrioid adenocarcinoma or CAH with or without laparoscopic evaluation of the pelvic cavity before initiating progestin treatment. Response rates were evaluated 6 months after the procedure, with conception encouraged as applicable following a complete response.

Results: Six patients with early EC and three with CAH underwent surgical resection. The complete response rate was 77% (100% in CAH and 66% in early EC), with two patients showing persistent disease after 6 months of treatment. No patients showed evidence of disease after a median follow-up of 23 months (range 8–124 months). In the patients who sought conception, the live birth rate was 60%. Three recurrences were observed within an average of 24 months after the initial complete response.

Discussion: Hysteroscopic resection for early EC and CAH with or without laparoscopy enables accurate staging and creates a favorable microenvironment for future childbearing without compromising the patients' oncological and reproductive outcomes.

Key words: endometrial cancer, fertility-sparing surgery, hysteroscopy, laparoscopy, levonorgestrel-releasing intrauterine device

Introduction

Endometrial cancer (EC) is the most common gynecological cancer in Taiwan[1], with most cases occurring in the sixth decade of life. Around 3%–5% of affected patients are under the age of 40 years[2], which poses a unique challenge for physicians aiming to preserve patient fertility while ensuring favorable oncologic outcomes.

*Correspondence to: Dr. Kim-Seng Law, Department of Obstetrics and Gynecology, Tungs' Taichung Metroharbor Hospital, No.699, Sec. 8, Taiwan Blvd., Taichung City 435, Taiwan (R.O.C.)

Fertility-sparing surgery has been advocated for women who are clinically diagnosed with stage 1 grade 1 EC, can comply with progestin treatment, and have a strong desire to conceive[3]. However, synchronous or metastatic ovarian involvement can occur in up to 29% of presumed stage 1 EC patients under the age of 40 years[4,5,6]. Furthermore, conventional progestin-only treatment combined with the inherent disadvantages of relying solely on conventional imaging studies incurs a high risk of upstaging or, worse, jeopardizing the outcomes.

Hysteroscopic resection with or without laparoscopic pelvic evaluation to eliminate gross endometrial lesions may be useful for a subset of patients

with early-stage EC diagnosed on clinical evaluation. This approach facilitates the more complete and accurate resection of the lesion and makes the endometrial microenvironment more favorable and responsive to subsequent progestin therapy[6-12].

This study aimed to investigate the impact of hysteroscopic resection with or without laparoscopy in fertility-sparing surgery in patients with early EC or complex atypical hyperplasia (CAH).

Methods

This study was approved by the Institutional Review Board of Tungs' Taichung Metroharbor Hospital. Nine patients diagnosed with stage 1 grade 1 EC (six patients) or CAH (three patients) between January 1, 2007, and October 31, 2018, were included. All patients were treated with curative intent using dilatation and curettage (D&C) followed by hysteroscopic resection. Hysteroscopic resection was performed under general anesthesia with a 10-mm 0° resectoscope. The uterus was distended using normal saline under an inflow pressure of 100 mmHg. A 5-mm electrode loop with 100 W of cutting power was used for partial myometrial resection of the tumor and the endometrium adjacent to the tumor. Laparoscopic evaluation of the abdominal and pelvic cavity was performed in all patients with EC and in one with CAH, with suspicious sites biopsied. The first two patients underwent retroperitoneal lymphadenectomy. Laparoscopic adhesiolysis and/or ablation of pelvic endometriosis were performed where appropriate.

After surgical intervention, all patients received a levonorgestrel-releasing intrauterine device (LNG-IUD) 20 μg (Mirena, Bayer) 1 week following the confirmation of pathological stage 1 grade 1 EC or CAH, with or without one of the following medications: oral megestrol acetate (160–320 mg QD), medroxyprogesterone acetate (MPA; 500 mg QD), or gonadotropin-releasing hormone agonist (leuprorelin; 3.75 mg IM QM) ± metformin (500 mg QD) for a total of 6 months. The LNG-IUD was removed 6 months after insertion during an outpatient hysteroscopy, during which endometrial curettage was performed to determine the final pathological response.

Complete response was defined as histological regression to the normal endometrium, whereas progression was defined as the worsening of CAH to EC or grade 1 stage 1 EC to a higher grade or stage on histology. Partial response was defined as regression from adenocarcinoma to atypical CAH or CAH to simple or complex hyperplasia without atypia and persistence without any histological changes before and after treatment.

Post-treatment conception was encouraged as soon as possible after the confirmation of a pathologically complete response with either spontaneous conception or assisted reproductive technology (ART). For patients not desiring pregnancy in the near future, the reinsertion of LNG-IUD with or without oral progestin was administered as maintenance therapy. Patients not willing to conceive in the future or those who had completed childbearing were advised to undergo definitive surgery and were closely followed up every 3 months during the first 2 years.

Results

The demographics of the study population are shown in Table 1. The mean age at the time of diagnosis was 32 years (range 27–34 years), the mean body mass index (BMI) was 28.6 kg/m^2, and the mean preoperative serum anti-Mullerian hormone (AMH) level was 4.73 ng/mL.

All patients with early EC underwent hysteroscopic resection and laparoscopic pelvic evaluation before progestin treatment, and two of the patients with CAH underwent hysteroscopic resection only. The oncological outcomes in the nine patients are shown in Table 2. A pathologically complete response was attained in 77% (7/9) (100% in CAH and 66% in EC) of patients after 6 months of treatment. Of the remaining patients, one had a persistent lesion, and another achieved a partial response (from EC to CAH). Both patients underwent definitive treatment with laparoscopic-assisted vaginal hysterectomy and bilateral salpingectomy with transposition of the ovaries.

Three patients experienced disease recurrence. Patient 1 showed recurrence after 96 months of follow-up with an initial complete response. The patient had given birth to a live term baby. Remission was achieved again after reinsertion of the LNG-IUD, but the attempt for a second baby failed due to chronic anovulation and male-factor infertility. She experienced a second recurrence after 18 months (114 months from the initial diagnosis) and

Table 1. Demographics of stage 1, grade 1 endometrial cancer patients

No.	Age at diagnosis (years) (32.1 ± 4.4)	BMI (kg/m^2) (28.6 ± 6.8)	AMH (4.73 ± 3.6)	Gravidity	Parity	ER/PR	Diagnosis	Stage	Grade	Follow-up (median = 23 months)
1	23	31.0	1.55	0	0	+ / +	Endometrioid cancer	I	1	124
2	34	28.0	7.60	0	0	+ / +	Endometrioid cancer	I	1	84
3	30	22.6	7.30	0	0	+ / +	Endometrioid cancer	I	2	55
4	29	41.7	-	0	0	+ / +	Endometrioid cancer	I	1	12
5	32	24.7	10.70	0	0	+ / +	Endometrioid cancer	I	1	10
6	34	27.8	4.84	0	0	+ / +	Endometrioid cancer	I	1	9
7	33	36.5	0.59	0	0	+ / +	Endometrioid cancer (EIN)	0	-	23
8	37	23.9	4.06	2	2	- / +	Complex atypical hyperplasia	-	-	25
9	37	21.2	1.17	0	0	+ / +	Complex atypical hyperplasia	-	-	8

Values are presented as mean ± standard deviation, unless otherwise stated. BMI, body mass index; AMH, anti-Mullerian hormone; ER/PR, estrogen receptors/progesterone receptors; EIN, endometrial intraepithelial neoplasia.

Table 2. Progesterone treatments and outcomes among patients with early stage endometrial cancer

No	Conservation treatment	Disease status	Tumour reaction	Conceive	Oral progesterone	IUD	ART utilisation	Live birth	Recurrence	Treatment after recurrence
1	TCR + Laparoscopy	NED	Resolved	Yes	Farlutal	Mirena	No	Yes	Yes	Hysterectomy + BS
2	TCR + Laparoscopy	NED	Resolved	Yes	Metformin	Mirena	Yes	Yes	Yes	TCR + Laparoscopy + Mirena
3	TCR + Laparoscopy	NED	Resolved	Yes	Farlutal + Metformin + Megace	Mirena	Yes	No	No	
4	TCR + Laparoscopy	NED	Persistent	No	-	Mirena	No	No	No	Hysterectomy + BS
5	TCR + Laparoscopy	NED	Persistent	No	Metformin	Mirena	No	No	No	Hysterectomy + BS
6	TCR + Laparoscopy	NED	Resolved	No	-	Mirena	No	No	No	
7	TCR + Laparoscopy	NED	Resolved	Yes	Farlutal + Metformin	Mirena	Yes	No	No	
8	TCR	NED	Resolved	Yes	Farlutal + Megace + Leuprolide acetate	Mirena	Yes	Yes	No	
9	TCR	NED	Resolved	No	-	Mirena	No	No	No	

TCR, transcervical resectoscopy; NED, no evidence of disease; IUD, intrauterine device; ART, assisted reproductive technology; BS, bilateral salpingectomy.

underwent definitive surgical management with laparoscopic-assisted hysterectomy and bilateral salpingectomy with preservation of both ovaries. The patient was followed up at our department every 3 months with no evidence of disease at the time of writing.

Patient 2 experienced recurrence at 59 months following an initial complete response. The patient had also given birth to a healthy term baby. She underwent hysteroscopic resection and reinsertion of the LNG-IUD and attained complete response at the time of writing.

The third recurrence was observed in Patient 3 after 21 months with initial regression (from EC to CAH). Remission was attained after retreatment with progestin. She did not have a clinical pregnancy due to a failed embryo transfer following the first complete remission. A second recurrence with EC grade 2 was observed 61 months from the first diagnosis. The patient was treated with a second hysteroscopic resection with LNG-IUD combined with oral dienogest (Visanne, Bayer) and subsequently showed no further evidence of disease.

The obstetric outcomes of those who sought conception are shown in Table 2. Among five attempted pregnancies, three (60%) involved the deliveries of single term babies. One patient (Patient 3), who had conceived through in-vitro fertilization/embryo transfer, had three embryo transfers aborted soon after implantation. Another patient (Patient 7) with low serum AMH had three follicle harvests but failed to conceive through ART.

Discussion

Fertility-sparing surgery is recommended for early EC patients of reproductive age who wish to preserve their childbearing ability[3,4,7-9,11,13-28]. The best candidates are patients with early EC (endometrioid histology stage 1 grade 1 without myoinvasion) who are able to receive progestin and have a strong desire to conceive shortly after treatment. Most importantly, the patient should be aware of the non-conventional nature of the treatment protocol[3,28].

The major concerns with fertility-sparing surgery are the inaccuracy of conventional clinical staging[29,30] and the risk of ovarian metastasis or synchronous ovarian cancer in young women with early EC, which has an incidence ranging from 4.5% to 29%[4-6,26,31]. Therefore, ovarian involvement in patients with early EC need to be ruled out, and this is most accurately done through surgical staging. Additional benefits of laparoscopic evaluation include pelvic adhesiolysis, ablation of pelvic endometriosis, and ovarian drilling in polycystic ovary syndrome, which might positively impact future pregnancies.

Previous studies have reported that up to 40% of patients with CAH have invasive EC[32,33]. In these cases, fractional D&C and complete resection are recommended, as they allow for comprehensive pathological evaluation. Hysteroscopic resection enables a more precise resection of the lesion and therefore more accurate disease staging by assessing the depth of myometrial invasion. This technique also facilitates a more favorable microenvironment upon which progestin can act after the surgery.

Previous studies by Mentrikoski *et al*. (2012) and Wheeler *et al*. (2007) have proposed 6 months as the most appropriate cut-off time for the assessment of pathological response in patients receiving progestin for fertility-sparing treatment. This was also verified in a phase II study by Ushijima *et al*. (2007), where a complete response was attained in 92% cases after 26 weeks of treatment.

Our series demonstrated oncological (77%) and reproductive response rates (60%) comparable to those of historical cohorts[13,17,18,23,24,26,27,34,35]. Considering the short interval of pathological assessment (6 months post-progestin vs. 9–12 months in other series), this was a satisfactory response. The favorable outcome could be attributed to better stratification of patients to the true stage 1 grade 1 group and resection of the endometrial lesion, which optimized the effect of the LNG-IUD inserted thereafter. LNG-IUD has been found superior to oral progestin alone in the treatment of endometrial hyperplasia, but not in EC[36]. The combination of both oral progestin and LNG-IUD has been advocated by some authors[15,36,37] and it should be considered in the future due to its direct and persistent action, especially in those with obesity and chronic anovulation.

The recurrence rate of fertility-sparing treatment in EC has previously been reported to range from 24%–41%, with a mean time to recurrence of 15–35 months[18,21,23,24,27,37]. The recurrence rate in our study was similar at 43%, but we observed a longer mean time to recurrence of 53.6 months.

Definitive treatment with hysterectomy should be offered to patients who have completed their families and those without fertility aspirations because late recurrence can occur in the long term, as shown in previous studies and in our series. Although retreatment of recurrent disease is feasible[37], the high risk of subsequent recurrence remains a challenging clinical problem.

This study has limitations. First, this was a retrospective study that included only a small number of cases. Second, recall biases might have occurred during data retrieval for future analysis. Third, the heterogeneity of progestin treatment poses difficulties in assessing the consistent effect of progestin. Most importantly, a standardized method for resecting lesions should be established with laparoscopic sentinel lymph node assessments replacing complete lymphadenectomy in suitable cases.

Future protocols should establish consistent postoperative regimens to determine a better response. Further genetic testing for Lynch syndrome, also known as hereditary nonpolyposis colorectal cancer, should be considered for young women seeking fertility-sparing options.

Our study demonstrates that hysteroscopic resection and laparoscopic staging in young women with early EC opting for fertility-sparing surgery can yield comparable oncological and reproductive results with the benefit of more accurate staging and a favorable endometrial environment.

Funding: None

Disclosure statement: The author reports no conflict of interest.

Data deposition: Not applicable.

References

1. Lai JCY, Weng CS, Huang SM, et al. Incidence and lifetime risk of uterine corpus cancer in Taiwanese women from 1991 to 2010. Taiwan J Obstet Gynecol. 2017;56:68-72. DOI: 10.1016/j.tjog.2015.09.010
2. Duska LR, Garrett A, Rueda BR, Haas J, Chang Y, Fuller AF. Endometrial cancer in women 40 years old or younger. Gynecol Oncol. 2001;83:388-393. DOI: 10.1006/gyno.2001.6434
3. Laurelli G, Di Vagno G, Scaffa C, Losito S, Del Giudice M, Greggi S. Conservative treatment of early endometrial cancer: preliminary results of a pilot study. Gynecol Oncol. 2011;120:43-46. DOI: 10.1016/j.ygyno.2010.10.004
4. Walsh C, Holschneider C, Hoang Y, Tieu K, Karlan B, Cass I. Coexisting ovarian malignancy in young women with endometrial cancer. Obstet Gynecol. 2005;106:693-699. DOI: 10.1097/01.AOG.0000172423.64995.6f
5. Signorelli M, Caspani G, Bonazzi C, Chiappa V, Perego P, Mangioni C. Fertility-sparing treatment in young women with endometrial cancer or atypical complex hyperplasia: a prospective single-institution experience of 21 cases. BJOG Int J Obstet Gynaecol. 2009;116:114-118. DOI: 10.1111/j.1471-0528.2008.02024.x
6. Alonso S, Castellanos T, Lapuente F, Chiva L. Hysteroscopic surgery for conservative management in endometrial cancer: a review of the literature. Ecancermedicalscience. 2015;9:505. DOI: 10.3332/ecancer.2015.505
7. Montz FJ, Bristow RE, Bovicelli A, Tomacruz R, Kurman RJ. Intrauterine progesterone treatment of early endometrial cancer. Am J Obstet Gynecol. 2002;186:651-657. DOI: 10.1067/mob.2002.122130
8. Mazzon I, Corrado G, Masciullo V, Morricone D, Ferrandina G, Scambia G. Conservative surgical management of stage IA endometrial carcinoma for fertility preservation. Fertil Steril. 2010;93:1286-1289. DOI: 10.1016/j.fertnstert.2008.12.009
9. Shan BE, Ren YL, Sun JM, et al. A prospective study of fertility-sparing treatment with megestrol acetate following hysteroscopic curettage for well-differentiated endometrioid carcinoma and atypical hyperplasia in young women. Arch Gynecol Obstet. 2013;288:1115-1123. DOI: 10.1007/s00404-013-2826-8
10. Kalogera E, Dowdy SC, Bakkum-Gamez JN. Preserving fertility in young patients with endometrial cancer: current perspectives. Int J Womens Health. 2014;6:691-701. DOI: 10.2147/IJWH.S47232
11. Marton I, Vranes HS, Sparac V, Maricic I, Kuna K, Kopjar M. Two cases of successful pregnancies after hysteroscopic removal of endometrioid adenocarcinoma grade I, stage IA, in young women with Lynch syndrome. J Turk Ger Gynecol Assoc. 2014;15:63-66. DOI: 10.5152/jtgga.2013.69379
12. Yang B, Xu Y, Zhu Q et al. Treatment efficiency of comprehensive hysteroscopic evaluation and lesion resection combined with progestin therapy in young women with endometrial atypical Hyperplasia and endometrial cancer. Gynecol Oncol. 2019;153:55-62. DOI: https://doi.org/10.1016/j.ygyno.2019.01.014
13. Dijkhuizen FP, Mol BW, Brolmann HA, Heintz AP. The accuracy of endometrial sampling in the diagnosis of patients with endometrial carcinoma and hyperplasia: a meta-analysis. Cancer. 2000;89:1765-1772. DOI: 10.1002/1097-0142(20001015)89:8<1765::aid-cncr17>3.0.co;2-f
14. Jadoul P, Donnez J. Conservative treatment may be beneficial for young women with atypical endometrial hyperplasia or endometrial adenocarcinoma. Fertil Steril. 2003;80:1315-1324. DOI: 10.1016/s0015-0282(03)01183-x
15. Trimble CL, Kauderer J, Zaino R, et al. Concurrent endometrial carcinoma in women with a biopsy diagnosis of atypical endometrial hyperplasia: a Gynecologic Oncology Group study. Cancer. 2006;106:812-819. DOI: 10.1002/cncr.21650
16. Ushijima K, Yahata H, Yoshikawa H, et al. Multicenter phase II study of fertility-sparing treatment with medroxyprogesterone acetate for endometrial carcinoma and atypical hyperplasia in young women. J Clin Oncol. 2007;25:2798-2803. DOI: 10.1200/JCO.2006.08.8344

17. Jamie N. Bakkum-Gamez, Eleftheria Kalogera, Gary L. Keeney, Andrea Mariani, Karl C. Podratz, and Sean C. Dowdy. Conservative management of atypical hyperplasia and grade I endometrial carcinoma: Review of the literature and presentation of a series. Journal of gynecologic surgery. 2012;28:262-269. https://doi.org/10.1089/gyn.2012.0011
18. Gallos ID, Yap J, Rajkhowa M, Luesley DM, Coomarasamy A, Gupta JK. Regression, relapse, and live birth rates with fertility-sparing therapy for endometrial cancer and atypical complex endometrial hyperplasia: a systematic review and metaanalysis. Am J Obstet Gynecol. 2012;207:266.e1-266.12. DOI: 10.1016/j.ajog.2012.08.011
19. Gunderson CC, Fader AN, Carson KA, Bristow RE. Oncologic and reproductive outcomes with progestin therapy in women with endometrial hyperplasia and grade 1 adenocarcinoma: a systematic review. Gynecol Oncol. 2012;125:477-482. DOI: 10.1016/j.ygyno.2012.01.003
20. Mentrikoski MJ, Shah AA, Hanley KZ, Atkins KA. Assessing endometrial hyperplasia and carcinoma treated with progestin therapy. Am J Clin Pathol. 2012;138:524-534. DOI: 10.1309/AJCPM2TSDDF1MHBZ
21. Kim MK, Seong SJ, Kim YS, et al. Combined medroxyprogesterone acetate/levonorgestrel–intrauterine system treatment in young women with early-stage endometrial cancer. Am J Obstet Gynecol. 2013;209:358.e1-358.e4. DOI:https://doi.org/10/1016/j.ajog/2013/06/031
22. Park JY, Kim DY, Kim JH, et al. Long-term oncologic outcomes after fertility-sparing management using oral progestin for young women with endometrial cancer (KGOG 2002). Eur J Cancer. 2013;49:868-874. DOI: 10.1016/j.ejca.2012.09.017
23. Koskas M, Uzan J, Luton D, Rouzier R, Daraï E. Prognostic factors of oncologic and reproductive outcomes in fertility-sparing management of endometrial atypical hyperplasia and adenocarcinoma: systematic review and meta-analysis. Fertil Steril. 2014;101:785-794. DOI: 10.1016/j.fertnstert.2013.11.028
24. Simpson AN, Feigenberg T, Clarke BA, et al. Fertility sparing treatment of complex atypical hyperplasia and low grade endometrial cancer using oral progestin. Gynecol Oncol. 2014;133:229-233. DOI: 10.1016/j.ygyno.2014.02.020
25. Arendas K, Aldossary M, Cipolla A, Leader A, Leyland NA. Hysteroscopic resection in the management of early-stage endometrial cancer: report of 2 cases and review of the literature. J Minim Invas Gynecol. 2015;22:34-39. DOI: 10.1016/j.jmig.2014.08.782
26. Pronin SM, Novikova OV, Andreeva JY, Novikova EG. Fertility-sparing treatment of early endometrial cancer and complex atypical hyperplasia in young women of childbearing potential. Int J Gynecol Cancer. 2015;25:1010-1014. DOI: 10.1097/IGC.0000000000000467
27. Qin Y, Yu Z, Yang J, et al. Oral progestin treatment for early-stage endometrial cancer: a systematic review and meta-analysis. Int J Gynecol Cancer. 2016;26:1081-1091. DOI: 10.1097/IGC.0000000000000723
28. Koh WJ, Abu-Rustum NR, Bean S, et al.. Uterine Neoplasms, Version 1.2018, NCCN Clinical Practice Guidelines in Oncology. J Natl Compr Canc Network, version 1.2018. 2018;16:170-199. DOI: 10.6004/jnccn.2018.0006
29. Wheeler DT, Bristow RE, Kurman RJ. Histologic alterations in endometrial hyperplasia and well-differentiated carcinoma treated with progestins. Am J Surg Pathol. 2007;31:988-998. DOI: 10.1097/PAS.0b013e31802d68ce
30. Park JY, Seong SJ, Kim TJ, et al. Pregnancy outcomes after fertility-sparing management in young women with early endometrial cancer. Obstet Gynecol. 2013;121:136-142. DOI: 10.1097/aog.0b013e31827a0643
31. Song T, Seong SJ, Bae DS et al. Synchronous primary cancers of the endometrium and ovary in young women:A Korean Gynecologic Oncology Group Study. Gynecol Oncol. 2013;131:624-628. DOI: 10.1016/j.ygyno.2013.09.009
32. Kudesia R, Singer T, Caputo TA, et al. Reproductive and oncologic outcomes after progestin therapy for endometrial complex atypical hyperplasia or carcinoma. Am J Obstet Gynecol. 2014;210:255.e1-255.e4. DOI: 10.1016/j.ajog.2013.11.001
33. Abu Hashim HA, Ghayaty E, El Rakhawy M. Levonorgestrel-releasing intrauterine system vs oral progestins for non-atypical endometrial hyperplasia: a systematic review and metaanalysis of randomized trials. Am J Obstet Gynecol. 2015;213:469-478. DOI: 10.1016/j.ajog.2015.03.037
34. Wildemeersch D, Janssens D, Pylyser K, et al. Management of patients with non-atypical and atypical endometrial hyperplasia with a levonorgestrel-releasing intrauterine system: long-term follow-up. Maturitas. 2007;57:210-213. DOI: 10.1016/j.maturitas.2006.12.004
35. Varma R, Soneja H, Bhatia K, et al. The effectiveness of a levonorgestrel-releasing intrauterine system (LNG-IUS) in the treatment of endometrial hyperplasia—a long-term follow-up study. Eur J Obstet Gynecol Reprod Biol. 2008;139:169-175. DOI: 10.1016/j.ejogrb.2008.02.022
36. Hawkes AL, Quinn M, Gebski V, et al. feMME trial committee, and Obermair, A. Improving treatment for obese women with early stage cancer of the uterus: rationale and design of the levonorgestrel intrauterine device ± metformin ± weight loss in endometrial cancer (feMME) trial. Contemp Clin Trials. 2014;39:14-21. DOI: 10.1016/j.cct.2014.06.014
37. Park JY, Lee SH, Seong SJ, et al. Progestin re-treatment in patients with recurrent endometrial adenocarcinoma after successful fertility-sparing management using progestin. Gynecol Oncol. 2013;129:7-11. DOI: 10.1016/j.ygyno.2012.12.037

利用子宮鏡和腹腔鏡手術處理欲保留生育能力的早期子宮內膜癌和複雜非典型子宮內膜增生—單一機構經驗

劉錦成*

童綜合醫療社團法人童綜合醫院　婦產科

受文日期：民國 109 年 07 月 24 日；接受刊載：民國 109 年 10 月 21 日

摘要

背景及目的：分析使用黃體激素治療前以子宮鏡及或腹腔鏡處理早期子宮內膜癌（EC）或複雜非典型增生（CAH）的患者的腫瘤預後和生育的結果。

方法：分析在使用黃體激素治療之前曾接受子宮鏡及或腹腔鏡進行骨盆腔評估的早期子宮內膜樣腺癌或複雜性非典型增生的婦女。術後六個月評估其疾病緩解率，並在分析其受孕率。

結果：6 例早期子宮內膜癌患者和 3 例複雜非典型增生患者在開始黃體激素治療之前接受了手術治療。完全緩解率為 77%（複雜非典型增生為 100%，子宮內膜癌為 66%），其中有兩名患者在治療 6 個月後疾病依然存在。平均追蹤 23 個月（8-124 個月）後，沒有患者有復發現象。在欲懷孕婦女當中，活產率為 60%。在那些原本疾病完全緩解的病人當中，有三位於平均 24 個月內復發。

結論：使用子宮鏡及或腹腔鏡癌症分期處理早期子宮內膜癌可得到較準確的癌症分期及創造良好的受孕環境，也不影響患者的癌症預後及活產率。

關鍵詞：子宮內膜癌、保留生育能力的手術、子宮鏡、腹腔鏡、投藥式子宮內避孕器

* 通訊作者：劉錦成醫師　童綜合醫療社團法人童綜合醫院　婦產科　43503 臺中市梧棲區臺灣大道八段 699 號

Tungs' Medical Journal 15 (2021)
The 50th Anniversary of TTMHH 62-66 DOI: 10.3966/207135922021091505009

Case Report

Maternal Inheritance of Deletion of Chromosome 18 q21.3

Hueng-Chuen Fan[1,2], Chen-Tang Yue[1], Ching-Shiang Chi[1], Sin-Yi Liou[3], Cai-Ying Lin[2], Shin-Nan Cheng[1,*]

[1]Department of Pediatrics, [2]Department of Medical Research, [3]Child Development Center, Tungs' Taichung MetroHarbor Hospital, Taichung, Taiwan

Received: Nov. 20, 2020; Accepted: Dec. 08, 2020

Abstract

The 18q deletion syndrome is a rare chromosomal disorder. The phenotype is highly variable but is characterized by central nervous system abnormalities, head and neck dysmorphisms, cardiac anomalies, bone deformities, and cognitive and immune impairment. On chromosome structure analysis, the most common breakpoint of the long arm of the chromosome 18 is at q21.3, and most cases are paternally inherited. However, case reports regarding the specific 18q21.3 deletion are quite few. We report the clinical manifestations in a case of a male infant with 18q21.3 deletion, wherein his and his mother's cytogenetic findings showed a terminal deletion of the long arm of chromosome 18, whereas his father's karyotype was normal. Whole-blood chromosome analysis revealed significant information that narrowed down a possible diagnosis, and genetic information from the parents' karyotypes shed light on the inheritance pattern of the disease.

Key words: 18q deletion syndrome, paternal and maternal inheritance

Introduction

The 18q- syndrome [OMIM #601808] is one of the most common deletion syndromes in humans with an estimated prevalence of about 1 in 40,000 live births[1]. It is caused by a terminal deletion of the long arm of chromosome 18. The phenotypes are characterized by central nervous system abnormalities, head and neck dysmorphisms, cardiac anomalies, and bone deformities. Cognitive and immune impairment are also reported[1-3].

The most common cytogenetic finding of anomalies in chromosome 18 is a deletion of bands q21to qter [MIM #601808][4], but reports regarding the phenotypes of this deletion are scarce[5,6]. Approximately three-fourths of patients had *de novo* deletions, of which 85% were paternal in origin[1,7,8]. Here, we report the case of a male infant with 18q- syndrome who inherited the genetic anomaly from his mother.

*Correspondence to: Dr. Shin-Nan Cheng, Department of Pediatrics, Tungs' Taichung MetroHarbor Hospital, No.699, Sec. 8, Taiwan Blvd., Taichung City 435, Taiwan (R.O.C.)

Case Report

A 4-day-old male newborn, full term with a gestational age of 40 weeks, was the first child born to healthy, non-consanguineous parents after an uneventful pregnancy, delivered through Cesarean section due to prolonged labor. The newborn had a birth weight of 2450 g and APGAR scores of 9 and 10 at 1 and 5 minutes, respectively. No known teratogenic exposures occurred during the pregnancy. As he had presented with frequent vomiting, regurgitation, and lethargy after birth, he was transferred to a teaching hospital for further treatment. At arrival, the clinical examination of the infant revealed a weight of 2.3 kg (less than 3 percentile), height of 47 cm (5–15 percentile), occipito-frontal perimeter of 30.5 cm (less than 3 percentile), and dysmorphic features. Specifically, the infant had a large forehead, hypertelorism, mid-facial hypoplasia, micrognathia, low-set

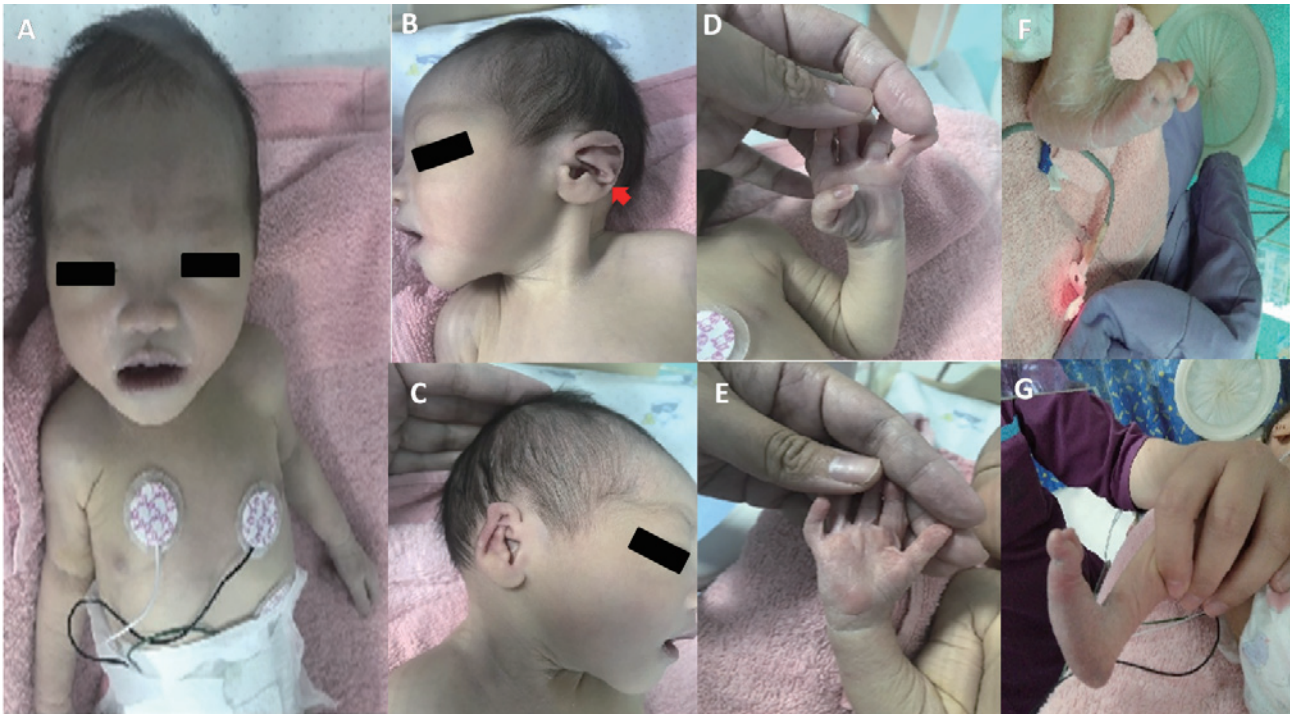

Fig. 1 Clinical features of a boy with a deletion of chromosome 18q21.3. (A) Large forehead, hypertelorism, mid-facial hypoplasia, carp-like lips, and micrognathia; (B) low-set ear with a prominent antihelix (red arrow) and a short neck; (C) the antihelix is not as prominent as the opposite ear; (D&E) small hands and clinodactyly of the 5th fingers; and (F&G) rocker bottom feet.

ears, and malformed earlobes with prominent antihelix, carp-like lips, short neck (Figures 1A–1C), bilateral small hands and clinodactyly of the 5th fingers (Figures 1D and 1E), and rocker bottom feet (Figure 1F and 1G). Neurological examination showed relative weakness of four limbs (3–4/5) and normal deep tendon reflex. Echocardiography showed a secumdum-type atrial septal defect, 0.61 cm (Figure 2A). Brain ultrasonography showed a bilateral thinner corpus callosum (Figures 2B and 2C). Chromosome analysis by Giemsa-trypsin-Giemsa banding showed a deletion of the long arm of chromosome 18, with a breakpoint at 18q21.3, that is, 46, XY, del (18)(q21.3) (Figure 3A). His mother's chromosome analysis showed a similar result, 46, XX, del (18)(q21.3) (Figure 3B). However, his father's karyotype was normal (Figure 3C).

Discussion

The clinical features of this syndrome are highly variable, including central nervous system problems (mental retardation, microcephaly, and hypotonia), eye problems (eye movement disorders, vision problems, and deep-set eyes), ear problems (prominent ears and hearing impairment due to aural stenosis or narrowing of the ear canals or aural atresia or absence of an ear canal), face dysmorphisms (midface hypoplasia, prominent forehead, a wide or carp-like mouth, and micrognathia), endocrine problems (short stature and hypothyroidism), heart problems (congenital heart defects, such as atrial septal defect and pulmonary atresia), urogenital abnormalities, skin problems, and bone problems (including clinodactyly and clubfoot). These features may be collectively noticeable if physicians conduct a detailed physical evaluation on any suspected subject.

In this case, the infant presented nearly all typical 18q- features, but his left prominent antihelix, rocker bottom feet, and thinner corpus callosum were unusual. These clinical findings suggest that the deletion of 18q21.3 may affect mechanisms in the organization of the brain and body parts such as the heart, ears, and bones. Feenstra et al.[9] correlated several phenotypes with the critical region defects, including microcephaly (18q21.33) and short stature (18q12.1–q12.3, 18q21.1–q21.33, and 18q22.3–q23), white matter disorders and delayed

myelination (18q22.3–q23), growth hormone insufficiency (18q22.3–q23), and congenital aural atresia (18q22.3). These correlations may reflect the patient's genetic defects that produced his wide spectrum of clinical features. Moreover, approximately three-fourths of patients had de novo deletions, of which 85% were of paternal in origin[1,7,8]. So far, only two papers have reported the maternal

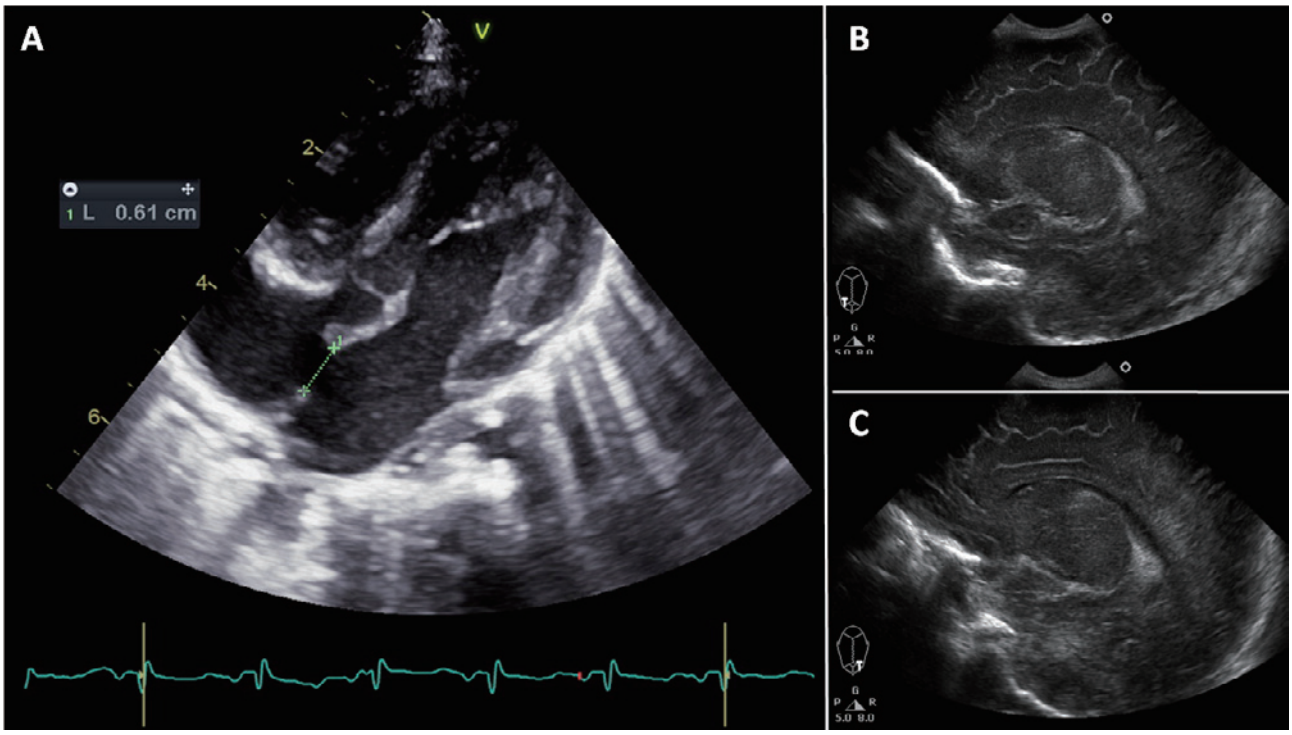

Fig. 2 Sonograms of heart and brain of a boy with a deletion of chromosome 18q21.3. (A) Subcostal 4-chamber view showing a large septal defect between the right and left atria (0.61 cm). Transcranial parasagittal view showing a thinner corpus callosum, (B) right and (C) left views.

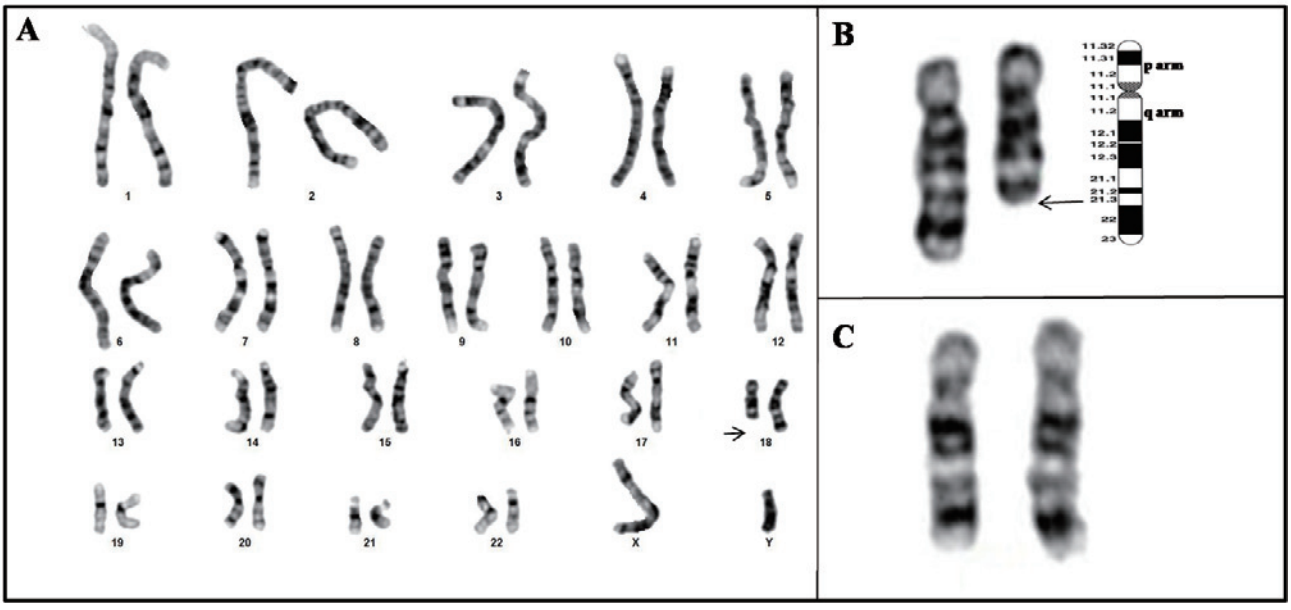

Fig. 3 G-banding karyotype illustrates (A) a deletion of the long arm of chromosome 18, with a breakpoint at 18q21.3 in the proband. (B) Maternal chromosome analysis showing the same deletion at the proband. (C) Normal paternal chromosome 18.

inheritance of chromosome 18 deletions[10,11]. Fryns et al.[11] found identical structural rearrangements between 18q21 and 14p11 in a mother and child, whereas Chen et al. noted the direct transmission of the deletion of 18q22.2 from a mother to her daughter. These cases all presented a short stature, facial dysmorphism, microcephaly, and mental retardation.

The 18q deletion syndrome is a heterogeneous condition with highly variable phenotypes. Since growth hormone insufficiency is mapped to the deletion of 18q22.3–q23, growth hormone therapy may be promising in individuals with 18q deletions, like this case. Psychological surveys should be conducted, and motor and cognitive stimulation may be helpful in subjects with 18q deletions, considering that all references suggest that this male infant has a very high possibility of developing mental retardation and developmental delay in the future. Moreover, we suggest that women with 18q deletion should receive genetic counseling regarding the possible direct transmission of the defect to their children and consider birth control and prenatal genetic studies during their reproductive age.

Reference

1. Cody JD, Pierce JF, Brkanac Z, Plaetke R, Ghidoni PD, Kaye CI, et al. Preferential loss of the paternal alleles in the 18q- syndrome. Am J Med Genet 1997;69:280-6.
2. Dostal A, Linnankivi T, Somer M, Kahkonen M, Litzman J, Tienari P. Mapping susceptibility gene locus for IgA deficiency at del(18)(q22.3-q23); report of familial cryptic chromosome t(18q; 10p) translocations. Int J Immunogenet 2007;34:143-7.
3. Semrud-Clikeman M, Thompson NM, Schaub BL, Leach R, Hester A, Hale DE, et al. Cognitive ability predicts degree of genetic abnormality in participants with 18q deletions. J Int Neuropsychol Soc 2005;11:584-90.
4. Zannolli R, Pierluigi M, Pucci L, Lagrasta N, Gasparre O, Matera MR, et al. 18q-syndrome and ectodermal dysplasia syndrome: description of a child and his family. Am J Med Genet A 2003;116A:192-9.
5. Ghidoni PD, Hale DE, Cody JD, Gay CT, Thompson NM, McClure EB, et al. Growth hormone deficiency associated in the 18q deletion syndrome. Am J Med Genet 1997;69: 7-12.
6. Su PH, Chen JY, Chen SJ, Yang MS, Kao IW, Tsai CY. Deletion of chromosome region 18q21.3-->qter in a patient: clinical, endocrine and imaging abnormalities. Acta Paediatr Taiwan 2007;48:23-7.
7. Martin AO, Simpson JL, Deddish RB, Elias S. Clinical implications of chromosomal inversions. A pericentric inversion in No. 18 segregating in a family ascertained through an abnormal proband. Am J Perinatol 1983;1:81-8.
8. Wertelecki W, Gerald PS. Clinical and chromosomal studies of the 18q- syndrome. J Pediatr 1971;78:44-52.
9. Feenstra I, Vissers LE, Orsel M, van Kessel AG, Brunner HG, Veltman JA, et al. Genotype-phenotype mapping of chromosome 18q deletions by high-resolution array CGH: an update of the phenotypic map. Am J Med Genet A 2007;143A:1858-67.
10. Chen CP, Lin SP, Chern SR, Lee CC, Huang JK, Wang W. Direct transmission of the 18q- syndrome from mother to daughter. Genet Couns 2006;17:185-9.
11. Fryns JP, Logghe N, van Eygen M, van den Berghe H. 18q- syndrome in mother and daughter. Eur J Pediatr 1979;130: 189-92.

母系遺傳的第十八對染色體長臂 q21 缺失

范洪春[1,2] 余震堂[1] 遲景上[1] 劉欣宜[3] 林采縈[2] 錢新南[1,*]

童綜合醫療社團法人童綜合醫院 [1]小兒部 [2]醫學研究部 [3]兒童發展中心

受文日期：民國 109 年 11 月 20 日；接受刊載：民國 109 年 12 月 08 日

摘要

第十八對染色體長臂缺失症後群是一種罕見的染色體異常疾病。其臨床表現是相當的多樣化；包括中樞神經系統、頭頸部、心臟、骨骼系統、認知以及免疫功能的異常等。從結構分析，第十八對染色體長臂的斷裂點最常在 q21.3 處，而且以散發型（sporadic）最多，遺傳學研究以父系遺傳為主。第十八對染色體長臂 q21 缺失症後群的臨床報告極少。在本篇文章中，我們除了描述一位患有第十八對染色體長臂 q21 缺失男嬰之臨床表徵外，我們也發現他的缺失是來自母親，而非父親。總之，當一個嬰兒表現出多樣的畸型，我們除了可利用其週邊血液進行染色體檢查之外，父母染色體的結果有時也能闡明疾病的遺傳模式。

關鍵詞：第十八對染色體長臂缺失症候群、父系母系遺傳

* 通訊作者：錢新南醫師 童綜合醫療社團法人童綜合醫院 小兒部 43503 臺中市梧棲區臺灣大道八段 699 號

Case Report

Chronic Myelomonocytic Leukemia with Hypereosinophilia in a Patient

Meng-Hsuan Tsai*

Division of Emergency Medicine, Tungs' Taichung Metro-Harbor Hospital, Taichung, Taiwan

Received: Dec. 03, 2020; Accepted: Dec. 28, 2020

Abstract

Hypereosinophilia (HE) is defined as an absolute eosinophil count > 1.5 × 10^9/L (or >1500 cells/μL) in the peripheral blood. Hypereosinophilia may be caused by events like allergic reactions, parasitic infections, drug reactions, paraneoplastic syndromes, and endocrine problems. In some cases, HE could be idiopathic and has limited clinical significance or is just secondary to other tissue damage like hypereosinophilic syndrome. However, hematological malignancies must be considered. We present a case with fever and hypereosinophilia that was eventually diagnosed as chronic myelomonocytic leukemia.

Key words: eosinophil, hypereosinophilia, chronic myelomonocytic leukemia

Introduction

The normal peripheral eosinophil count varies between 0.04–0.6 × 10^9/L. Peripheral blood eosinophilia can be classified as mild (0.5–1.5 × 10^9/L), moderate (1.5–5 × 10^9/L), or severe (>5 × 10^9/L) based on at least two measurements with an interval of ≥1 month in between and/or histologically proven tissue infiltration by eosinophils[1].

Peripheral blood eosinophilia can be caused by numerous allergic, infectious, and neoplastic disorders, which require a variety of different treatments. [2] The initial evaluation sought to identify disorders that require specific treatments, such as parasitic infection, drug hypersensitivity, leukemia, or non-hematologic cancer. We present a case of HE with no clear underlying causes that was eventually diagnosed based on careful history taking, head-to-toe physical examination, laboratory studies, chest radiography, and computed tomography.

*Correspondence to: Dr. Meng-Hsuan Tsai, Division of Emergency Medicine, Tungs' Taichung Metro-Harbor Hospital, No.699, Sec. 8, Taiwan Blvd., Taichung City 435, Taiwan (R.O.C.)

Case report

The patient was a 53-year-old male with a history of diabetes mellitus, chronic anemia (myelodysplastic syndrome in 2013), and intervertebral disc herniation at L5–S1. He visited the emergency department for intermittent fever that had persisted for 1–2 years with general malaise, headache, and arthralgia. The patient was a farmer who worked in the Miaoli country hillside with soil contact history, but he denied having ingested any raw food or untreated water consumption. No skin rashes, changes in bowel habits, or body weight loss were observed. Physical examination showed no specific findings except a palpable, enlarged spleen. Laboratory data indicated leukocytosis with a white blood cell count of 18800/μL, eosinophil count of up to 53.1%, segment count of 32.5%, lymphocyte count of 10.1%, monocyte count of 3.7%, basophil count of 0.6%, hemoglobin of 9.5 g/dL, and platelet count of 324 × 10^3/μL. C-reactive protein and procalcitonin levels were 5.19 mg/dL and 1.1 ng/mL, respectively. Markers of liver and renal function were at normal limits. Kidney, ureter, and bladder X-ray study revealed marked splenomegaly, a distinct contrast

to the study conducted in 2014 (Fig. 1). Endoscopy of the upper gastrointestinal tract and colon after admission was negative for parasites and ova. Stool routine analysis was also negative for parasites. The febrile episodes decreased with naproxen use. Bone marrow biopsy was performed, which showed refractory cytopenia with bilineage (myelocytic and megakaryocytic) dysplasia. This patient was eventually diagnosed with chronic myelomonocytic leukemia.

Discussion

Hypereosinophilia (HE) is defined as an absolute eosinophil count >1.5 × 10^9/L (or >1500 cells/μL) in the peripheral blood on two examinations with a 1-month interval in between[1,2]. Hypereosinophilic syndrome (HES) is defined by hypereosinophilia associated with eosinophil-mediated organ damage and/or dysfunction[5]. The signs and symptoms of HES result from the overproduction of eosinophils, which infiltrate and damage various tissues[3]. HE may result from clonal eosinophilic proliferation or from the overproduction of eosinophilopoietic cytokines such as interleukin 5 (IL-5)[3]. Eosinophils are primarily tissue-dwelling cells; they are several hundredfold more abundant in tissues than in blood. The degree of peripheral blood eosinophilia does not always accurately predict the risk of organ damage[4].

Eosinophilia is a dominant manifestation of a hematopoietic myeloid neoplasm or a secondary/reactive one of an underlying medical condition. [5] However, the degree of eosinophilia is rarely helpful in identifying the cause. The underlying disorders for eosinophilia are best distinguished by the patient's history, clinical presentation, and specific laboratory testing. [1] The most common causes are related to allergic disease, infectious disease, hematologic and neoplastic disorders, and endocrine problems. [3, 5] The workups of these patients include a complete blood test, blood smear, liver function test, serum chemistries, creatinine, and stool studies for ova and parasites. Further evaluation may include a bone marrow biopsy or bone scan[3].

In our patient, a complete blood test confirmed hypereosinophilia. Biochemistry data showed normal liver and renal function. No signs of target organ damage or involvement were indicated. Gastrointestinal endoscopy eliminated the differential diagnosis of parasitic infection. Therefore, the most likely cause for hypereosinophilia may have been myeloproliferative disorders. Bone marrow biopsy ultimately confirmed a diagnosis of chronic myelomonocytic leukemia, which may be due to underlying myelodysplastic syndrome.

Chronic myelomonocytic leukemia is characterized by peripheral blood monocytosis and bone

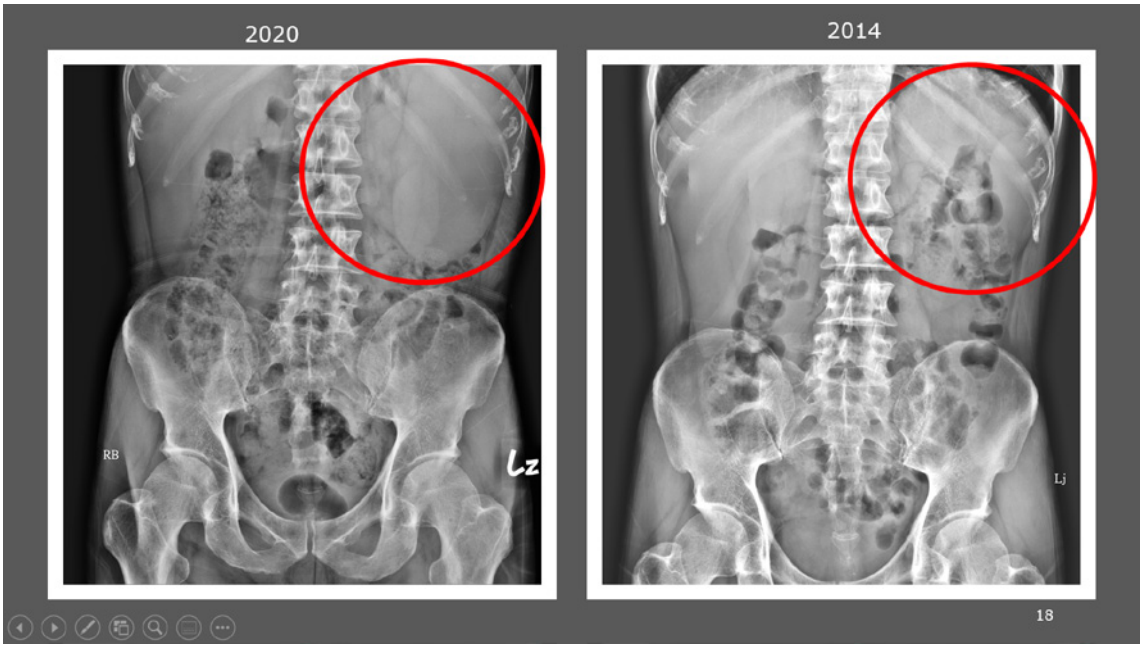

Fig. 1 Kidney, ureter, and bladder X-ray study in 2020 (left) showed markable splenomegaly which compared with a previous one in 2014 (right). Informed consent of the subject.

marrow dysplasia and often accompanied by cytopenia and splenomegaly. In rare cases with ≥1500 eosinophils/mL, chronic myelomonocytic leukemia must be distinguished from myeloid neoplasms with eosinophilia associated with specific genetic abnormalities. Myeloid and lymphoid causes of eosinophilia include myeloproliferative neoplasms with certain molecular abnormalities, including those involving *PDGFRA*, *PDGFRB*, *FGFR1*, *PCM1-JAK2*, and other rare gene rearrangements. Causes of eosinophilia secondary to neoplasms may also need differential diagnosis from T cell lymphomas and leukemias, Hodgkin lymphoma, and systemic mastocytosis[6].

The diagnosis of HE can always be obtained from thorough history taking, astute physical examination, laboratory tests, and, in particular, a high level of suspicion. This case emphasizes that malignancy should be considered when an unusual manifestation of HE is presented at an emergency room. An immediate workup is crucial to ruling out possible causes and thus to providing early and appropriate therapy, as demonstrated in this case.

References

1. van Balkum M, Kluin-Nelemans H, van Hellemond JJ, van Genderen PJJ, Wismans PJ. Hypereosinophilia: a diagnostic challenge. Neth J Med. 2018 Dec;76(10):431-436. PMID: 30569889
2. Helbig G, Kyrcz-Krzemień S. Diagnostic and therapeutic management in patients with hypereosinophilic syndromes. Pol Arch Med Wewn. 2011 Jan-Feb;121(1-2):44-52. PMID: 21346698.
3. Curtis C, Ogbogu P. Hypereosinophilic Syndrome. Clin Rev Allergy Immunol. 2016 Apr;50(2):240-51. doi: 10.1007/s12016-015-8506-7. PMID: 26475367.
4. Accessed 11/28/2020, at https://www.uptodate.com/contents/hypereosinophilic-syndromes-clinical-manifestations-pathophysiology-and-diagnosis
5. Curtis C, Ogbogu PU. Evaluation and Differential Diagnosis of Persistent Marked Eosinophilia. Immunol Allergy Clin North Am. 2015 Aug;35(3):387-402. doi: 10.1016/j.iac.2015.04.001. Epub 2015 Jun 23. PMID: 26209891.
6. Accessed 12/23/2020, at https://www.uptodate.com/contents/chronic-myelomonocytic-leukemia-clinical-features-evaluation-and-diagnosis

慢性髓性白血病以高嗜伊紅性血症表現之病例報告

蔡孟軒*

童綜合醫療社團法人童綜合醫院　急診醫學部

受文日期：民國 109 年 12 月 03 日；接受刊載：民國 109 年 12 月 28 日

摘要

高嗜伊紅性血症是一少見的血液疾患，主要表現是周邊血液或是組織間的嗜伊紅性血球細胞增加。其定義為絕對嗜伊紅性血球大於 1.5 x 109/L（或血液中嗜伊紅性血球 >1500 細胞 / 毫升）。高嗜伊紅性血球症可能會因過敏反應、寄生蟲感染、藥物刺激、腫瘤伴生神經症候群以及內分泌失調等因素相關，在某些患者身上，高嗜伊紅性血球症可為原發性，表現為無任何臨床症狀，亦可伴有其他組織器官因嗜伊紅性血球侵犯所產生的損害，此時稱為高嗜伊紅性血症；此外血液方面的惡性腫瘤也必須列入考量。在此我們探討一位伴有發燒及高嗜伊紅性血球症的患者，之後診斷出是慢性髓性單球性白血病。

關鍵詞：嗜伊紅性球、高嗜伊紅性血症、慢性髓性白血病

* 通訊作者：蔡孟軒醫師　童綜合醫療社團法人童綜合醫院　急診醫學部
43503 臺中市梧棲區臺灣大道八段 699 號

Case Report

Torsion of Huge Ovarian Borderline Brenner Tumor in Pregnancy: A Case of Successful Term Delivery

Yu-Hsuan Lin[1], Kim-Seng Law[2,*], Jong-Shiaw Jin[3], Liang-Ying Wu[1]

[1]General Medicine, [2]Department of Obstetrics and Gynecology, [3]Department of Pathology, Tungs' Taichung Metroharbor Hospital

Received: Sep. 04, 2020; Accepted: Nov. 09, 2020

Abstract

Brenner tumors are extremely rare epithelial ovarian neoplasms that are often asymptomatic and difficult to diagnose during pregnancy. Only four cases have been reported in the literature. Here, we describe the case of a 30-year-old pregnant woman with a large (26 × 20 × 8 cm^3), left-side, ovarian, borderline stage Ia Brenner tumor complicated with torsion during the first trimester. This patient successfully underwent unilateral salpingo-oophorectomy during the first trimester, to eventually deliver a term male baby without any complications.

Key words: Brenner tumor, borderline ovarian tumor, torsion of ovarian tumor, early pregnancy

Introduction

Brenner tumors are a rare subtype of epithelial ovarian neoplasm, accounting for only 2%–3% of all ovarian tumors. The first Brenner tumor was described in 1898 by MacNaughton-Jones[1], whereas Fritz Brenner reported three cases in 1907 and named the tumor "oophoroma folliculare." Brenner tumors usually occur unilaterally and are characterized by an epithelial lining composed of clusters of transitional cells that resemble the urinary tract epithelium. About 20% of these manifest as mixed epithelial tumors with other ovarian cancers and mainly feature a mucinous component[2]. However, most Brenner tumors are benign, with only 5% becoming malignant. Brenner tumors during pregnancy are extremely rare, with only four cases reported in the literature[3-6]. Here, we present the case of a pregnant woman with a large left-side ovarian Brenner tumor complicated with torsion found incidentally during the first trimester.

*Correspondence to: Kim-Seng Law, MD. M Sc Department of Obstetrics and Gynecology, Tungs' Taichung Metroharbor Hospital, No.699, Sec. 8, Taiwan Blvd., Wuqi Dist.,Taichung City 43503, Taiwan, (R.O.C.)

Clinical Case

A 30-year-old G1P0A0 woman with an unremarkable medical history presented with a large ovarian tumor found during routine antenatal ultrasound. A viable intrauterine fetus 6 weeks and 5 days age of gestation (AOG) with positive fetal heartbeat was also noted. The patient reported no abdominal pain, constipation, diarrhea, dysuria, frequency, or vaginal discharge. Physical examination found the abdomen soft and slightly protuberant, with no tenderness over the uterus and bilateral adnexa. A prominently palpable mass over the left pelvic area was identified.

Abdominal ultrasound revealed a large ovarian tumor (about 18.9 × 9.16 cm^2) with internal excrescence and a thick cystic wall, as well as an anteverted uterus. Pelvic magnetic resonance imaging (MRI) without intravenous contrast showed a large multiloculated cystic lesion with a likely soft-tissue component in the left adnexal region suspected as ovarian epithelial tumor (Figure 1). Significant laboratory findings were β-HCG at 6631.83 mIU/mL (normal range, <10.0 mIU/mL) and CA-125 at 107.5 U/mL (normal range, <35 U/mL). The patient was admitted

for exploratory laparotomy based on the suspicion of a large ovarian tumor and her ongoing pregnancy.

The patient was placed under general anesthesia. Upon opening the abdominal cavity, a large, grayish, smooth-surfaced tumor was noted, arising from the left ovary and measuring about 20 cm with torsion (Figure 2). The right ovary had no significant findings. The uterus was retroverted, boggy, and slightly enlarged with intrauterine pregnancy. Straw-colored ascites (about 50 cm^3) over the cul-de-sac were collected for cytology. Palpation found no tumor implantation over the mesentery, omentum, and upper diaphragm. Moreover, no enlarged retroperitoneal lymph nodes were noted. Left salpingo-oophorectomy with dissection of left lymph nodes was performed.

Frozen-section biopsy revealed a large mucinous borderline ovarian tumor, measuring 26 × 20 × 8 cm^3 and weighing 2756 g, with the Fallopian tube (10 × 0.6 cm^2) (Figure 3). The general appearance of the tumor was smooth, brown-gray, well-encapsulated, and multiloculated with mucinous yellow-brown fluid contents. Histological analysis (Figure 4) was consistent with the diagnosis of a borderline Brenner tumor (also known as an atypical proliferative Brenner tumor). The tumor was composed of large crowded nests of cells, resembling transitional-type epithelia with abundant fibromatous stroma. Additionally, metaplasia of the proliferative mucinous glands with crowding was noted. Focal cellular atypia without micro-invasion was observed. Immunohistochemistry results, which indicated CK7(+) and CK20(−), differentiated the tumor from urothelial carcinoma.

The patient was discharged 3 days after operation and resumed regular antenatal visits at our outpatient department. At 40 weeks and 1 day, she presented with a bloody discharge and a ruptured membrane, which prompted delivery. After admission, Group B *Streptococcus* infection was confirmed and treated with ampicillin. Cesarean section (CS) was performed due to a secondary arrest of labor, and a 3200-g male baby was delivered with Apgar scores of 8 and 9 at 1 and 5 minutes, respectively.

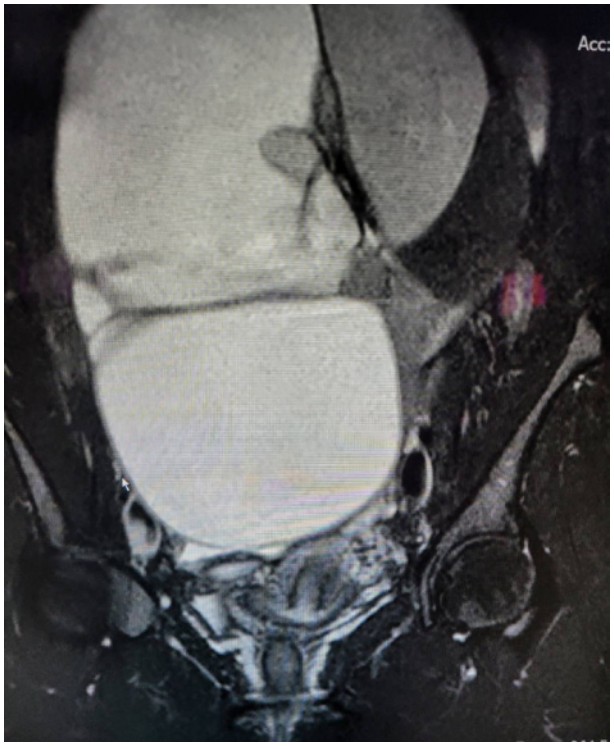

Fig. 1 MRI showing a huge ovarian tumor with multiloculated and soft-tissue components.

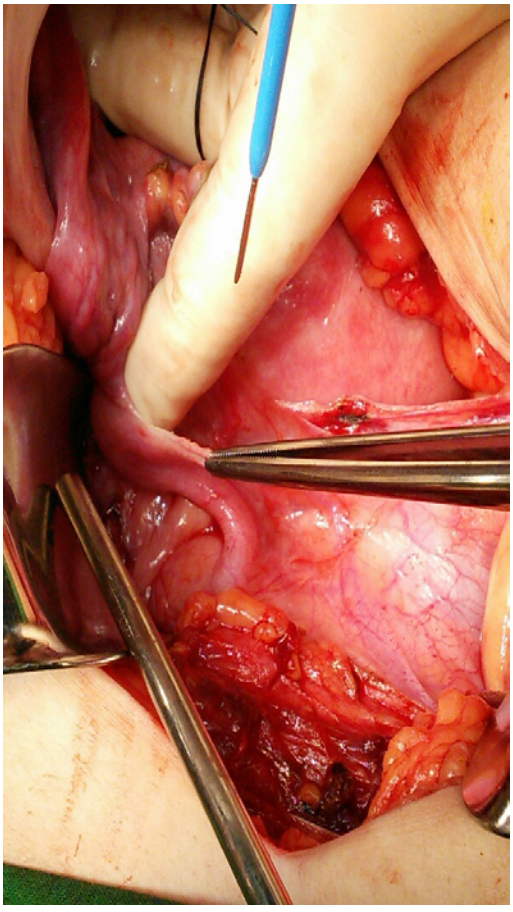

Fig. 2 A large, smooth, grayish tumor arising from the left ovary measuring about 20 cm, with torsion.

Discussion

The epithelial variant is the most common histologic type of ovarian tumor with five known subtypes: (1) serous, (2) mucinous, (3) endometrioid, (4) clear cell, and (5) Brenner tumors[7]. Brenner tumors are rare, accounting for only 2%–3% of all ovarian tumors, and are more likely to occur in postmenopausal women (Table 1).

The patient's age was similar to that of a pregnant woman with the largest Brenner tumor (age range, between 30 and 35 years). The women in the other reported cases except that of Gedikbasi et al.[6] had one gravida, whereas most of the Brenner tumors were detected before the third trimester. Briggs and Katchy[4] and Gedikbasi et al.[6] found Brenner tumors incidentally during CS.

Most pregnant women with adnexal tumors are asymptomatic. The incidence of adnexal tumors during pregnancy is about 1%–2%, approximately 1%–6% of which are malignant[1,8]. Ovarian cancer is the second most frequent gynecologic cancer complicating pregnancy. Common presentations of ovarian cancer include abdominal or back pain, constipation, abdominal swelling, and urinary symptoms. Although, a palpable adnexal mass may be identified through routine antenatal physical examination, most adnexal masses < 5 cm are benign simple cysts. Most adnexal cystic masses detected in the first trimester may spontaneously resolve by the early phase of the second trimester[9]. Those with persistent adnexal masses ≥ 5 cm in diameter are considered mature cystic teratomas[10]. A review suggested that adnexal masses 6–8 cm in diameter have a higher rate of torsion (22%) than either smaller or larger masses. This review also proposed that tumors ≥ 10 cm at initial diagnosis had a higher risk of malignancy versus smaller sizes[11]. The distinct finding in the present case is that torsion does occur in huge tumors, which was, additionally, not malignant. Moreover, notably, the patient did not present any symptoms of ovarian cancer.

An accurate diagnosis of an ovarian tumor is difficult to make during pregnancy because

Fig. 3 A large ovary tumor measuring 26 × 20 × 8 cm and weighing 2756 g was resected.

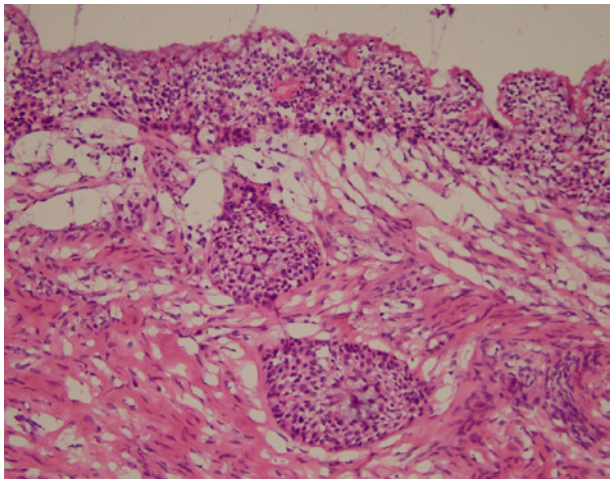

Fig. 4 Histological examination revealing large crowded nests of cells resembling transitional-type epithelia, with abundant fibromatous stroma.

Table 1. Review of the published reports for Brenner tumor in pregnancy

Report	Age	Parity	Size of mass (cm)	Symptoms/sign
Beckmann	33	G1P1001	Not stated	Detected at 8 weeks AOG
Briggs and Katchy	35	G1P0	10	Incidentally found while CS at 37 weeks for pre-eclampsia/breech
Yang DM	30	G1P0	8 x 5	Detected at 15 weeks, resected at CS
Ali Gedikbasi	35	G3 P2	8 x 7 x 5.5	Incidentally found while CS at 35 weeks for pre-eclampsia
Current case	30	G1P0	26 x 20 x 8	Detected at 6 weeks 5 days AOG

AOG - age of gestational; CS - Caesarean section

pregnancy-associated symptoms may conceal any clinical presentations of a stealthy tumor, regardless of size. An ultrasound can visualize measurements and the nature of the tumors by analyzing the echogenicity and scanning arteries with color Doppler, thus providing information on tumor size, structure, and growth. Therefore, we recommend a prior ultrasound scan whether the therapeutic decision is surgery or palliative treatment. MRI is another method of preoperatively determining the nature of the mass, given its excellent resolution for soft-tissue pathology in the absence of significant radiation exposure.

Brenner tumors are composed of transitional cells within dense stroma. They are related to other ovarian tumors in 30% of cases and are visible as multilocular, hypoechoic cystic masses with solid components. These tumors typically present as a small, mostly solid mass on ultrasound with a dense fibrous stroma on MRI. Extensive amorphous calcification is often present within the solid component [12]. In our case, the MRI showed a large, multiloculated cystic lesion with soft-tissue components.

Although serum tumor markers may provide crucial information regarding the nature of the tumors, these markers may, paradoxically, increase at some stages in life because of their involvement in fetal development. Notably, CA-125, one of the significant tumor markers in benign ovarian tumors, may also increase in conditions such as epithelial ovarian cancer[13] and during the first trimester of pregnancy[14]. Controversially, Seki et al. reported that although CA-125 levels were significantly lower in women in the first trimester of pregnancy than in patients with ovarian cancer, a considerable overlap exists between them. Conversely, Amampai et al.[15] reported that only 9.1% of the studied patients showed abnormal CA-125 levels in the first trimester, with the median serum CA-125 level measured at 16.44 U/mL (range, 5.94–77.54 U/mL). The elevated CA-125 level observed in our case is most likely due to pregnancy than malignancy, so were the elevated β-HCG levels.

Clinicians should prudently plan the scope of the treatment, including consequent impacts on maternal and fetal health such as possible morbidity. Fertility preservation should also be considered, especially with a viable fetus in situ.

The general consensus for surgical intervention are the size of the tumor (>10 cm in diameter), tumor growth observed during follow-up, and potential malignant changes on radiologic imaging (including solid, cystic, papillary and septal features[16]. Emergent conditions such as torsion, ruptured adnexal mass, or possible obstruction of labor are also indicated for surgery, specifically, resection if with a large tumor. Of the four cases of Brenner tumors in the literature, three were resected during CS. Two of them (Briggs et al.[4]; Gedikbasi et al.[6]) were detected incidentally during CS due to small sign, whereas Yang found their Brenner tumor at 15 weeks AOG. Beckmann et al. discovered the tumor in their case at 8 weeks AOG and performed a hysterectomy with unilateral oophorectomy due to uterine fibroids and an adnexal mass.

Conclusion

Our case report verifies the difficulty of diagnosing ovarian tumors during pregnancy, specifically Brenner tumors. However, ultrasonography and MRI can adequately provide visualization that can aid diagnosis since Brenner tumors present distinctive morphological features. Our case presented a massive tumor with torsion but without any signs of malignancy, which contradicts existing findings. Furthermore, although most Brenner tumors have solid components, this case featured soft-tissue components within the lesions. These findings expand on currently known characteristics of Brenner tumors and emphasize the need for radiologic imaging for better diagnostic accuracy, especially if found during pregnancy.

References

1. Jones MH: Uterine fibroid with anomalous ovarian tumor. Am J Obstet Gynecol 1978;132:471-2.
2. Waxman M: Pure and mixed Brenner tumors of the ovary: clinicopathologic and histogenetic observations. Cancer 1979;43:1830-9.
3. Beckmann CR: Brenner tumor during pregnancy. A case report. J Reprod Med 1983;28:681-3.
4. Briggs ND, Katchy KC: Brenner tumor as encountered in a southern Nigerian Hospital. Int J Gynaecol Obstet 1988;27: 455-8.
5. Yang DM, et al.: Brenner tumor of the ovary with extensive stromal luteinization presenting in pregnancy: report of a case and review of the literature. J Matern Fetal Neonatal Med 2002;12:281-3.

6. Gedikbasi A, et al.: Brenner tumor in pregnancy: clinical approach and pathological findings. J Obstet Gynaecol Res 2009;35:565-8.
7. Chen VW, et al.: Pathology and classification of ovarian tumors. Cancer 2003;97:2631-42.
8. Oehler MK, Wain GV, Brand A: Gynaecological malignancies in pregnancy: a review. Aust N Z J Obstet Gynaecol 2003;43:414-20.
9. Giuntoli RL, 2nd, Vang RS, Bristow RE: Evaluation and management of adnexal masses during pregnancy. Clin Obstet Gynecol 2006;49:492-505.
10. Schmeler KM, et al.: Adnexal masses in pregnancy: surgery compared with observation. Obstet Gynecol 2005;105: 1098-103.
11. Yen CF, et al.: Risk analysis of torsion and malignancy for adnexal masses during pregnancy. Fertil Steril 2009;91: 1895-902.
12. Chiang G, Levine D: Imaging of adnexal masses in pregnancy. J Ultrasound Med 2004;23:805-19.
13. Van Calster B, et al.: Discrimination between benign and malignant adnexal masses by specialist ultrasound examination versus serum CA-125. J Natl Cancer Inst 2007;99: 1706-14.
14. Seki K, et al.: Increased serum CA 125 levels during the first trimester of pregnancy. Acta Obstet Gynecol Scand 1986;65:583-5.
15. Amampai R, Suprasert P: Cancer Antigen 125 during Pregnancy in Women without Ovarian Tumor Is Not Often Rising. Obstet Gynecol Int 2018;2018:8141583.
16. Aggarwal P, Kehoe S: Ovarian tumours in pregnancy: a literature review. Eur J Obstet Gynecol Reprod Biol 2011; 155:119-24.

早期妊娠併巨大低惡性卵巢布氏腫瘤扭轉術後足月生產：成功案例報告

林瑜萱[1] 劉錦成[2,*] 金忠孝[3] 吳亮瑩[1]

童綜合醫療社團法人童綜合醫院 [1]一般科 [2]婦產部 [3]病理部

受文日期：民國 109 年 09 月 04 日；接受刊載：民國 109 年 11 月 09 日

摘要

布氏腫瘤（Brenner tumor）為一種罕見卵巢上皮腫瘤。臨床上通常無症狀，且很難在懷孕中鑑別診斷。目前在英文文獻中僅有四例懷孕中發現的布氏腫瘤個案。此篇個案報告探討一位 30 歲妊娠女性，在懷孕第六週產檢時意外發現一 26 x 20 x 8 公分巨大卵巢布氏腫瘤，合併扭轉，經輸卵管及卵巢切除術後在足月順利產下胎兒。

關鍵詞：布氏腫瘤、卵巢扭轉、懷孕早期、輸卵管及卵巢切除術

* 通訊作者：劉錦成醫師 童綜合醫療社團法人童綜合醫院 婦產部 43503 臺中市梧棲區台灣大道八段 699 號

童綜合醫學雜誌投稿相關規則

95.9.01 製訂
110.06.23. 修訂（第 13 版）

童綜合醫學雜誌線上投稿暨評閱系統：http://www.ipress.tw/J0143。本雜誌刊載與醫學有關之論述，包括原著論文（Original Articles）、病例報告（Case Reports）、綜論（Review Articles）、短論（Communications、包括 Brief Communications）、影像判讀（Images）、臨床病理討論（Pathology Page）、編著的話（Editorials）等。惠稿請送 43503 臺中市梧棲區臺灣大道八段 699 號童綜合醫學雜誌編審委員會。（E-mail:Tungs_Journal@ms.sltung.com.tw）

壹、投稿前注意事項

1. 惠稿請以英文撰寫，本雜誌接受電子檔投稿或經由線上投審稿系統：http://www.ipress.tw/J0143 投稿，電子檔投稿請直接將稿件 WORD 檔寄至編審委員會信箱：Tungs_Journal@ms.sltung.com.tw。
2. 著作中若牽扯到版權所有之內容，作者需取得其使用權，法律責任由作者負責。
3. 投稿同時請附上著作權讓與同意書。所有作者必須實際參與並同意該論述。本院於接受稿件且印刷完成後，將致贈稿酬並贈送 20 份抽印本給通訊作者，如需額外抽印本請於校稿時言明，並酌收成本費用。第一作者若需抽印本可提出申請，依份數酌收成本費用。
4. 本刊對於原稿經徵得作者之同意得伸縮或修改之。如不合本刊宗旨者，得退還之。
5. 凡刊載於本雜誌之著作，若涉及「研究用人體檢體採集」及「人體試驗」等情事，應遵守該注意事項。除不須 IRB 審查之細胞、細菌、動物實驗外，回溯性研究、資料庫分析、問卷量性研究等皆須於文章中註明 IRB 編號〔需含機構名稱〕；病例報告及影像判讀等文章需取得病人知情同意並於內文註明，以落實保障受檢人權益。
6. 論文中如涉及使用脊椎動物進行科學應用計畫者，應檢附該計畫業經所屬機構動物實驗管理小組審議認可之文件，以落實實驗動物之人道管理。

貳、寫作原則

1. 原著論文（Original Articles）按下列順序撰寫：摘要、前言、材料與方法、結果、討論與結論、誌謝、參考文獻、附表、圖片說明、圖片（含照片）。每篇字數 3000 字以內，摘要 300 字以內，參考文獻 40 篇以內。
2. 病例報告（Case Reports）按下列順序撰寫：摘要、前言、病例、討論、參考文獻、附表、圖片說明、附圖、照片。凡病患顏面部位之相片必須遮去眼睛部位，表示尊重隱私。診療資料或臨床經過之圖表，原則上均限六個月以內。每篇字數 1500 字以內，摘要 150 字以內，參考文獻 10 篇以內。
3. 綜論（Review Articles）不必按原著論文格式撰寫，但每篇字數 3500 字以內，摘要 300 字以內，參考文獻 60 篇以內。
4. 短論（Brief Communications），臨床上、技術上的精簡論著，每篇字數 750 字以內，摘要 150 字以內，參考文獻 7 篇以內。
5. 影像判讀（Images）、臨床病理討論（Pathology Page）圖例說明每篇字數 500 字以內，摘要 150 字以內，參考文獻 3 篇以內。
6. 編者的話（Editorials），每篇字數 2000 字以內，摘要 150 字以內，參考文獻 7 篇以內。
7. 其他細節，請參閱國際指導委員會（International Steering Committee）發表之生物醫學雜誌稿件統一規格（Uniform Requirements for Manuscripts Submitted to Biomedical

Journals，見 The New England Journal of Medicine 336:309-315,1997）。

8. 將可接受投稿之稿件種類之摘要字數、字數、參考文獻及圖表相關上限規定，整理於下表：

稿件種類	字數限制		參考文獻	圖 / 表
	摘　　要	內文字數		
原著論文 (Original Article)	≦ 300	≦ 3000	≦ 40	≦ 5
病例報告 (Case Report)	≦ 150	≦ 1500	≦ 10	≦ 3
綜論 (Review Article)	≦ 300	≦ 3500	≦ 60	≦ 6
短論 (Brief Communication)	≦ 150	≦ 750	≦ 7	≦ 1
影像判讀 (Images)、 臨床病理討論 (Pathology Page)	≦ 150	≦ 500	≦ 3	≦ 2
編者的話 (Editorial)	≦ 150	≦ 2000	≦ 7	≦ 1

參、投稿須知

1. 稿件須符合「生物醫學雜誌投稿之統一規定」[1]，請以電腦隔行 double space 書寫，並編行號及頁碼，中文字型以標楷體，英文字型以 Time New Roman 12 號字大小，稿紙之左右緣爲 2.54 公分，上下緣爲 3.17 公分。
2. 第一頁爲標題頁，須列出中文及英文之論文題目、中英文作者姓名、所屬機構及單位之中英文稱號（分屬不同單位，請以阿拉伯數字標出作者與單位）、聯絡人姓名、電話及中英文通訊錄。
3. 第二、三頁爲中文及英文之摘要及關鍵詞（請提供 3 至 5 個關鍵詞或簡短片語），中英文摘要須完全相同，摘要分段撰寫，依序爲背景及目的（Background and purpose）、方法（Methods）、結果（Results）及討論（Discussion）。
4. 相同貢獻作者請加註說明，如研究主題的設定、參與決定研究設計、進行統計分析、詮釋研究結果、以及各章節撰稿等貢獻。
5. 圖表應專業製作，一張紙僅一個附圖或附表，依引用順序以阿拉伯數字標出排列。附表須有標題及說明且不可以照片形式。圖片或照片電子檔（.jpg）必須清晰、分明。附圖須有簡單說明（Legend），並另頁撰寫。光學或電子顯微鏡照片，請註明擴大倍率或比例。

註：[1] 根據「生物醫學雜誌投稿之統一規定」第五版，刊載於 Annals of Internal Medicine 1997;126(1): 36-47.

肆、參考文獻

未經發表之論文或摘要不得列爲參考文獻，但可於本文中說明並註明「未發表」（unpublished observations）。博碩士論文可引用。已被任何雜誌接受刊發但仍未發表之著作，請列出雜誌名稱及年份，並註明「in press」。

原著論文、病例報告、綜論、短論、影像判讀、臨床病理討論、編著的話按下列格式撰寫：

A. 雜誌及期刊

中文例〔作者姓名：題目。雜誌簡稱 年號；卷數：起訖頁數〕

薛玉梅、陳建仁：皮膚砷癌之流行性病學特徵與危險因子。中華衛誌 1996; 15: 1-26。

英文例〔英文原稿中引用的參考文獻，其雜誌或期刊之簡稱應參照 Index Medicus 型式〕

1. Feely J, Wilkinson GR, Wood AJ. Reduction of liver blood flow and propranonol metabolism by cimetidine. N Engl J Med 1981;304:691-6.

2. Kaplan NM. Coronary heart disease risk factors and antihypertensive drug selection. J cardiovasc Pharmacol 1982; 4(suppl 2): 186-365.（引用雜誌附冊時）
3. Tada A, Hisada K, Suzuki T, Kadoya S. Volume measurement of intracranial hematoma by computedtomography. Neurol surg (Tokyo) 1981; 9: 251-6.〔In Japanese: English abstract〕（引用文獻之作者之本文爲非英文，但有英文摘要）。
4. Bhasin S, Storer TW, Berman N, Callegari C, Clecenger B, Phillips J, et al. The effects of supraphysiologic doses of testosterone on muscle size and strength in normal men. N Engl J Med 1996; 335: 1-7.（作者超過 6 位時，只須列出前 6 位，其它以「等」(et al) 代替）

＊期刊若有「數位物件識別碼 (digital object identifier, DOI)」，則於文獻末。

＊＊內文文獻標示以中括號、數字、上標呈現。

B. 單行本：

中文例 [作者姓名：書名，版數（卷數）。發行地；出版公司，年代：引用部份頁數]。

楊志良：生物統計學新論，一版。台北；巨流圖書公司，1984：33-8.

英文例 [英文單行本的書名，除介系詞及連接詞外，第一字母需大寫]

(1) Plum F, Posner JB. Diagnosis of Stupor and Coma. 3rd ed., Philadelphia: Davis, 1980:132-3.

C. 多重作者之單行本：

中文例 [有關文章作者姓名：題目 。編輯者姓名：書名 。版數（卷數）。發行地：出版公司，年代；引用部份頁數]。

蔣欣欣：護理與健康。顧乃平：護理專業導論。一版。台北：匯華出版公司，1991：83-121。

英文例 Levinsky NG: Fluid and electrolytes. In: Thorn GW, Adams RD, Braunwald E, lsselbacher K, Petersdprf RG eds. Harrison’s Principles of Internal Medicine. 8th ed. New York: Mcgraw-Hill, 1977;364-75.

D. 參考文獻引用時，若兩名以下作者請列出姓氏。兩名以上則列出第一名之姓氏，其他以「等」(et al) 代替，並以阿拉伯數字方括弧表示於引用之後。

例：One of the first well documented reports of ECH poisoning with fatality in young children was reported by Miller et al. in 1970[2].

E. 參考文獻引用網路資料請列出文獻名稱及出處以及引用時間

(Accessed Month day, 2016, at http://www.house.gov/xxxx/min/inves_xxx/index_accord.htm.)

伍、著作權

若著作人投稿於本刊經收錄後，同意授權本刊得再授權國家圖書館或其他資料庫業者，進行重製、透過網路提供服務、授權用户下載、列印、瀏覽等行爲。並得爲符合各資料庫之需求，酌作格式之修改。若爲摘譯、譯稿或改寫稿，需附原作者之正本同意書，並附原文影本一份；來稿如涉及版權，概由作者自負文責。

Instruction to contributors

The Tungs' Medical Journal provides a forum for all fields of medicine, including Editorials, Review Articles, Original Articles, Case Reports, Brief Communications, Images, and Pathology Page. Authors are welcome to submit manuscripts to Tungs' Medical Journal.

Preparing Your Manuscript:

1. The manuscript must be submitted as a Word document to the Editor on online system: http://www.ipress.tw/J0143, or to E-mail address: Tungs_Journal@ms.sltung.com.tw.
2. The author is responsible for the content of the manuscript. If the content is related to copyright, author needs to obtain the right to use and is legally responsible for it.
3. Please attached the copyright and consent form on submission. All author(s) listed must actually participate in and agree with the conclusion. Upon receiving and completion of printing, the author(s) will receive 20 free copies and compensation. If extra copy is needed, please notify during editing, and this is subjected to charges.
4. The manuscript may be rejected if incompatible with the journal's mission. After acquiring consent from the author(s), the editor may edit the manuscript.
5. Any manuscript related to "the human specimen for research" or "clinical trial", must follow the guidelines to obtain an IRB approval for the right of participants. In addition to cell, bacteria, and animal experiments that do not require IRB review, retrospective research, database analysis, quantitative research, etc. are required the IRB number (including the institution name). Case report and Image articles should receive patients' consent and the written "consent of the subject" should be indicated in the text to protect the rights of patients.
6. For any the manuscript related to the use of animals, it needs to be approval of The Institutional Animal Care and Use Committee to ensure the humane management.

Manuscript format:

1. Editorials are limited to 2000 words, with 150 words of abstract and 7 references.
2. Review articles should provide the reader with a balanced overview of an important and topical subject in the field. This should be limited to 3500 words, with 300 words of abstract and 40 references.
3. Original articles should be presented in the following order: Abstract, Introduction, Materials and Methods, Results, Discussion and Conclusion, Acknowledgements, References, Attachments, Tables, Legends for illustration, and Figures (photographs). This should be limited to 3000 words, with 300 words of abstract and 40 references.
4. Case reports should be arranged by the following sequence: Abstract, Introduction, the Clinical case, Discussion, References, Attachments, Table, Legends for illustration, and Figures. Patients' eyes should be covered for privacy. Diagnosis information or the chart of clinical process should be within 6 months. This should be limited to 1500 words, with 150 words of abstract and 10 references.

5. Brief communications should be concise presentations of preliminary clinical results and technological improvements. This should be exceeded 750 words, 150 words of abstract and 7 references.
6. Images and Pathology page should be limited to 500 words, with 150 words of abstract and 3 references.
7. For other details, please refer to International Steering Committee, for Uniform Requirements for Manuscripts Submitted to Biomedical Journals, please refer to The New England Journal of Medicine 336:309-315,1997.

Specifications for the different article categories

Article Category	Word count limit		No. of references allowed	No. of tables/ figures allowed
	Abstract	Min text*		
Original Articles	≦300	≦3000	≦40	≦5
Case Reports	≦150	≦1500	≦10	≦3
Review Articles	≦300	≦3500	≦60	≦6
Brief Communications	≦150	≦750	≦7	≦1
Images, Pathology Page	≦150	≦500	≦3	≦2
Editorials	≦150	≦2000	≦7	≦1

*Refers to the main body of text only, i.e., does not include article title, abstract, table headings/tables, figure legends and references.

Manuscript preparation:

Manuscript should be double-spaced, line number, numbered pages, and comply with the “uniform requirements for manuscripts submitted to biomedical journals”. The first page is the title page, which include title, name of author(s), organization and unit, contact name, phone number, e-mail address and mail address (in both Chinese and English). The second and the third page is for abstract (Chinese content needs to consist with English content) and key words (please include 3 to 5 keywords or phrases in Chinese and English), and should be written in paragraphs following by background and purpose, methods, results and discussion.

Co-corresponding author should mention the contributions on manuscript, such as initiation of research topics, the study design, statistical analysis, interpretation of findings, chapters writing involved, et al.

Please attach two original copies including attachments, charts and legends. Chart should be professional, with only one figure or one table per page, and is arranged in consecutive orders and numbered in Arabic characters. Table should have a title and appropriate interpretation. Picture should be 5” x 7” in size, black and white, glossy and numbered in consecutive orders of appearance.

Reference:

Unpublished articles or abstracts cannot be listed as references, but could be noted as “unpublished

observations". Doctoral dissertation or master thesis can be used. Any articles being accepted by magazines but not published yet, please note the name of magazine, year and note "in press".

Original researches, case reports, review articles, communications (includes brief communications), images in clinical medicine, editorial follows the following format:

1. Abbreviations used should follow the format of Index Medicus for all journal titles. When authors are less than 6 people, list all author(s), when more than 6, only list the first 6 followed by "et al." for the rest.
2. References in the text should be placed where relevant. When a reference article is cited, only the primary author is cited; however, if only two authors are present, both should be listed.
3. Citation should show as [numbers] and use Superscript mark.

Examples of Reference:

1. Periodicals:

   Yang KTA, Chen HD: A semi-automated method for edge detection in the evaluation of left ventricular function using ECG-gated single-photon emission tomography. Eur J Nucl Med 1994;21:1206-11.

2. Monographs:

   Plum F, Posner JB: Diagnosis of Stupor and Coma. 3rd ed. Philadelphia: Davis, 1980:132-3.

3. Monographs with multiple authors:

   Levinsky NG: Fluid and electrolytes. In: Thorn GW, Adams RD, Braunwald E, Isselbacher K, Petersdprf RG eds. Harrison's Principles of Internal Medicine, 8th ed. New York: Mcgraw-Hill, 1977:364-75.

4. References from website

   Please indicate the title, source, and the retrieving date

   (Accessed Month day, 2016, at http://www.house.gov/xxxx/min/inves_xxx/index_accord.htm.)

Copyright:

童 綜 合 醫 學 雜 誌

編著的話

綜　論

原　著

病例報告

ISSN 2071-3592

童綜合醫學雜誌

中華民國九十六年十二月創刊
預定出版日期：每年六、十二月三十日出刊

出版編輯部：
童綜合醫學雜誌編審委員會
地址：43503 臺中市梧棲區臺灣大道八段 699 號
E-Mail：Tungs_Journal@ms.sltung.com.tw
Tel：〈04〉26581919 ext 59045　Fax：〈04〉26582193

印 刷 者：
大光華印務部　Tel：〈02〉2302-3939（代表號）
地址：10851 台北市萬華區廣州街 32 號 6 樓　Fax：〈02〉2302-2036